

University of Dundee

DOCTOR OF PHILOSOPHY

A novel hypothesis for plant capacitance

Dietrich, Ralf

Award date:
2013

Awarding institution:
University of Dundee

[Link to publication](#)

General rights

Copyright and moral rights for the publications made accessible in the public portal are retained by the authors and/or other copyright owners and it is a condition of accessing publications that users recognise and abide by the legal requirements associated with these rights.

- Users may download and print one copy of any publication from the public portal for the purpose of private study or research.
- You may not further distribute the material or use it for any profit-making activity or commercial gain
- You may freely distribute the URL identifying the publication in the public portal

Take down policy

If you believe that this document breaches copyright please contact us providing details, and we will remove access to the work immediately and investigate your claim.

Download date: 17. Feb. 2017

DOCTOR OF PHILOSOPHY

A novel hypothesis for plant capacitance

Ralf Dietrich

2013

University of Dundee

Conditions for Use and Duplication

Copyright of this work belongs to the author unless otherwise identified in the body of the thesis. It is permitted to use and duplicate this work only for personal and non-commercial research, study or criticism/review. You must obtain prior written consent from the author for any other use. Any quotation from this thesis must be acknowledged using the normal academic conventions. It is not permitted to supply the whole or part of this thesis to any other person or to post the same on any website or other online location without the prior written consent of the author. Contact the Discovery team (discovery@dundee.ac.uk) with any queries about the use or acknowledgement of this work.



Plant Science Division, College of Life Science,
University of Dundee at The James Hutton Institute

A novel hypothesis for plant capacitance

Ralf Christian Dietrich

Thesis submitted to the University of Dundee
for the degree of Doctor of Philosophy,
September 2012

CONTENT

CONTENT	ii
TABLES	v
FIGURES	vi
ABBREVIATIONS	xi
ACKNOWLEDGEMENT	xii
LIST OF ILLUSTRATIONS	xiii
DECLARATION	xiv
ABSTRACT.....	xv
1 INTRODUCTION	1
1.1 Non-invasive measurement techniques with the focus on soil and root research.....	6
1.1.1 Techniques for root measurement that use electromagnetic radiation	6
1.1.2 Measuring with electricity	13
1.2 The capacitance measurement of plants in the ground	25
1.2.1 A general overview.....	26
1.2.2 Experimental findings and their interpretation	27
1.2.3 The Dalton model for root capacitance	29
1.2.4 Factors that may affect root capacitance measurement	30
1.2.5 Testing the Dalton model	33
1.3 Definition of electrical capacitance (F) and basic theory	34
1.4 Aims and outline of thesis	39
2 GENERAL METHODS AND PRELIMINARY EXPERIMENTS	42
2.1 General methods	42
2.1.1 Plant growth.....	42
2.1.2 Measuring capacitance and resistance	45
2.1.3 Determination mass, plant dimensions and the soil water content	48
2.1.4 Statistics.....	49

2.2	Preliminary experiments.....	50
2.2.1	Introduction	50
2.2.2	Material and methods	51
2.2.3	Results and discussion.....	53
2.2.4	Conclusions	64
3	TESTING THE DALTON MODEL OF CAPACITANCE FOR BARLEY IN HYDROPONICS.....	66
3.1	Introduction	66
3.2	Material and methods	68
3.3	Results and discussion	72
3.4	Conclusions	85
4	ELECTRICAL CAPACITANCE OF PLANTS IN SOLID MEDIA	87
4.1	Introduction	87
4.2	Material and methods	88
4.3	Results	94
4.4	Discussion.....	100
4.5	Conclusion.....	101
5	EFFECT OF PLANT TISSUE GEOMETRY AND CONNECTION SCHEME ON CAPACITANCE, USING POTATO PARENCHYMA AND ELECTRICAL ANALOGIES	103
5.1	Introduction	103
5.2	Material and methods	104
5.2.1	Potato tuber experiments	104
5.2.2	Electrical analogies.....	111
5.3	Results and discussions.....	114
5.3.1	Plant tissue- and electrode-related effects on capacitance and the simulation of plant experiments.....	114
5.3.2	Electrical circuit analogies.....	131
5.4	Conclusions	140
6	GENERAL DISCUSSION AND CONCLUSIONS.....	142
6.1	Objectives	142

6.2	Re-evaluation of the physical basis for the electrical capacitance of plants in hydroponics	143
6.3	Re-evaluation of the physical basis for the electrical capacitance of plants in solid media	145
6.4	Reevaluating the physical basis for the electrical capacitance of plant material in general	147
6.5	Knowledge that was gained for practical application	149
6.6	Future work.....	150
7	REFERENCES	151
	APPENDIX.....	167

TABLES

Table 1-1. Examples of measurement methods that show promise for field-based phenomics...	3
Table 1-2. Details of studies and parameters obtained for linear relationships between capacitance and root system size.	4
Table 2-1. Composition of nutrient solution	44
Table 2-2. Timelines of and, experimental conditions for, preliminary experiments (I – III) ...	52
Table 2-3. Linear regression equations for capacitance against root mass and number.....	55
Table 2-4. Mean parameters of 94 individual nodal roots from 11 whole root systems	60
Table 2-5. Linear regression equations for eight unbranched nodal roots	61
Table 3-1. Linear regressions for capacitance against the root cross-sectional area and sum of circumferences of individual roots at the solution surface.	79
Table 5-1. Bore-sizes of potato tuber cores.....	104
Table 5-2. Linear regression equations for capacitance against distance between plant electrode and water surface for partly submerged potato cores	125
Table 5-3. Linear regression equations for the relationship between capacitance and the reciprocal of cumulative distance/area for potato tuber cores with three sections of different diameter.	126
Table 5-4. Average capacitances and impedances for barley grown in hydroponics and compost	138

FIGURES

1

Figure 1-1. 3D images of pre-germinated maize seeds	9
Figure 1-2. MRI images (top) and photo (bottom) of a maize root system.	10
Figure 1-3. Neutron radiography image of a root system of <i>Lupinus L</i> in relatively dry sand..	11
Figure 1-4. Typical ranges of electrical resistivities of earth materials	20
Figure 1-5. Electrode arrays for electrical resistivity surveys: (a) Four-point electrode configuration in a two-layer model. (b) Acquisition of a 2D apparent resistivity pseudosection using a dipole–dipole array	22
Figure 1-6. Relationship between the volumetric water content and the electrical resistivity for different soil types	22
Figure 1-7. Scheme of capacitance measurement on a plant rooting in substrate.....	27
Figure 1-8. Left: schematic diagram of a plate capacitor. Right: Symbol for a capacitor.	35
Figure 1-9. Scheme of a resistance-capacitance circuit (RC circuit)..	38

2

Figure 2-1. Two hydroponic systems differing in their water regime.....	44
Figure 2-2. Measuring capacitance with different electrode types..	46
Figure 2-3. A root system submerged in hydroponic solution forms a meniscus.	47
Figure 2-4. Results of experiment I.....	54
Figure 2-5. (a, b) Results of experiment II.....	56
Figure 2-6. (a) Capacitance with time and (b) in relationship with root fresh mass of 27 root systems.	58
Figure 2-7. (a) A matrix scatter plot showing the relationships between capacitance and different root size factors (Table 2-4), i.e. root fresh mass (M , g), length (L , mm), volume (V , mm^3), surface area (A_s , mm^2), and the root cross-sectional area (A_c , mm^2) and circumference (Φ , mm) at the solution surface of 94 individual nodal roots. The relationships between capacitance and (b) A_c and (c) Φ are shown as larger plots.....	60

Figure 2-8. Relationship between capacitance and (a) distance and (b) the reciprocal of the distance between plant electrode and solution surface for eight nodal roots.....	61
Figure 2-9. Interpolative biplots of the dimensions (a) capacitance (C), root mass (M), and root number of 61 individual barley roots from experiment I; (b) C, root system mass and shoot mass of 16 barley plants from experiment II; (c) C, M, root volume (V, mm ³), root surface area (A _s , mm ²), root circumference at the solution surface (Φ, mm), and root cross-sectional area at the solution surface (A _c , mm ²) of 94 barley roots from experiment III; and (d) C, Φ, A _s of the same roots as in (c).	63
 3	
Figure 3-1. Resistance-capacitance (RC) circuits according to the Dalton (1995) model	68
Figure 3-2. Experimental apparatus	69
Figure 3-3. Capacitance measurements performed on whole root systems and single roots	71
Figure 3-4. Relationship between capacitance and fresh mass of 16 whole root systems	73
Figure 3-5. Relationships between capacitance and (a) fresh mass and (b) the sum of cross-sectional areas at the solution surface.	74
Figure 3-6. Examples of relationships between capacitance (C) and (a) the distance (D) between the plant electrode and the solution surface and (b) the fresh mass (M) of submerged root tissue when roots were raised incrementally out of solution. (c) The relationship between C and the reciprocal of the distance (1/D) between plant electrode and solution surface. (d) The relationship between C measured after and before complete trimming of the submerged root.	76
Figure 3-7. (a) Relationship between capacitance and the distance between the plant electrode and the solution surface, when roots were lowered incrementally into solution. (b) The relationship between capacitance measured after and before trimming of the submerged root.....	77
Figure 3-8. The relationships between (a) capacitance (C) and the position of the electrode on the root system, and (b) the sum of root cross-sectional areas (ΣA _c) at the solution surface and the electrode position on the root system, and (c) between C and ΣA _c .	78
Figure 3-9. Relationship between the capacitances of roots measured in solution against capacitance measured at an equivalent separation of electrodes on roots removed from solution..	80
Figure 3-10. Resistance–capacitance (RC) circuits according to the revised model.	81

Figure 3-11. The relationships between capacitance and the reciprocal of cumulative

$$\text{distance/area} \left[\sum_{i=1}^n \frac{\Delta d_i}{A_i} \right]^{-1} \text{ for a whole root system, a seminal root and an}$$

unbranched nodal root. 83

4

Figure 4-1. Controlled irrigation treatments performed in Experiment 3. 92

Figure 4-2. (a) Relationship between the capacitance of compost and its water content. (b) Relationship between the capacitance of soil and its water content. (c) Relationships between the capacitance of compost, of soil measured in the laboratory and soil measured in the field and electrode separation. (d) Relationships between the capacitance of compost, of soil measured in the laboratory and of soil measured in the field and the reciprocal of electrode separation..... 95

Figure 4-3. Relationship between the capacitance of wheat plants and their root dry mass. 96

Figure 4-4. (a) Capacitance relative to fully wetted compost for barley plants in dry compost, compost wetted at the surface, and thoroughly wetted compost. (b) Capacitance relative to fully wetted soil of tillers of barley plants growing in the field. 97

Figure 4-5. (a) Capacitance of 35 barley plants growing in compost as the water table was increased. (b) Relationship between capacitance and the area of tissue in the stem cross-section of 20 barley plants measured with the water table at the compost surface. (c) Relationship between the shoot capacitances of 43 barley plants measured before and after their excision..... 98

Figure 4-6. (a) Illustration showing the position of insertion of electrodes in tillers of neighbouring barley plants and in soil. (b) Capacitance measured between two electrodes in the soil, electrodes inserted at the base and at a height of 1 cm in an individual tiller 99

Figure 4-7. Relationship between the measured capacitance and the capacitance predicted for the combination of tillers described in Figure 4-6..... 100

5

Figure 5-1. Cutting potato tuber cores with (a) even and (b) stepped cross-section. 105

Figure 5-2. (a) Scheme of a longitudinal section through a potato tuber. (b) Annotated drawing of a transverse section through a tuber. 107

Figure 5-3. Measuring capacitance of whole potato tubers in tap water.....	107
Figure 5-4. Measuring the capacitance with electrodes of the same and of different type.....	108
Figure 5-5. Potato core submersion experiments analogous to the barley roots and root systems in nutrient solution (Fig. 3-3) the core and capacitance measured.	109
Figure 5-6. Simulating field barley experiments (Fig. 4-6) with two potato tuber cores.....	110
Figure 5-7. (a) Scheme of the electrical breadboard, (b) an exemplary RC circuit, and (c) schematic illustration of this RC circuit on the breadboard.	113
Figure 5-8. (a) Relationship between the capacitance (C , nF) and electrode separation (d , cm) of nine potato tuber cores of bore-size 2, 3, and 4 (Table 5-1). (b, c) Relationship between C per cross-sectional area and (b) d and (c) the reciprocal of d	116
Figure 5-9. Hypothesised electrical fields in plant tissue.....	117
Figure 5-10. (a) Relationship of capacitance (C) and electrode separation (d) for 10 cores of potato tuber cores of various diameters. (b) Relationship between C per cross-sectional area and the reciprocal of d for the same cores. (c) Relationship between C per circumference and the reciprocal of d for the same cores.	118
Figure 5-11. Relationship of capacitance and (a) cross-sectional and (b) circumference for surface-dried potato cores of different diameter.	120
Figure 5-12. (a) Capacitance normalized by the cross-sectional area and measured with pairs of blade-electrodes, needle-electrodes, and strip-electrodes and combinations of two different electrodes of 12 potato tuber cores.....	121
Figure 5-13. (a,c) Relationship of the capacitance of partly submerged potato tuber cores and core mass in water and (b,d) the core cross-sectional area at the water surface..	122
Figure 5-14. Relationship between the capacitance of potato tuber cores and (a) the distance between plant electrode and water surface (D), (b) the tissue mass in water, and (c) the reciprocal of D	124
Figure 5-15. Relationship between (a) capacitance (C) and the distance between water surface and plant electrode (d , cm) and (b) between C and reciprocal of cumulative d per cross-sectional area.....	126
Figure 5-16. The relationship between (a) capacitance and (b) the cross-sectional area of four potato tuber cores that were incrementally raised out of water and position of the water surface on the cores.	127
Figure 5-17. Relationship between the capacitance of four potato cores with stepped circumference measured in air and (a) electrode separation and (b) capacitance measured in water. Relationship between the capacitance of four different cores	

- with stepped circumference measured in air and (c) electrode position along the core and (d) capacitance measured in water..... 129
- Figure 5-18.** (a) Capacitances of the components in Figure 5-6d. (b) Relationship between the total capacitance and the reciprocal of cumulative reciprocals of the component-capacitances..... 131
- Figure 5-19.** (a) Breadboard scheme and (b) RC circuit for the successive removal of capacitors from a set of capacitors connected in parallel. Relationship between capacitance and the number of capacitors for a set of (c) equally and (d) unequally large capacitors..... 133
- Figure 5-20.** (a) Breadboard scheme and (b) RC circuit for the successive adding of capacitors to a series. Relationship between capacitance (nF) and the number of capacitors for (c) equally and (d) unequally large capacitors. (e) Relationship between capacitance measured and predicted following Eqn 13..... 135
- Figure 5-21.** (a) Breadboard scheme and (b) RC circuit for the successive measurement of capacitors in a series. (c) Relationship between capacitance and the capacitor positions (P) in the series..... 137
- Figure 5-22.** The capacitance of a capacitor and a resistor connected in series normalized by the capacitance of the capacitor plotted against the resistance of the resistor..... 139

ABBREVIATIONS

A_c	Cross-sectional area (mm^2)
Φ	Circumference (mm)
C	Capacitance ¹ is the ability of a capacitive body to store electrical charge. The SI unit is farad (F). One F is the amount of capacitance when one coulomb (C) of charge is stored with one volt (V) applied to a capacitive body.
Q	Charge ¹ is an electrical property of matter that exists because of an excess or deficiency of electrodes. It can be either positive or negative. The SI unit is coulomb (C). One coulomb is the charge possessed by 6.25×10^{18} electrons.
V	Voltage ¹ is the amount of energy or work per unit charge to move electrons from one point to another. The SI unit is volt (V). One volt is the potential difference between two points when one joule (J) of energy is used to move one coulomb (C) of charge is moved from one point to the other.
X_c	Capacitive reactance ¹ is the opposition of a capacitor to sinusoidal current and is expressed in Ohms (Ω).
Z	Impedance ¹ is the total opposition to sinusoidal current in an RC circuit. It is the sum of resistance (R) set up by resistors and capacitive reactance (X_r) set up by capacitors and is expressed in Ohms (Ω).

¹ Definitions for physical phenomena from Floyd (2010)

ACKNOWLEDGEMENT

Ralf Christian Dietrich was funded by a University of Dundee / James Hutton Institute PhD studentship. The James Hutton Institute receives funding from the Scottish Government Rural and Environment Science and Analytical Services Division (RESAS).

I would like to thank my late wife Manuela Franzelli-Dietrich for her support and patience, and my mum for all her support. Thanks to all the friends and fellows at the James Hutton Institute who helped me get through difficult experiments and moments. My special thanks go to Lyn Jones for his support and motivation, Glyn Bengough for keeping me on track and Philip White for sharing his philosophy of science with me. Their guidance, support and motivation have been invaluable.

LIST OF ILLUSTRATIONS

Capacitance measurement on a barley root system in hydroponic solution	41
Capacitance with two plant electrodes on an unbranched barley nodal root	65
Barley plants in a sand-mix column in the greenhouse	86
Capacitance measurement on cores cut from potato tubers	102
Barley plant removed from hydroponic solution at harvest	141

DECLARATION

The author of this thesis declares that, unless stated otherwise, all references have been consulted by the author; that the work of which the thesis is a record has been done by the author; and that it has not been previously accepted for a higher degree.

Ralf Christian Dietrich, Dundee, 25th January 2013

ABSTRACT

Many authors have reported linear correlations between electrical capacitance, measured between an electrode inserted at the base of a plant and an electrode in the rooting substrate, and root mass. The measured capacitance is conventionally interpreted using the electrical model of F.N. Dalton in which roots are regarded as cylindrical capacitors wired in parallel. This model was tested for barley (*Hordeum vulgare*) grown hydroponically using treatments that included: raising roots out of solution, and cutting roots at positions below the solution surface. Although good linear correlations were found between capacitance and mass for whole root systems, when roots were raised out of solution, capacitances were non-linearly related to submerged root mass. Excision of roots in the solution had negligible effect on measured capacitance. The latter observations conflict with Dalton's model. Capacitance correlated linearly with the cross-sectional area of root tissue at the solution surface, and inversely with distance between plant electrode and solution surface. A new model for capacitance was proposed and tested with cereal plants growing in solid substrates. Capacitances of plants in various substrates were measured under contrasting water regimes. Substrate capacitances increased with increasing water content. At water contents approaching field capacity, substrate capacitances were at least an order of magnitude greater than those of plant tissues. Wetting the substrate locally around a plant stem base was both necessary and sufficient to record maximum capacitance, which was correlated with stem cross-sectional area. Capacitance measured between two electrodes could be modelled as an electrical circuit in which component capacitors (plant tissue/ substrate) are wired in series, with capacitances of components connected to the same electrode acting in parallel. All results were consistent with the new model. Whilst the measured capacitance can, in some circumstances, be correlated with root mass, it is not a direct assay of root mass.

1 INTRODUCTION

The world population will grow by a third at least in the next 40 years (United Nations, 2010). Arable land, however, is limited. More than forty percent of Earth's land surface is currently used as cropland or pasture (Monfreda *et al.*, 2007). In the last decades agricultural land expansion was achieved mainly by deforestation of tropical forests (Gibbs *et al.*, 2010) and driven by population growth and an increasing global demand for food (e.g. DeFries *et al.*, 2010; Geist and Lambin, 2001). Newly cleared land however shows a net-release of carbon dioxide (West *et al.*, 2010), promoting climate change. The changing climate, in turn, threatens the existing arable land (e.g. Dasgupta *et al.*, 2009; Rahmstorf and Ganopolski, 1999). Therefore, it is crucial for researchers, breeders and farmers to have of a quick method for identifying crops and cultivars that grow optimally under given or changing conditions in regard to variables such as yield, biomass and stress tolerance. Field-based phenomics include a wide range of parameters (Table 1-1) to determine biomass, growth, water-relations and vigour of crop-plants. Many phenomics-techniques work with electro-magnetic waves. This often restricts their application to the aboveground parts of a plant. The belowground part, however, the root system, is crucial for plant growth, because it facilitates the uptake of water and nutrients and its transport to the places of photosynthesis and thus growth.

The major obstruction to root research is the inaccessibility of the organs. Root excavation and visual scoring is time- and labour-intensive so that often only a small selection of representative plants is investigated (e.g. Trachsel *et al.*, 2011). Therefore and because of the implied destruction of the plant, excavation appears rather unsuitable for growth studies. Thus, a lot of work was invested in developing non- or minimally-invasive techniques for monitoring root growth in the substrate in recent years.

The technique, which is object of the thesis, is the electrical capacitance measurement on plants in the ground. The equipment required is, in contrast to most other methods, cheap and simple to apply in both field and laboratory. Although capacitance has been used as a non-destructive measure of root system size for > 30 years and often good linear correlations have been reported between capacitance and root mass (Table 1-2), the underlying electrical pathways are still unknown. A model by F. N. Dalton (1995), predicting a linear relationship between these two variables, has become accepted widely. The aim of this thesis was to investigate the applicability of capacitance measurement for the estimation of plant root mass.

This chapter provides an overview of non-invasive measurement techniques of root research.

The first section 1.1 describes different methods and discusses their limitations, each in a short section. The capacitance measurement on plants is discussed in more detail in the second section 1.2. The third section 1.3 provides the basic theory of electrical capacitance while section 1.4 outlines the aims of the thesis.

Table 1-1. Examples of measurement methods that show promise for field-based phenomics, taken from White *et al.* (2012).**Key:** IR = Infrared; NIR = near infrared

Trait class	Target trait	Index or method	Applications or relevant traits	Point (P) or image-based (I)	Wavelengths
Pigment constituents	Chlorophyll	Normalized difference vegetation index (NDVI) Canopy chlorophyll content index (CCCI)		P	Red, NIR 720 and 790 nm
	Carotenoids	Green atmospherically resistant vegetation index (GARI)	Chlorophyll concentration, rate of photosynthesis	P/I	550 and 860 nm
Non-pigment constituents	Cellulose	Cellulose absorption index (CAI)	Bioenergy potential	P	2100 nm
	Nitrogen	NDVI & CCCI	Plant nitrogen status	P	670, 720, 790 nm
	Lignin	Cellulose absorption bands	Stress response; bioenergy potential	P	
Photosynthesis	Photosystem II activity	Photochemical reflectance index (PRI)	Diurnal radiation use efficiency	P	531 and 570 nm
	Photosystem II activity	Chlorophyll fluorescence	Stress effects on photosynthesis	P/I	
Water relations	Transpiration or canopy conductance	Canopy temperature (CT) Crop water stress index (CWSI)	Instantaneous transpiration and hence crop water status.	P/I	Thermal IR
	Canopy water content	Normalized difference water index (NDWI)	Crop water status	P	860 and 1240 nm
	Water content	Leaf water thickness (LWT)		P	1300 and 1450 nm; 1500 - 1700 nm
Plant growth	Leaf area index	NDVI	Overall growth	P	Red, NIR
	Plant biomass	NDVI	Overall growth	P	590 and 880 nm; 670 and 770 nm
		NWI	Overall growth	P	850, 880, 920 and 970 nm
Plant architecture	Canopy height	Close-range photogrammetry	Light interception, overall growth, lodging resistance	I	Visible or NIR
		Ultrasonic	Canopy height and width	P	(Ultrasonic)
		Depth camera	Canopy height and width; leaf orientation and size	I	Infrared
Phenology	Maturity	Time series of index	Tracking leaf senescence	I	400 - 900 nm
		Time series of fluorescence	Anthocyanin levels	P	Visible
	Flower number	Image analysis	Plant development	I	Visible
	Multiple stages	Analysis of time series of indices	Seedling emergence, senescence	P+I	400 - 900 nm

Table 1-2. Details of studies (plant species, growth medium, and electrical frequency at which capacitance was determined) and parameters obtained for linear relationships between capacitance and root system size.

Notes

* final harvest date only (several previous harvest dates gave poorer correlations, possibly a result of dry soil)

** capacitance was measured first with several, and second with only one, electrode in soil

*** capacitance was measured with one electrode in soil at 5, 10 or 15 cm from the plant

**** combined data from 8 genotypes in vermiculite, 6 in field

Key: FM: Fresh Mass, DM: Dry Mass, RL: Root Length, SA: Surface Area, n = number of replicates

Publication	Plant species	Growth medium	Frequency (kHz)	R ² values				n
				FM	DM	RL	SA	
Chloupek (1972)	<i>Zea mays</i>	Sand (container)	0.8	0.736	0.728	0.731	0.663	24
	<i>Allium cepa</i>	Sand (container)	1	0.566	0.545	nd	0.529	14
	<i>Helianthus annuus</i>	Sand (container)	5	0.916	0.897	0.92	nd	15
	<i>Avena sativa</i>	Clay soil (container)	5	0.566	0.464	nd	nd	15
	<i>Helianthus annuus</i>	Clay soil (container)	5	0.692	0.432	nd	nd	10
	<i>Brassica napus</i>	Not specified		0.081	nd	nd	nd	18
Chloupek (1977)	<i>Daucus carota</i>	loam soil (field)	1	0.514				113
	<i>Helianthus annuus</i> (**)	Sand	1	0.549, 0.554				15
	<i>Helianthus annuus</i> (***)	Sand	1	0.523, 0.543, 0.566				15
Kendall <i>et al.</i> (1982)	<i>Trifolium pratense</i>	Solution	1		0.672			21
	<i>Medicago sativa</i>	Silt loam soil (field*)	1		0.436			20
Dalton (1995)	<i>Solanum lycopersicum</i>	Solution	1		0.877			12
van Beem <i>et al.</i> (1998)	<i>Zea mays</i> (****) 35 d	Vermiculite	1	0.85				32
	<i>Zea mays</i> (****) 70 d	Vermiculite	1	0.27				32
	<i>Zea mays</i> (****) 56 d	Loam soil (field)	1	0.41, 0.53				36
Ozier-Lafontaine & Bajazet (2005)	<i>Amaranthus tricolor</i>	Solution	1	0.937				5
	<i>Solanum lycopersicum</i>	Solution	1		0.987			11
	<i>Solanum lycopersicum</i>	Clay loam soil (container)	1		0.829			15

Preston <i>et al.</i> (2004)	<i>Populus deltoides</i> × <i>Populus nigra</i>	Potting compost (container)	1	0.866	0.895	33
Rajkai <i>et al.</i> (2005)	<i>Helianthus annuus</i>	Sandy soil (container)	1	0.832 (needle), 0.921 (clamp)		12
McBride <i>et al.</i> (2008)	<i>Zea mays</i> (Expt 1, 4 genotypes)	Turface®, granular medium (container)	1		0.779, 0.647, 0.823, 0.364	30, 30, 30, 30
	<i>Zea mays</i> (Expt 2, 4 genotypes)	Turface®	1		0.761, 0.846, 0.646, 0.726	30, 30, 30, 30
Bengough <i>et al.</i> (2009)	<i>Triticum aestivum</i> (35 genotypes)	Gravel–sand mix (containers)	1		0.753	67
Tsukahara <i>et al.</i> (2009)	<i>Prunus persica</i>	Soil (field)	1	0.897	0.896	27
	<i>Pyrus pyrifolia</i> (on <i>Pyrus</i> <i>betulaefolia</i> rootstock)	Soil (container)	1		0.806	18
Pitre <i>et al.</i> (2010)	<i>Salix viminalis</i> × <i>Salix schwerinii</i>	Soil (pots), sandy soil (field)	1		0.81, 0.49	16, 8
Chloupek <i>et al.</i> (2010)	<i>Daucus carota</i>	Soil (field)	1	0.525		92

1.1 Non-invasive measurement techniques with the focus on soil and root research

This sub-chapter introduces different technical approaches for non-invasive root phenomics.

First, techniques using electromagnetic radiation are presented, then techniques using electrical current. Each section drafts the mechanistic basis of the approach and discusses its potentials and limitations.

Non-invasive measurement techniques are essential for the research of root characteristics and function. Roots in soil elude tactile or optical screening approaches. The removal of the soil shield grants access to roots, but also affects root development. Root characteristics, such as architecture, morphology, physiology, and development are adapted to the rooting medium to perform the primary root functions, anchorage and resource acquisition (Waisel *et al.*, 2002). Removed from their medium, roots start to adapt so that observations cannot be related to soil conditions any more. Therefore, techniques that work beyond the visible spectrum of light are crucial for root phenomics.

1.1.1 Techniques for root measurement that use electromagnetic radiation

This chapter drafts the theory of electromagnetic waves and introduces in five sections the major root measurement techniques that are based on electromagnetic wave transmission.

An electromagnetic wave is defined as energy transmission in form of oscillating electrostatic and magnetic fields (Woodward and Sheehy, 1993). The wave form is a result of pulses, caused by electron relaxation at the source. When transmitted electromagnetic waves hit an object and interact with its nuclei or electrons they become absorbed or get scattered. Thus, the degrees of ray attenuation and characteristics of ray scattering provide information about the nature of the

object, e.g. its position, density and element composition. The radiating² character of electromagnetic waves allows their usage as screening device in three or even four dimensions. Since CCD³ cameras extend the imaging capabilities far beyond the visible light spectrum to very high frequencies (e.g. X-ray), they can be used to image roots in soil (Vandenhirtz *et al.*, 2010). On the other side of the visible light spectrum, radar waves are used to map and quantify roots in soil. The techniques that are suitable for root research use rays with frequencies ranging from GHz (radar) to pHz (x-ray). Rays of higher frequency struggle to penetrate the bulk soil (Section *Using X-rays*) while rays of lower frequency do not offer sufficient resolution. Thus, seismic wave measurements are only found for niche applications, e.g. for the detection of decaying wood in tree trunks (al Hagrey, 2007).

Measuring with visible light

Window-based rhizotrons and minirhizotrons may influence the root growth that they are supposed to observe (e.g. due to gaps adjacent to the rhizotron window). Conversely, steamed windows cause underestimations. These problems were addressed by double-walled windows which put a constant pressure on the outer wall to tighten the gap and increase the visibility (Merrill *et al.*, 2005). Two-D-light transmission imaging (Garrigues *et al.*, 2006) uses visible light, too, the root systems growing within a thin layer of sand. However, the method is restricted to specific sands and provides insufficient resolution for detailed root phenotyping.

Using electromagnetic fields

The nuclear magnetic resonance technique (NMR) visualizes the response pattern of atomic nuclei within a magnetic field to an electromagnetic pulse. The atom nuclei of some elements bear a spin and are weakly sheltered by an electron shell, e.g. ¹H or ¹³C. Spinning nuclei generate a small magnetic field that possesses a magnetic moment. The application of a strong

² Radiation is the term for energy transmission with uniform velocity in straight lines in all directions.

³ CCD; charge-coupled device. Such devices translate electromagnetic waves into electrical signals

electromagnetic field forces all nuclei to align in the field. The magnetic moment of the target nuclei ^1H and ^{13}C , however, is too weak to align and they become excited. When a perpendicular electromagnetic pulse disrupts the applied field, relaxation occurs and the target nuclei emit energy in the form of heat and resonance radiation at characteristic frequencies. Thus, the target nuclei are locatable within a sample, such that internal structures of biological samples can be visualized with high spatial resolution using magnet resonance imaging (MRI). The technique can be used for monitoring fluxes of carbon and water in root systems (Bottomley *et al.*, 1986; Schulze-Till *et al.*, 2009; Jahnke *et al.*, 2009). MRI-resolution can be used on whole plants (Van As, 2007; Van As *et al.*, 2009). MRI is well suited for visualizing cylindrical plant organs, i.e. carrot roots (*Daucus carota* L.), radish (*Raphanus sativus* L.), sugar beet (*Beta vulgaris* L.), seeds (*Pinus moticola* Dougl. ex D. Don), sweet potato tuber (*Ipomoea batatas* L.) and tree trunks (Jahnke *et al.*, 2009; Van As *et al.*, 2009; Iwaya-Inoue *et al.*, 2004; Terskikh *et al.*, 2005; Homan *et al.*, 2007). Though portable NMR apparatus⁴ are available, they are less suitable for measuring below-ground parts of plants, because the device is designed as a cuff (Windt *et al.*, 2011) and applications on roots would require root excavation (Blümli, 2007).

Using X-rays

X-ray computed tomography (CT) is based on the attenuation of X-rays. The rays interact with the electron shell of a sample so that ray attenuation becomes a function of material density. The density patterns of soil are complex due to a mixture of water, air and solids. Thus, X-ray CT provides detailed information on the soil structure and allows the discrimination of textural layers and the detection of cracks and voids in soil (Moradi *et al.*, 2009; Elliot and Heck, 2007). Conversely, the high density of soil limits the size of the sample and the resolution. Two-dimensional CT images can be thought of as slices, because they correspond to what would be seen, if a sample were sliced along the scan plane (Ketcham and Carlson, 2001). The slices

⁴ Information available at <http://www.portable-nmr.eu>

represent a certain thickness of the object that depends on the settings and resolution of the scanner, with volume elements of CT slices are called voxels (volumetric picture elements). The size of the voxels, and thus the resolution, depends on various factors including the electron density within the slice (Perret *et al.*, 2007). Ketcham (2011) estimated that CT resolution is limited to 1000–2000-times the object cross-section diameter. A further factor limiting the sample size is the field of view. Haberthür *et al.* (2010) used micro X-ray setup with a field view of 1.52×1.52 mm. They doubled the field view by 360° sample-rotation and further increased it by interpolating sub-scans and could visualize a rat lung of 4.1 mm diameter with a voxel size of $1.46 \mu\text{m}$.

X-ray CT has been used to visualise samples of roots in soil. Gregory *et al.* (2009) scanned containers of 2.5 cm diameter (Fig. 1-1) with a voxel size of $15 \mu\text{m}$. With increasing sample size and thus voxel size the detection of fine roots suffers. Gregory *et al.* (2003) detected roots of 0.48 mm diameter. Both Gregory *et al.* (2003) and Perret *et al.* (2007) reported that root length was underestimated.

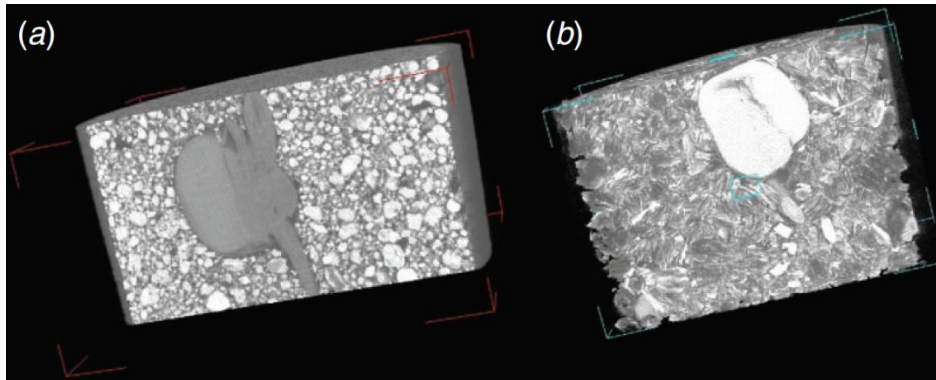


Figure 1-1. 3D images of pre-germinated maize seeds grown for 48 h in (a) soil (sieved to <2 mm) and (b) vermiculite, taken from Gregory *et al.* (2009). The images were obtained by scanning at 145 kV and 201 mA with the X-Tek HMX CT scanner.

Blurring is a further problem of X-ray CT and occurs at the boundary of root and soil (Fig. 1-2 top). Boundary blurring is caused by variable X-ray attenuations, due the mixture of air, root and water (Gregory *et al.*, 2003) and depends on soil characteristics. Gregory *et al.* (2009)

observed less blurring in sand than in soil, due to the higher attenuation contrast for roots in sand. By image processing, the boundaries between roots and soil can be reconstructed. Air-related voxels are “peeled” from sub-voxels leaving a “skeleton” that represented the root tissue (Lontoc-Roy *et al.*, 2006) (Fig. 1-2).

Although X-ray CT is recommended as technique for studying root architecture and growth dynamics, (Lontoc-Roy *et al.*, 2006; Tracy *et al.*, 2011; e.g. Hargreaves *et al.*, 2009), it has several shortcomings: X-ray CT poses a ionizing radiation hazard and is therefore restricted to laboratory studies; the setup-costs are in a five-digit range (Gregory *et al.*, 2003); and measurement is relatively slow. Hundreds of slices are required for one 3D image each requiring about one hour of scanning (Gregory *et al.*, 2003). Recent improvements drastically shorten the scanning time, but can sometimes image artefacts (Gregory *et al.*, 2009).

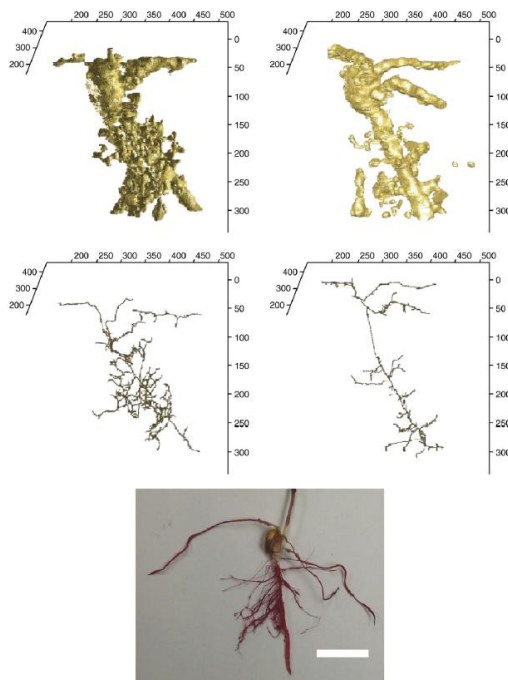


Figure 1-2. MRI images (top) and photo (bottom) of a maize root system, taken from Lontoc-Roy *et al.* (2006): Isolated root systems (top) and the corresponding skeletons (middle) of a maize seedling CT scanned in homogeneous sand in dry (left) and water-saturated (right) conditions, as compared to a digital photograph of the real root system (bottom), once removed from the soil, washed and coloured with red ink (Bar=2 cm). Scales were not defined, but appear to show the voxel number.

Using neutron transmission to investigate roots

In contrast to X-rays, neutrons attenuate by interactions with the unsheltered protons of the sample. Thus, neutron radiography visualizes the ^1H -rich sample components, e.g. roots in soil (Fig. 1-3). Neutron attenuation, as a function of time and water content, allows estimation of water fluxes (Oswald *et al.*, 2008). Neutron radiography has been used to detect fine roots even in large samples (root diameter ≥ 0.2 mm) (Moradi *et al.*, 2009). The limitations of NR for root research occur at extreme soil water contents. Wet soil causes a high attenuation, whilst dry soil reduces the root–soil contrast, due to root dehydration (Moradi *et al.*, 2009). Another major shortcoming of the technique is the few laboratories that can conduct neutron imaging (Moradi *et al.*, 2009).

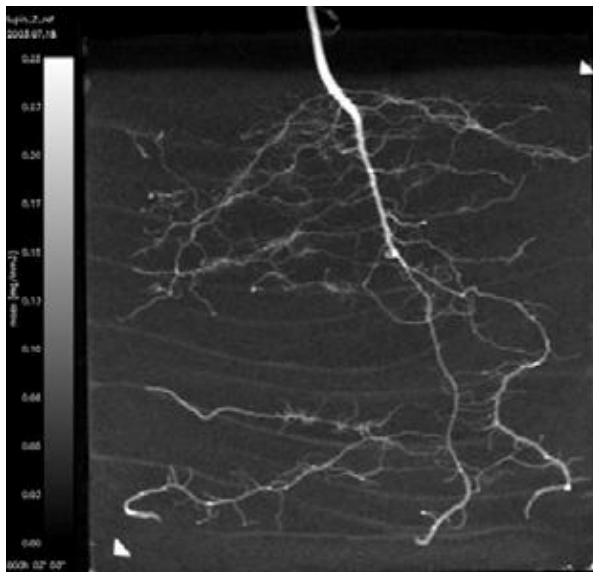


Figure 1-3. Neutron radiography image of a root system of *Lupinus L* in relatively dry sand, taken from Oswald *et al.* (2008): grey values represent water content calibrated as volume fraction of the sand porous medium, with the grey scale ranging from 0 to 25% water content. Values above 25% are shown in white to allow better visibility of the roots.

Using radar to investigate roots

The techniques discussed so far are feasible in the laboratory. In field studies, however, ground-penetrating radar has the advantage that the technique uses electromagnetic waves. Radar requires no screen to detect wave attenuation that is caused by wave scattering. In contrast, the radar captures scattered waves that provide information about the nature of materials in the ground, e.g. the soil moisture content (Vereecken *et al.*, 2008). A transmitter antenna pulses an electromagnetic wave into the ground (e.g. Vendl, 2009). At boundaries of materials with different permittivity, waves are partly scattered. The waves reflected back to the surface are detected with receiving antennas. The key factor is the time between wave pulse and capture, because the velocity of the waves depends on the electrical permittivity of a material. The wave-velocity is proportional to the inverse square root of the sample permittivity (Daniels, 2000), while the strength of the reflection depends on the difference in material permittivity at the boundary (Hirano *et al.*, 2009). Thus, ground penetrating radar can determine the position and size of materials in the ground that differ in their electrical permittivity. Radar waves have lower frequencies than visible light (0.01 GHz to 1 GHz), enabling them to travel deep into soil. This advantage, however, is greatly compensated by the low resolution that is immanent to low frequencies. For applications that require less depth (< 80 cm) and high spatial resolution, researchers use radars with working frequencies of 1.5 GHz to 2 GHz (e.g. al Hagrey, 2004; Cui *et al.*, 2011).

The root mapping with GPR uses differences in permittivity between roots and soil. The relative permittivity⁵ (relative dielectric constant) of water is approximately 80, while that of the other soil components varies between 1 (air) and 7 (solids) (Ley *et al.*, 1994; Wu *et al.*, 2011). Thus, GPR can detect water-rich roots in dry soil (e.g. Butnor *et al.*, 2001; Zenone *et al.*, 2007). Both groups found drained sandy soil an optimal condition for the radar-based root detection. Root detection in clayish and loamy soil, however, suffered from low permittivity contrasts.

⁵ the permittivity of a material related to the permittivity of free space (dimensionless)

Another factor affecting the quality of root detection was noise, caused by gravel, pebbles and rough terrain.

Cui *et al.* (2011) found a resolution limit for the detection of fine roots at 5 mm root diameter. Although the group was satisfied with their root mass estimation per radar, they saw a general problem of this application in the discrimination of overlapping and clustering of roots. Hirano *et al.* (2009) addressed this problem by burying root pieces at different intervals in sandy soil and also compared buried root pieces with different water contents. The discrimination limits were root piece intervals of 20 cm, a root water content of 20%, a root depth of 80 cm, and a root diameter of 19 mm. The researchers worked with 0.9 GHz in contrast to Cui *et al.* (2011), who achieved a considerably better resolution with their 2 GHz radar. A shortcoming of the ground penetrating radar technique is that setup costs are > £ 10k (Vendl, 2009).

1.1.2 Measuring with electricity

This section introduces different techniques of measuring the electrical properties of natural systems including living systems. All methods are based on the application of electrical current and the comparison between the input and the output current. The (proposed) mechanistic basis is drafted for each approach and the proposed application discussed. The capacitance measurement on plants will be introduced and discussed separately in Section 1.2.

Electrical measurements are generally cheaper than techniques basing on electromagnetic wave measurement (*S. Techniques for root measurement that use electromagnetic radiation*). They are usually easy to apply in both laboratory and field studies. Commonly two to four electrodes apply electrical current and receive the output (many electrodes and more complex apparatus are required for 2D- and 3D-tomography). A meter measures then capacitance and either, resistivity or conductance. Spatial differences between input and output current allow the imaging of internal structures, while temporal changes allow monitoring processes.

Water is a key factor for electrical measurements in natural systems

The measurement of electrical characteristics in samples requires an electrical pathway between the electrodes used. In natural systems, water provides an electrical pathway and generates electrical capacitance and impedance. Its dielectric constant (78–80, at 1kHz) is relatively high. Thus, water distribution affects electrical measurements in biological and geological studies.

Applications of electrical capacitance measurement (ECM) in soil and plant systems

This section introduces some established applications of capacitance measurements in soil and plant systems. Similar to ground penetrating radar, capacitance measurement provides information about a sample's permittivity. The permittivity of soil is considered as a function of the volumetric soil water content (θ), because the permittivity of dry soil is relatively small. Soil-capacitance probes (e.g. θ -probes) are routinely used for measurement of soil water content (Robinson *et al.*, 2005). Theta-probes are accurate to $\pm 1 \text{ cm}^3 \text{ cm}^{-3}$ although may overestimate the soil water content in certain soils (Robinson *et al.*, 1999; Robinson *et al.*, 1998). Robinson *et al.* (2005) assumed that probes fail to identify the real soil permittivity, because θ -estimation neglects the ionic soil conductivity particularly important in sodic soil. The workers proposed a circuit model that corrected θ -estimation in sandy soils better than in clayey soil. Robinson *et al.* (2005) suggested that the reason for this was an underestimation of bulk soil electrical conductivity. Kitzito *et al.* (2008) questioned soil-specific calibration and hypothesized that the sensitivity of capacitance measurement to (a) soil conductivity, (b) soil texture and (c) soil temperature may be overcome by using higher measurement frequencies. In fact, they proposed a single calibration curve that was independent of these factors. Wu *et al.* (2011) favoured lower measurement-frequencies, but their correction model became inaccurate at extreme soil water contents. Celinski and Zimback (2010)⁶ used the C-sensitivity to soil texture and salinity for the prediction of clay and sand content. They found good correlations for capacitance with chemical attributes, such as soil pH and cation exchange capacity.

⁶ Content was taken from the abstract only, because the paper text was in Portuguese.

ECM has also been used for the estimation of water content in wood pellets and tea leaves (Fuchs *et al.*, 2008; Mizukami *et al.*, 2006).

In forestry research, capacitance measurement was tested for detecting different gradients of wood decay in tree trunks and was found to be a function of the water content of wood (Tattar *et al.*, 1974). Lekas *et al.* (1990) inserted two electrodes, one above the other, in the trunks of different tree species and observed a seasonal pattern in their capacitance readings that were species- and site-specific. Capacitance increased in spring and decreased in autumn following an increased root uptake activity with a large and rapid increase measured after heavy rainfall following a longer dry period. The researchers found good correlations between capacitance and diameter of breast height (dbh) and observed capacitance sensitivity to stem temperature. Lekas *et al.* (1990) concluded that ECM is capable of measuring cambial growth and sap flow though suggested avoiding electrode insertion at sun-exposed places. Qu, Wang and Liang (2005) reviewed results in forestry studies that were obtained with ECM and suggested tree capacitance as index for growth rate, for foliar biomass, for dbh, and as hazard system for environmental stress.

Other scientists used ECM for the determination of fruit size (Kato, 1997) and for monitoring biofilm thickness (Maurício *et al.*, 2006). MacCuspie *et al.* (2008) tested the method for the discrimination between viruses in infected tissue. In medicinal research, ECM was tried for investigation of skin water barrier functions (e.g. Boyce *et al.*, 1996; Wickett *et al.*, 1993); for monitoring oedema evolution after inflammation (Yamada *et al.*, 2004); and for differentiation between carcinoma and normal parenchyma (b; Inagaki *et al.*, 2004b).

Applications of electrical capacitance measurement on cells

Commonly the dielectric character of the plasma membrane bilayer is considered as source of plant capacitance, e.g. Dalton (1995). In regard to findings of cell capacitance measurements,

this is clearly a simplification. Early findings suggested that the electrical capacitance of a cell depends on more factors than just the geometrical properties of the plasmalemma. A lot of this work was done on green algae for two reasons: Small single celled algae (e.g. *Chlorella*) allow measurement of their capacitance in a suspension which makes it comparable with the capacitance of plant organelles (Hope, 1955). Furthermore, giant green algal cells (e.g. *Acetabularia*) ease the insertion of micro electrodes into the cytoplasm, e.g. for voltage-clamping experiments (Tittor *et al.*, 1983; Beilby and Beilby, 1983).

Hope (1955) filled the gap of a plate capacitor with suspensions of mitochondria, chloroplasts and *Chlorella* sp.. cells and measured their capacitance (AC at 1 Hz to 4 kHz frequency). For all suspensions he observed an increase of capacitance up to 5Hz followed by a continuous decrease with increasing frequency, suggested to be due to “leakage” of electrolytes. The mean capacitance at 1 Hz frequency increased in the order *Chlorella* ($1.0 \pm 0.4 \text{ F m}^{-2}$), chloroplast ($1.6 \pm 0.0 \text{ F m}^{-2}$), mitochondria ($2.8 \pm 1.2 \text{ F m}^{-2}$). The author assumes that such differences would be due to differences in the membrane structure, i.e. variations in thickness and other factors influencing the dielectric constant.

For voltage clamping two micro-electrodes are inserted into a giant algae cell and a third electrode is connected with the surrounding medium. One of the inserted electrodes conducts the current into the cell, while the other electrodes either measure the resting potential across the plasmalemma (approx. -170 mV) or adjust the potential to a desired value between 0 mV and -400 mV. Within this range a superimposed sine wave is able to excite a cell. Variations in the relaxation time after an excitation allow conclusions on the nature of the capacitance.

Beilby and Beilby (1983) measured the capacitance of *Chara corallina* cells at different frequencies. The relaxation time at low frequencies (1 – 10 Hz) was relatively long and attributed by the authors to transport effects of ions through the plasmalemma, because such effects are relatively slow. Measurements at higher frequencies, however, showed the dielectric characteristics of the membrane only. The authors measured a resting potential capacitance of 0.22 F m^{-2} . Capacitance varied between 0.1 and 1.0 F m^{-2} for other potentials. Beilby and Beilby (1983) suspected that this was caused by variations in the acid and alkaline conditions at the cell surface. They also observed that capacitance lagged the excitation (and thus conductance) and assumed that the cause were excitation-induced changes of the interfacial ion concentrations of Cl^- , Ca^{2+} and K^+ . Thereby, the authors widened the scope of plant cell capacitance by the aspect of bi- and interfacial ion concentrations and membrane permeability.

Tittor *et al.* (1983) used voltage-clamping over a wider range of frequencies (1Hz to 10kHz) for *Acetabularia* to test the hypothesis that cells of the marine ulvophyean green alga *Acetabularia*

would provide a five-times higher capacitance, than “nearly all biological membranes” (0.01 Fm^{-2}), because of a very high density of electrogenic Cl^- binding enzymes (pumps) within the plasmalemma. Unfortunately, the authors provide no reference for their value which is by one order of magnitude lower at least than the capacitance Hope (1955) or Beilby and Beilby (1983) found in their experiments using internodal cells of the freshwater charophycean green alga *Chara corallina*. Tittor *et al.* (1983) proposed a modified Hodgkin–Huxley model (Hodgkin and Huxley, 1952) that differs from the original by disclaiming significant capacitive effects by passive ion flow through either ion channels or ATP-binding transport proteins in the plasmalemma. Using equations based on their hypothesis Tittor *et al.* (1983) calculated two capacitances from a measured impedance value. As a function of the surface area of the plasmalemma, one value was said to represent the bilayer capacitance while the other value represented the number of Cl^- -pumps. The mean of calculated “membrane capacitances” measured for eight potentials ($0.009 \text{ Fm}^{-2} \pm 0.004 \text{ Fm}^{-2}$, $n=35$) was found to be significantly lower than the calculated “pump capacitance” ($0.033 \text{ Fm}^{-2} \pm 0.019 \text{ Fm}^{-2}$, $n=35$) although Tittor *et al.* (1983) observed, like Beilby and Beilby (1983), high variations and no trend over the range of applied voltages (-70 mV to -240 mV). From their pump capacitance the authors estimated a pump density of 50 nmol m^{-2} . However, the authors limit their interpretation to the species *Acetabularia*, because for another giant-celled ulvophycean green alga *Valonia* living under similar environmental conditions similar capacitance values were found (Zimmermann *et al.*, 1982) which could be correlated with external pH and turgor pressure. The two studies agree in that next to the bilayer capacitance charge carrier at the plasma membrane surface affect plant cell capacitance.

Zhang *et al.* (1990) also calculated plant capacitance from impedance measurements but for different plant tissues. The team tested the Hayden model (Hayden *et al.*, 1969) which proposes that next to plasma membrane capacitance there would be two resistances, one for the symplasmic and one for the apoplasmic current pathway. The authors proposed that impedance would become apoplasmic with decreasing frequency and symplasmic with increasing frequency, and found that both symplasmic resistance and capacitance decreased with increasing frequency and concluded on the existence of a symplasmic capacitor. Zhang *et al.* (1990) suggested that the vacuole rather than other cell organelles played a major role as symplasmic capacitor, because of its large size.

Recent work on plant cell capacitance was mainly done with cell suspensions, termed dielectric measurement, as the capacitance is proportional to the dielectric constant of a sample, when spatial arrangement of the capacitor components, i.e. plates, cylinders or pin-electrodes. Measurements can be conducted *in situ* in the medium (e.g. in a bioreactor). Online monitoring

of cell concentration, biomass and growth is possible (e.g. Degouys *et al.*, 1993; Mishima *et al.*, 1991; Markx *et al.*, 1991) and allow conclusions on the physiological state of biological cells, as the capacitance values reflect the effects of cell disruption and lysis (e.g. Asami and Yamaguchi, 1999; Matanguihan *et al.*, 1994; Morita *et al.*, 1999). Cell capacitance is found by subtracting the capacitance of the suspending medium from the capacitance of the cell suspension (Degouys *et al.*, 1993; Matanguihan *et al.*, 1994). The frequency commonly ranges between 0.1 MHz and 6 MHz (Kiviharju *et al.*, 2008).

Asami and Yamaguchi (1992) measured the capacitance of cell suspensions (AC, 1kHz to a few hundred MHz) and found three changes of the dielectric constant (dielectric dispersions) for plant protoplasts. They attributed them to the surface layer and internal membranes of cells. Asami and Yamaguchi (1992) proposed a single-shell model for cells containing no intracellular organelles (e.g. erythrocytes), a double-shell model for cells with a large vacuole or nucleus (e.g. lymphocytes), and a double-shell model including vacuoles for plant protoplasts. Based on these models Asami *et al.* (1996) found capacitances of 0.62 and 0.68 F m⁻² for the plasma membrane; 0.91 and 0.95 Fm⁻² for the tonoplast; and 1 F m⁻² for organelle membranes for plant protoplasts of *Brassica campeteris* and *Tulipa gesneriana*. The values are between those found by Hope (1955) and Beilby and Beilby (1983).

Asami (1995) proposes an imaging application of dielectric measurement: This researcher set up a scanning dielectric microscope by moving a pointed electrode over a sample of biological cells in aqueous medium. A metal plate carried the sample and served as counter electrode. The best contrast was achieved at 30 kHz frequency. Asami (1995) suspected that the plasma membrane would be short-circuited and thus “electrically transparent” at higher frequencies.

Electrical capacitance tomography (ECT) for imaging differences in permittivity

Electrical capacitance tomography is a complex variation of capacitance measurement that can be used to map spatially the electrical permittivity of fluids in tubes. Capacitance tomography in two dimensions (2D) requires four to eight pairs of parallel plate electrodes arranged in a ring. Three dimensional (3D) imaging is realized either by interpolation of 2D-images (frames) from a single ring or by arranging several rings in a tube (multi-frames; (e.g. Banasiak and Soleimani, 2010; Banasiak *et al.*, 2009; Banasiak *et al.*, 2010). The 3D approach is also termed

electrical capacitance volume tomography (ECVT; (Warsito *et al.*, 2007). Recently, Soleimani *et al.* (2009) proposed a 4D algorithm for real time image computing from multi-frame ECT data. ECT has been used for the visualization of industrial processes, such as two-phase flow in pipes (e.g. Niedostatkiewicz *et al.*, 2009; Gamio *et al.*, 2005), flames in a combustion chamber (Waterfall *et al.*, 2001), ice movement in water (Jiang *et al.*, 2009) or high-shear mixing and granulation (Rimpiläinen *et al.*, 2011). There were no reports found for ECT-applications in plant research, though it is possible, e.g. for monitoring sap flow in tree trunks or water content in rooted soil. The lack of interest might be due to the availability of established techniques, such as electrical resistivity tomography.

Electrical capacitance tomography (ECT) for imaging differences in permittivity

Electrical capacitance tomography is a complex variation of capacitance measurement that can be used to map spatially the electrical permittivity of fluids in tubes. Capacitance tomography in two dimensions (2D) requires four to eight pairs of parallel plate electrodes arranged in a ring. Three dimensional (3D) imaging is realized either by interpolation of 2D-images (frames) from a single ring or by arranging several rings in a tube (multi-frames; (e.g. Banasiak and Soleimani, 2010; Banasiak *et al.*, 2009; Banasiak *et al.*, 2010). The 3D approach is also termed electrical capacitance volume tomography (ECVT; (Warsito *et al.*, 2007). Recently, Soleimani *et al.* (2009) proposed a 4D algorithm for real time image computing from multi-frame ECT data. ECT has been used for the visualization of industrial processes, such as two-phase flow in pipes (e.g. Niedostatkiewicz *et al.*, 2009; Gamio *et al.*, 2005), flames in a combustion chamber (Waterfall *et al.*, 2001), ice movement in water (Jiang *et al.*, 2009) or high-shear mixing and granulation (Rimpiläinen *et al.*, 2011). There were no reports found for ECT-applications in plant research, though it is possible, e.g. for monitoring sap flow in tree trunks or water content in rooted soil. The lack of interest might be due to the availability of established techniques, such as electrical resistivity tomography.

Measuring the electrical resistivity in natural systems

Resistivity (ρ) is the specific electrical resistance of a conductive material (Floyd, 2010).

Environmental factors affecting soil resistivity often also affect soil capacitance. In accordance, ρ was found to be a function of soil water content, soil texture (Fig. 1-4), and soil temperature (e.g. Aaltonen, 2001; Celano *et al.*, 2011). The porosity of soil and the ionic composition of the pore fluids were found to govern ρ -values for different soil textures (e.g. Michot *et al.*, 2003; Paillet *et al.*, 2010; Robain *et al.*, 1996; Samouëlian *et al.*, 2005). Paillet *et al.* (2010) surveyed ρ at two sites to map forest soil properties and found significant correlations at both sites for CEC, clay, silt and humidity and at one site for pH, sand, and bulk density. They concluded that the availability of cations and a close particle contact increased the soil conductivity in clay and silt and thus decreased ρ . Resistivity was used to detect cracks in soil (Samouëlian *et al.*, 2003), and has been used for salinity mapping and in coastal fresh water aquifers (e.g. Nowroozi *et al.*, 1999; Samsudin *et al.*, 2008).

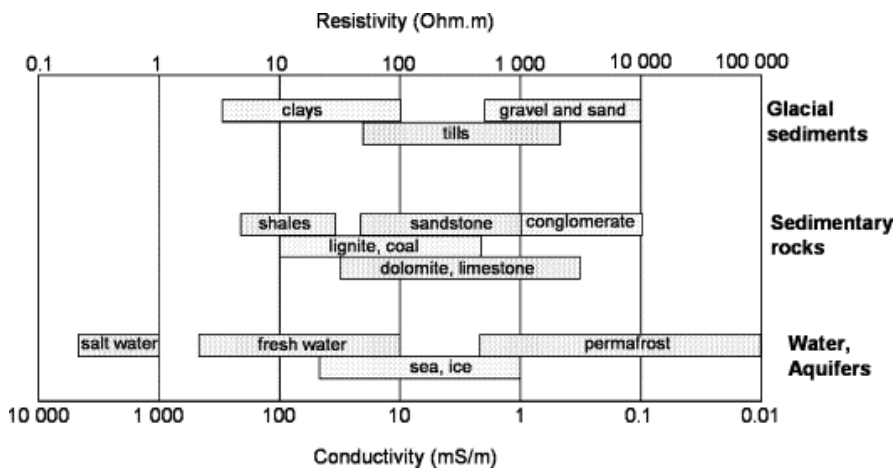


Figure 1-4. Typical ranges of electrical resistivities of earth materials (Samouëlian *et al.*, 2005).

Electrical resistivity is often measured using four electrodes. The method uses direct or alternating current of a low frequency: One pair of electrodes applies an electrical current to the

soil, while another pair measures the resulting potential difference. The resulting pattern of electrical potential reflects the resistivity properties within the subsurface (Fig. 1-5a). Different electrode arrays (e.g. Wenner array, twin-probe array, or dipole-dipole array; Fig. 1-5b) affect the resolution. Resistivity is a function of the soil water content, though the function varies for different soil types (Fig. 1-6). Multi-electrode setups are used on greater areas, or to increase the resolution, or to screen in three dimensions (e.g. al Hagrey, 2006; Amato *et al.*, 2009). Electrical resistivity tomography is used in geological and environmental research to visualize soil water movement in the vadose zone (e.g. Michot *et al.*, 2003; al Hagrey, 2006; Garré *et al.*, 2011); to investigate soil/root water relations (e.g. Werban *et al.*, 2008; al Hagrey and Petersen, 2011; Goulet and Barbeau, 2006; Srayeddin and Doussan, 2009); and to determine root biomass and root diameter in soil (e.g. Amato *et al.*, 2009; Rossi *et al.*, 2011). Amato *et al.* (2009) tested ρ in a borehole setup as measure for root biomass of herbaceous plants that grew in containers with sandy soil and silt loam soil, respectively. The workers judged ρ suitable for the mapping and quantitative estimation of root biomass. However, the estimation of root length density (RLD) was confounded by ρ -variations caused by soil texture and water content, when RLD was low. A borehole setup, however, facilitates the detection of roots in deeper soil layers (Amato *et al.*, 2009; al Hagrey and Petersen, 2011).

Based on the findings of Tattar *et al.* (1974), al Hagrey (2007, 2006) tried mapping wood decay in trees as a function of ρ and could (i) map gradients of wood decay, (ii) discriminate phloem, sapwood, and heartwood in trunks, and (iii) discriminate soft and woody roots. A combined surface and borehole resistivity survey even allows the detection of fine roots in soil (≥ 2 mm diam.; (al Hagrey and Petersen, 2011).

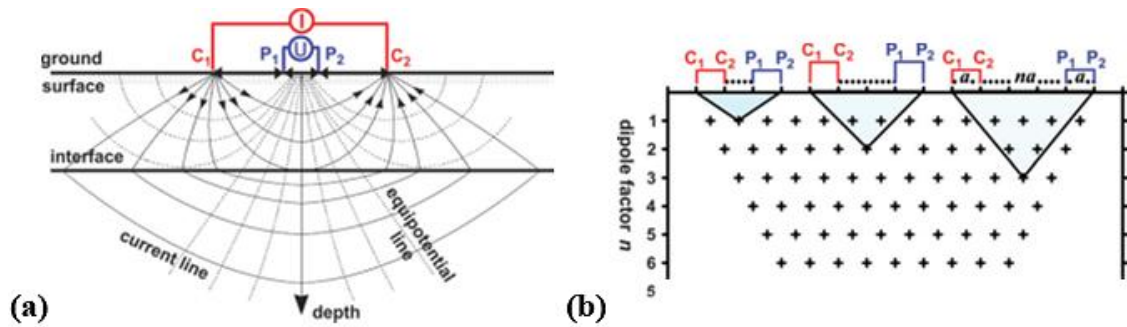


Figure 1-5. Electrode arrays for electrical resistivity surveys (al Hagrey 2007): (a) Four-point electrode configuration in a two-layer model of resistivities ρ_1 and ρ_2 . I, current; U, voltage; C, current electrode; P, potential electrode. (b) Acquisition of a 2D apparent resistivity pseudosection using a dipole–dipole array (C1 C2 P1 P2); a, dipole spacing; n, dipole factor.

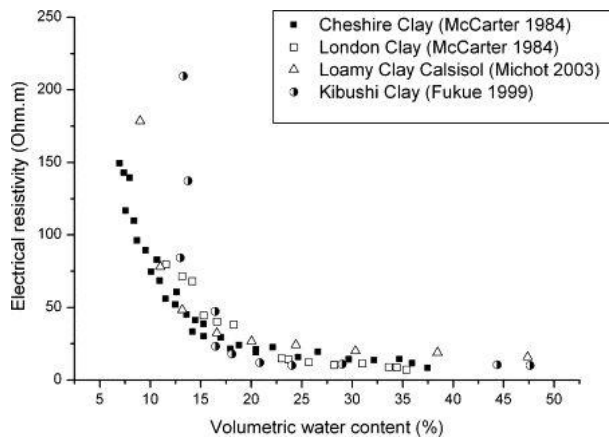


Figure 1-6. Relationship between the volumetric water content and the electrical resistivity for different soil types, taken from Samouëlian *et al.* (2005): Values issued by Fukue *et al.* (1999); Michot *et al.* (2003); McCarter (1984).

Electrical impedance spectroscopy (EIS)

In plant science electrical impedance spectroscopy measures the impedance of a biological sample or system over a wide range of frequencies. The imaginary part of impedance, the reactance (X_c) is frequency-related (Eqn 5) and can be plotted against resistance (R), the real part of impedance in form of a Nyquist plot. A Nyquist plot allows conclusions on the dielectric and resistive properties of the sample in form of a half circle. In complex systems

impedance spectroscopy is used to examine different components of the system. Components with different permittivities cause sub-half circles within the Nyquist plot and indicate a serial connection between capacitive materials. Therefore, impedance spectroscopy was used as complementary method for studying capacitance measurement on roots (Ozier-Lafontaine and Bajazet, 2005; Rajkai *et al.*, 2002, 2005) as well as stand-alone method for root growth measurement (Repo *et al.*, 2005). Repo *et al.* (2005) let willow cuttings (*Salix myrsinifolia* Salisb.) grow in hydroponics. Similar to Figure 1-7, one of two electrodes was attached to the woody stem and the other electrode was inserted in the hydroponic solution. The group measured impedance for 40 days. A high negative correlation was found between root fresh mass and impedance ($r = -0.70$) and fresh mass and reactance ($r = -0.65$), but not for resistance (R). Apart from root measurement, biologists used EIS to investigate the cold acclimation of trees (e.g. Repo *et al.*, 2002; Repo *et al.*, 2000; Räisänen *et al.*, 2007) and freeze-thawing injuries of vegetables (Zhang *et al.*, 2002; Wu *et al.*, 2008).

Root resistivity measurement

Cao *et al.* (2010) hypothesized resistivity to be a function of root size and root water content. The workers let cuttings of willow (*Salix schwerinii* E. L. Wolf) grow hydroponically. Similar to Figure 1-7, one of two electrodes was attached to the stem and the other was inserted in the hydroponic solution. High negative correlations were found between ρ and both root surface area ($r = -0.93$) and the number of lateral roots ($r = -0.91$). Gradual immersion of roots caused a decrease of ρ with increasing root immersion depth. Resistivity halved, when the stem came into contact with the solution. The removal of roots from the immersed stem, however, had negligible effect on the ρ -values. A close correlation was found between ρ and the reciprocal of the stem cross-sectional area in solution. An electrical analogue was proposed that discriminates between resistivity due to (a) the solution, (b) the root-solution interface, (c) the

stem-solution interface and (d) by the stem out of solution. The group judged ρ -measurement as a suitable method to investigate root growth dynamics and root function.

Earth impedance technique

The so called earth impedance method (e.g. Aubrecht *et al.*, 2006; Čermák *et al.*, 2006; Butler *et al.*, 2010) has been suggested to give a measure of the total root water absorbance zone (Aubrecht *et al.*, 2006). Based on assumptions of Ozier-Lafontaine and Bajazet (2005) and Dvořák, Černohorská and Janáček (1981) that the reactance X_c would be negligible in comparison with resistance at low frequencies, the earth impedance is measured with alternating current at 100 to a few hundred Hertz (Aubrecht *et al.*, 2006; Urban *et al.*, 2011). One current electrode is inserted in soil, the other current electrode penetrates the stem and two potential electrodes measure the voltage response. One potential electrode is inserted in the sapwood of the stem at the soil surface and the other potential electrode inserted at various positions in the soil until an optimum position is found. ρ increased with increasing distance between tree and electrode (Aubrecht *et al.*, 2006). The increase was large at a short distance and became weaker the further the electrode was set away from the tree. The ρ -value measured at the beginning of the linear part of ρ -increase was suggested to be a direct measure of the local root absorbance area, though the scientific basis for this is relatively poor: Čermák *et al.* (2006) found at best indications that the method is capable of determining the root water absorbance area. Urban, Bequet & Mainiero (2011) tested the validity of the earth impedance method by testing seven hypotheses that based on the theoretical construct of this approach and could verify none of them.

Urban *et al.* (2011)'s main findings were:

- Impedance measured at woody tree roots at various electrode distances increased with increasing electrode distance.

- Tree root systems were immersed into a solution with one electrode in solution and another inserted into a root above the solution. Raising the tree root systems out of solution caused an increase of impedance. This observation was in agreement with results obtained by Cao *et al.* (2010). Urban *et al.* (2011) interpreted this as the result of a longer electrical pathway.
- Neither excavation, nor the chopping of considerable parts of the root system caused a change in the impedance. This observation was in agreement with results of root trimming observed by others (Cao *et al.*, 2010; Kendall *et al.*, 1982; Matsumoto *et al.*, 2001).
- Intensive fertilizing of the soil around trees caused a ρ -decrease by 20%. This agrees with the study of Paillet *et al.* (2010) which reports that a high cation exchange capacity of soil was correlated with low resistivity readings.

In conclusion, electrical measurements on roots were affected by (1) the electrode distance, (2) the distance between electrode and substrate, and (3) the ionic composition of the rooting medium, but importantly not by root trimming.

1.2 The capacitance measurement of plants in the ground

This section describes how the electrical capacitance is measured and provides a general overview. It introduces the work, results and conclusions of researchers that investigated capacitance as a function of root system size and presents the most widely accepted conceptual model for the capacitance measurement on plants suggested by Dalton (1995). Finally, soil and plant factors are discussed that might possibly affect the measurement of capacitance.

1.2.1 A general overview

The equipment requires a handheld capacitance-meter and a pair of electrodes (Fig. 1-7). Its simplicity and easy application in laboratory and the field have led to an increasingly wide use of the technique, though many questions remain concerning the interpretation and general validity of such capacitance measurements. Close correlations between capacitance and different root size parameters such as mass, surface area and length have been reported for many species (Table 1-2). From all hypotheses and concepts proposed to explain findings of close correlations between capacitance and root mass (e.g. Dalton, 1995; Ozier-Lafontaine and Bajazet, 2005; Rajkai *et al.*, 2002; Chloupek, 1977; Chloupek *et al.*, 2010) the Dalton model is the most widely accepted. It proposes a linear relationship between the root mass and capacitance, which is why the method is also commonly called root capacitance measurement. It has been used as measure of root system size (Kendall *et al.*, 1982; van Beem *et al.*, 1998; Chloupek *et al.*, 1999; McBride *et al.*, 2008; Chloupek *et al.*, 2006), for plant breeding purposes; for the study of root growth (e.g. Dalton, 1995; Kendall *et al.*, 1982; van Beem *et al.*, 1998; McBride *et al.*, 2008; Preston *et al.*, 2004) and to estimate root mass of trees (e.g. Preston *et al.*, 2004; Pitre *et al.*, 2010; Psarras and Merwin, 2000; Tsukahara *et al.*, 2009; Blomme *et al.*, 2004). Possibly the largest study on root capacitance measurement was conducted by Chloupek *et al.* (2010) who measured the capacitance of several thousand plants of various cultivars over four years. In this data set close correlations between capacitance and root mass however were relatively rare. Capacitance measurement has never-the-less been proposed as a quick and non-destructive screening method for plant root systems size (e.g. Dalton, 1995; Chloupek, 1972; Bengough *et al.*, 2009; Rajkai *et al.*, 2002; Kendall *et al.*, 1982; Chloupek, 1977; van Beem *et al.*, 1998; McBride *et al.*, 2008; Preston *et al.*, 2004; Pitre *et al.*, 2010; Tsukahara *et al.*, 2009).

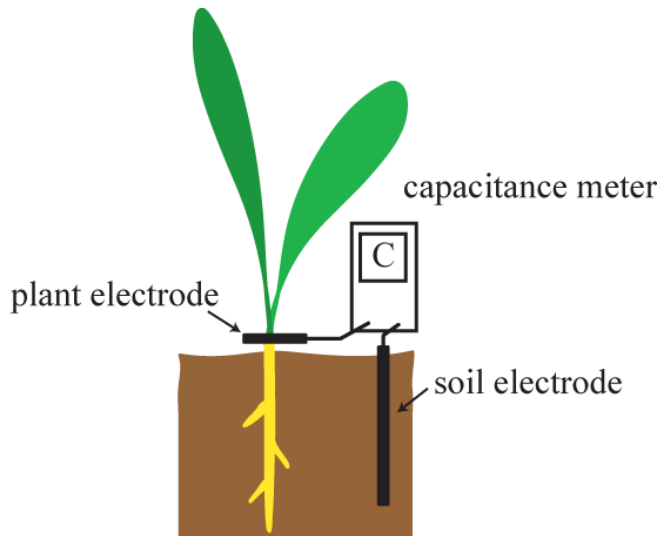


Figure 1-7. Scheme of capacitance measurement on a plant rooting in substrate: Higher plants usually consist of an aboveground shoot (green) and a belowground root system (yellow), including also ‘stem’/’shoot’ tissue. Capacitance is measured by establishing a resistance-capacitance circuit between the plant and the rooting substrate (brown) with a capacitance-meter. One of two electrodes is inserted in the substrate (substrate electrode), while the other is attached to the plant shoot (plant electrode) near the soil surface.

1.2.2 Experimental findings and their interpretation

Chloupek (1972) was the first to relate the capacitance measured for plants in soil to root system size parameters such as fresh mass and surface area (Table 1-2). Chloupek (1977) found good correlations between capacitance and mass for several species of crop (see Table 1-2), though not for rape (*Brassica napus* L.). In this paper he assumed that capacitance is "generated" at the gap between soil and root surface cells, but also assumed that many inner root tissues contributed capacitance, too. The poorer correlations between capacitance and root mass found for rape he explained by the rather spherical shape of its major tap root. Chloupek (1977) stated that soil capacitance would have no effect on the capacitance measurement of a plant in wet soil. He argued that the high conductivity of soil would make its capacitance irrelevant. Later, Chloupek, Skácel and Ehrenbergova (1999) mentioned that soil capacitance “contaminates” the root capacitance measurement and stated that root capacitance could therefore not be an absolute measure of root system size. But Rajkai, Vegh and Nasca (2005) found evidence that

the capacitances of root and soil are connected in series, indeed, having measured capacitance and impedance of soil, root pieces, and roots in soil over a wide range of frequencies.

Chloupek, Forster & Thomas (2006) proposed a different capacitor model that considered soil and root material as the plates of one capacitor and their boundary layer as dielectric. Later, Chloupek *et al.* (2010) considered root tissue and soil to be equivalent to two dielectrics with an electric field at their boundary. The various explanations for capacitance (Chloupek (1977); Chloupek *et al.* (1999, 2006, 2010) do not offer a rigorous explanation of the mechanistic basis of the technique.

Plant capacitance, soil capacitance, and soil water content

Though soil capacitance is known as function of soil water content (S. 1.1.2) and both soil and plant capacitance are proposed to be connected in series (Rajkai *et al.*, 2005), there were no studies found in the literature that properly explained their inter-relations. Poor correlations were consistently found, however, between capacitance and root mass when capacitance was measured under dry soil conditions (Kendall *et al.*, 1982; Chloupek *et al.*, 2010; van Beem *et al.*, 1998). Dalton (1995) measured the capacitance of a plant in sand for different sand water contents and observed a plateau of rather consistent capacitance values between 0.35–0.85 cm³ cm⁻³ water content. Rajkai *et al.* (2005) measured the capacitance of plants in soil at field capacity ($\theta = 0.23 \text{ cm}^3 \text{ cm}^{-3}$), in capillary-saturated ($\theta = 0.27 \text{ cm}^3 \text{ cm}^{-3}$) and in water and found equally good correlations between the capacitance of root mass. Furthermore the group observed that the capacitance of soil was at least an order of magnitude higher than that of a plant in soil at the commonly used measurement frequency of 1 kHz. With decreasing frequency the difference between the capacitances increased further.

In conclusion, the estimation of the root system size by capacitance measurement requires relatively wet soil. Wet soil shows a high soil capacitance. Since soil capacitance and plant

capacitance appear to be connected in series, it might be concluded that the plant capacitance governs the measurement only in wet soil, because then it is much lower than the soil capacitance. This follows from the following equation

$$\frac{1}{C_{total}} = \frac{1}{C_{plant}} + \frac{1}{C_{soil}} \quad (1)$$

where C_{plant} is the plant capacitance and C_{soil} the soil capacitance. This explains why correlations between capacitance and root mass were poor in dry soil, due to the smaller soil capacitance dominating the capacitance reading. The relationship between both capacitances however depends of the measurement-frequency used.

1.2.3 The Dalton model for root capacitance

The most widely-accepted model to explain the capacitance of root systems was put forward by Dalton (1995). He proposed a simple resistance-capacitance model to describe the underlying electrical pathways between an electrode in the root substrate and an electrode inserted into the base of the shoot. The model considers roots to be equivalent to cylindrical capacitors. It suggests that the plasma membranes of root cells serve as dielectrics (Dvořák *et al.*, 1981) separating the soil solution from the inner solution and generating capacitance. Accordingly, the boundary layers between the plasma membranes of root cells and these solutions are seen as equivalent to capacitor plates. Thus, the capacitance of a root system would be linearly related to its size, analogous to the addition of capacitors when they are connected in parallel, given by

$$C_{total} = C_1 + C_2 + \dots + C_i \quad (2)$$

where C_1, C_2, \dots, C_i represent the capacitance of individual roots. Dalton's model (1995) has gained wide acceptance, because the linear relationship between the capacitance and the size of

a plant root system it predicts has been found for many different plant species in many different substrates (Table 1-2).

Dalton (1995) surmised that the suberized plant tissue of fully developed endodermis would act as an insulator. Hence the root capacitance would be provided predominantly by “active” apical parts of the root. The model equates xylem and phloem vessels with wires that conduct the current to the plant electrode aboveground. Thus, Dalton (1995) concluded that root-C would provide information about both the mass and the physiological “activity” of roots. Dalton (1995) observed what he called a “hyperbolic decrease of capacitance” with increasing distance between the shoot electrode and the soil surface and explained this by a network of resistance–capacitance elements in the shoot connected in series (Eqn 13).

Although Dalton’s (1995) key prediction of a linear relationship between C and root mass is supported by a number of studies (Table 1-2), there are several examples of findings disagreeing with the model. These will be discussed in more detail in a later section (1.2.5).

1.2.4 Factors that may affect root capacitance measurement

This section discusses technical, environmental and plant-related factors that are thought to affect the root capacitance.

(a) The capacitance of the rooting medium

Rajkai *et al.* (2005)’s model suggests that an accurate estimation of root capacitance requires either that the substrate capacitance is substantially higher than that of the root system, or that it is known. Indeed, there is a general consensus that root capacitance is only a relative measure and best performed under uniformly wet conditions (e.g. van Beem *et al.*, 1998; Chloupek *et al.*, 1999; Preston *et al.*, 2004; Pitre *et al.*, 2010).

(b) Ionic composition of soil solution

Different electrical measurement techniques show strong sensitivities to the ionic composition of soil solution (Section 1.1.2). Dalton (1995) tested whether different ionic compositions of a hydroponic solution would affect the root capacitance measurement, but came to no final conclusion, due to a lack of adequate data. Results of soil resistivity studies suggest that capacitance might increase with increasing soil salinity (e.g. Paillet *et al.*, 2010; Samouëlian *et al.*, 2005; Urban *et al.*, 2011).

(c) Soil temperature

Temperature has often been found to affect capacitances measured in soil and plants (e.g. Kizito *et al.*, 2008; Lekas *et al.*, 1990; Blomme *et al.*, 2004). Blomme *et al.* (2004) were one of the few research groups who found no correlation between capacitance and root system mass at all, despite measuring in wet soil. They suggested that temperature fluctuations on the ground and at the shoot caused variations in the capacitance reading. The group measured root capacitance of banana trees (*Musa L.*). Banana plants have a spherical pseudo-stem that is partly located belowground and consists of rolled leaves (Blomme *et al.*, 2004). The researchers concluded that this specific plant anatomy could have been another cause for the lack of a relationship between capacitance and root mass.

(d) Electrode type and placement

Ozier-Lafontaine & Bajazet (2005) were concerned about “parasitic” capacitance, caused by electrode polarization. The polarization of electrodes has an effect on capacitance measurement (Schwan, 1992), but according to Schwan’s equation the polarisation has a relatively weak effect on the total capacitance, given by

$$C = C_s + \frac{1}{\omega^2 R^2 C_p} \quad (3)$$

Here, C_s is the sample capacitance with $\omega = 2\pi f$ angular frequency, C and R the measured values and C_p the capacitance provided by electrode polarisation. Moreover, ionic polarization and relaxation is a time-related process and root capacitance is usually measured within seconds and with alternating current, commonly 1 kHz frequency (Table 1-2). Therefore, the effect of electrode polarization may be small for root capacitance measurement, as long as capacitance is not measured continuously over a longer period of time.

The placement, arrangement and number of soil electrodes were found to have negligible effects on the capacitance reading (Ozier-Lafontaine and Bajazet, 2005; Chloupek, 1977), although the tested distances between soil electrode and plant did not exceed 15 cm. The placement of the plant electrode, however, greatly affected the capacitance reading (Dalton, 1995; Ozier-Lafontaine and Bajazet, 2005; Preston *et al.*, 2004). The workers observed a capacitance-decrease with increasing distance between plant electrode and ground. Preston *et al.* (2004) reported a closer relationship between capacitance and root mass at higher distances between plant electrode and ground. Dalton (1995) interpreted the change of capacitance with electrode height as the result of a serial capacitor "network" for the shoot (in contrast to the parallel network for the root system in soil).

McBride *et al.* (2008) measured root capacitance separately for different plants growing in the same containers, before they measured all plants simultaneously. They penetrated the shoots of two to four plants with a wire which served as plant electrode and found that simultaneously measured capacitances met the sum of separately measured capacitances. The workers suggested using simultaneous capacitance measurements to suppress plant-to-plant variations.

(e) Plant electrode attachment

In the first root capacitance studies the plant electrode was commonly attached by penetrating the shoot with a needle (e.g. Dalton, 1995; Chloupek, 1972; Ozier-Lafontaine and Bajazet, 2005; Rajkai *et al.*, 2002; Matsumoto *et al.*, 2001; Chloupek, 1977). Later, clamping devices were used as plant electrodes (e.g. Bengough *et al.*, 2009; Kendall *et al.*, 1982; Chloupek *et al.*, 2010; van Beem *et al.*, 1998; Preston *et al.*, 2004; Pitre *et al.*, 2010). Rajkai *et al.* (2005) compared needle- and clamp-electrodes. The researchers found good correlations between capacitance and root mass for both devices (Table 1-2), although smaller values were measured with a clamp. While the difference in the capacitance readings was negligible for plants in solution, capacitances measured with a clamp were by 17% to 19% smaller, when measured in moist soil.

(f) Root physiology and anatomy

No evidence was found that root physiology or root anatomy or both affected root capacitance.

1.2.5 Testing the Dalton model

The Dalton (1995) model predicts a direct proportionality between electrical capacitance and root mass in a moist rooting medium. Several observations in the literature, however, question the validity of the model. These are:

1. The excision of roots from hydroponics solution had negligible effects on capacitance (Kendall *et al.*, 1982; Matsumoto *et al.*, 2001)
2. When capacitance was plotted against root mass, the linear regression lines regularly showed an intercept far from the origin (e.g. Dalton, 1995; Chloupek, 1977; van Beem *et al.*, 1998; McBride *et al.*, 2008; Pitre *et al.*, 2010). This suggests that capacitance is not directly proportional to root mass. An offset of the linear regression line was commonly explained as a function of soil water content, although this did not appear satisfyingly justified.

3. When capacitance was measured at different growth stages, the relationship between capacitance and root system mass was non-linear. The ratio of capacitance per root system mass was higher at early growth stages (Pitre *et al.*, 2010) and decreased at later growth stages (e.g. Dalton, 1995; van Beem *et al.*, 1998; McBride *et al.*, 2008; Preston *et al.*, 2004). Although, the change in ratio could explain offset intercepts of linear regression lines in point (2.), this was not taken into account in the literature. Decreasing ratios at late growth stages were rather explained by maturing processes (e.g. Dalton, 1995).

These findings are not consistent with the Dalton (1995) model, suggesting that further study is required.

1.3 Definition of electrical capacitance (F) and basic theory

This section describes the physical background of electrical capacitance phenomenon.

Introductory electrical principles can be found in respective standard books (e.g. Floyd, 2010; Atkins, 1994).

The capacitance of a plate capacitor is determined by the plate area, the plate separation and the permittivity of the insulating material between the plates.

Electrical capacitance is the ability of an object to store electrical charge. It is expressed in units of farads (F) and equals charge⁷ stored per voltage⁸. A body with the ability to store charge is termed a capacitor (Fig 1-9). In their simplest form capacitors consist of two parallel

⁷ Charge is an electrical property of matter that exists because of an excess or deficiency of electrons. It can be either positive or negative and is expressed in coulombs (C)

⁸ Voltage is the amount of energy or work per unit charge to move electrons from one point to another and is expressed in volts (V)

conductive plates or sheets separated by an insulating material (Fig. 1-8). William Whewell termed such materials “dielectric” to describe their ability to allow to pass an electric field (Patel and Markx, 2008).

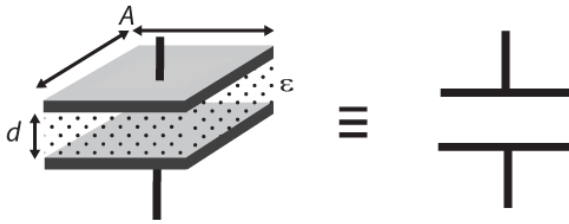


Figure 1-8. Left: schematic diagram of a plate capacitor. Capacitance equals the product of parallel plate area (A), the permittivity (ϵ) of the insulating material (dots), and the reciprocal of the plate separation (d) between the plates (Eqn 4). Right: electrical symbol for a capacitor.

Applying voltage to a resistance–capacitance (RC) circuit causes a negative charge flow from the voltage source to one of the plates. Electrons accumulate at the plate, as they cannot pass the dielectric. The same number of electrons is removed from the opposite plate, as like charges repel each other causing the plates to polarize. Energy is stored in form of an electric field within the dielectric. The storage capacity depends on the permittivity of the dielectric. There is no perfect insulator and therefore every dielectric shows a material-dependent leakage in form of a low electron flow.

Permittivity

The absolute permittivity of the dielectric (ϵ) is a measure of its ability to establish an electric field. Thus, ϵ is proportional to the capacitance (Eqn 4). Putting an insulating material between two capacitor plates increases its capacitance. The permittivity of a material is therefore related

to the permittivity of free space⁹ (ϵ_0) and called the dielectric constant (ϵ_r). The absolute permittivity is therefore the product of ϵ_0 and the dielectric constant. Furthermore, the capacitance is proportional to the parallel plate area (A). Charles Augustin Coulomb found that the magnitude of an electric field decreases by their spatial separation (e.g. Hall, 2008). Thus, capacitance is related to these three factors permittivity, plate area and plate separation (d) via the equation

$$C = \frac{A\epsilon}{d} \quad (4).$$

The polarisation of capacitor plates “charges” the capacitor. This process is measurable as a decrease in current and an increase in voltage. As a consequence, direct current cannot pass a capacitor, unless the capacitor breaks down. A breakdown occurs when the voltage generates an electric field that exceeds the dielectric strength¹⁰ of the insulator. Dielectric strength and therefore the maximally achievable capacitance are affected by temperature, humidity and the current frequency.

The characteristics of the dielectric phase-shifts with respects to voltage for the sinusoidal wave pattern of the alternating current

Switching off the voltage source causes the discharge of the capacitor. Electrical current then flows in the opposite direction. This principle allows alternating current (AC) to pass a capacitor without the necessity of an electron flow across the insulating dielectric. James Clerk Maxwell called this phenomenon “displacement current” (Hall, 2008). The steadily changing direction of AC follows a sinusoidal wave. The process of electron accumulation on one plate and electron repulsion at the other plate, however, is time-related. The electron flow that is

⁹ The permittivity of vacuum (ϵ_0) is $8.85 \cdot 10^{-12}$ F/m

¹⁰ Dielectric strength (ϵ) is the insulating capacity of a material and expressed in MV/m

induced on the other plate follows an sinusoidal wave, too, but the wave is shifted in phase (ϕ) with respect to voltage. The phase-shift is a function of electron displacement per time and an index of how well a capacitor passes alternating current. The phase-shift depends on the characteristics of the dielectric (thickness, area, permittivity) and on the specific conductance (σ)¹¹ of the conductors and the frequency (f) of the current.

The reactance of a capacitor

Decreasing frequency gives a capacitor more time to store charge increasing its (electric field) opposing the electrical current. This opposition is called capacitive reactance (X_c)¹². The inverse proportionality of X_c to f and capacitance is expressed by

$$X_c = \frac{1}{2\pi fC} \quad (5)$$

with 2π as constant of proportionality. Both the reactance and the resistance (R) that is due to the nature of the conducting devices, form the overall opposition to current, the impedance (Z), given by

$$Z = R + X_c \quad (6).$$

Resistance is determined by the physical dimensions and resistivity of the conductors.

Resistance is the real part of impedance, whilst reactance is represented as the imaginary part of impedance (this is a mathematically convenient terminology enabling simple calculations of phase shifts). The material and design of the capacitor and its conductors provide resistance.

Therefore capacitors are always referred to as a part of an RC circuit (Fig. 1-9).

¹¹ The specific conductance of a conductor is also termed conductivity (σ). It is the reciprocal of resistivity and measured in Sieverts per meter.

¹² Capacitive reactance (X_c) is the opposition of a capacitive element to alternating current and is expressed in Ohms (Ω)

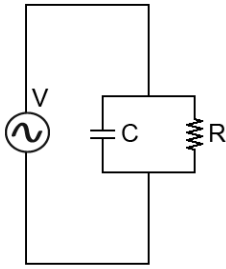


Figure 1-9. Scheme of a resistance-capacitance circuit (RC circuit). The voltage source (V) applies alternating current (encircled wave symbol) to the circuit that consists of a capacitor (C) and a resistor (R) opposing the electrical current.

In the discussion of electro-chemical and electro-physical properties of biological samples or systems, some terms are often used synonymously, such as impedance and resistivity or capacitance and permittivity.

Conductivity, resistivity and capacitance in biological systems

In biological systems, ions carry the electron flow. Ion mobility, charge, and concentration determine the conductivity of a conducting material. The inverse of conductivity is the resistivity, or specific resistance (ρ)¹³. The resistivity is a measure of the opposition a capacitive material puts up to an applied electrical current and relaxation time (τ), the time a capacitor needs to polarize. With increasing frequency the ions lag behind the voltage with polarization increasingly, a phenomenon termed dielectric dispersion. At extremely high frequencies no capacitance can be measured, because the ions and dipoles in the dielectric effectively become immobile. Dielectric spectroscopy uses the dielectric dispersion and measures capacitance over a wide range of frequencies for investigating complex relative permittivities in biological systems, such as in plant cells (Asami and Yamaguchi, 1992).

¹³ The specific resistance of a material is also termed resistivity (ρ). It is the reciprocal of conductivity and measured using an Ohmmeter.

1.4 Aims and outline of thesis

The aim of this thesis was to explore the mechanistic basis of plant capacitance measurement and specifically to evaluate its potential as a non-invasive technique for the investigation of root characteristics. For that purpose, the conducted experiments aimed to

1. test different measurement durations, electrode placements and electrode types;
2. test the Dalton (1995) model in hydroponics and then in soil;
3. investigate the role of both soil capacitance and plant capacitance in ECM.

Chapter 2 describes the generally used methods and presents the results of preliminary experiments. Preliminary experiments were conducted to explore

1. the optimal type of plant electrode for consistent capacitance measurement;
2. the optimal placement of electrodes for consistent capacitance measurement; and
3. the dynamics of root capacitance in long-time observations.

The findings are discussed and related to findings in other studies.

Chapter 3 presents a series of experiments testing the Dalton (1995) model with barley (*Hordeum vulgare* L.) in hydroponics by a range of treatments that included:

- raising individual roots and whole root systems out of a hydroponic solution;
- cutting roots below the solution surface;
- varying the distance between plant electrode and solution surface; and
- measuring roots in air.

A new model is proposed.

Chapter 4 presents experiments that investigated the role of soil water in root capacitance measurement and tested the newly proposed model for barley and wheat (*Triticum* sp. L.) in compost and soil systems. The new model is further developed.

Chapter 5 presents a series of experiments with potato tubers (*Solanum tuberosum* L.) that investigated the role of the plant electrode and reproduced the key experiments of chapters three and four. The RC circuits that follow from the new model for the key experiments were then tested with man-made capacitors and resistors on an electrical breadboard.

Chapter 6 includes the general discussion of the results from the experimental chapters and final conclusions. Future work is suggested.



2 GENERAL METHODS AND PRELIMINARY EXPERIMENTS

Chapter 2 outlines the general methods used in the thesis, and presents preliminary experiments that investigated variations in root capacitance measurement for barley plants in hydroponics.

2.1 General methods

The first section introduces the general methods used to grow plants in different media and the measurement their electrical properties. The specific details of experiments that use these techniques are described in sections 2.2, and chapters 3, 4, and 5 of this thesis.

2.1.1 Plant growth

Plant materials: Experiments were conducted on barley (*Hordeum vulgare* L., cvs Optic, Siberia), 35 cultivars of wheat (*Triticum aestivum* L.), and potato tubers (*Solanum tuberosum* L. cvs Maris Piper, Sterling).

Barley grown in hydroponic systems

Barley caryopses (cv. Optic) were surface sterilised by soaking in a saturated 2% calcium hypochlorite solution for 15 minutes, then rinsed three times in distilled water. The caryopses were germinated on paper towel moistened with sterile distilled water in a sterile Petri dish in the dark at 16°C for four days. Three days after sowing (DAS) seedlings at similar stages of development were transferred to a controlled environment room at the James Hutton Institute, Dundee, UK (Building AG, Latitude 56.4577°N, longitude 3.0718°W). Plants were illuminated for 18 hours daily with photon irradiance (PAR; 400–700 nm) of 320 mmol m⁻² s⁻¹ at plant height. The day/night temperature regime was 18°C/12°C. Initially seedlings were either

directly transferred to vertically aligned plastic tubes of 50 mm diameter, 1 m length and two litres volume (Fig. 2-1a,b) containing a nutrient solution (Table 2-1) or spent an interim period in a 10L basin filled with the same nutrient solution aerated by porous stones (ELITE, Hagen Inc., Toronto, Canada) placed beside the seedlings (Fig. 2-1a). To avoid problems with maintaining an accurate water level during aeration an alternative water regime was devised in which the solution was cycled between the tubes, a basin enclosing the tubes, and a canister in which the solution was aerated (Fig. 2-1b). All tubes were plugged at the bottom with rubber plugs so that each tube contained about 1.95L of solution plus one seedling. In contrast to the standard water regime (Fig. 2-1a), the alternative did not require daily replacing of solution losses by evaporation and transpiration. Further advantages were that it allowed measuring capacitance over long periods at (i) constantly high solution levels and (ii) consistent ionic compositions of the solution, independent from the ion-uptake of a plant.

Figure 2-1. Two hydroponic systems differing in their water regime: Plants grew individually in tubes containing nutrient solution. Solution was aerated with air bubbles produced by porous stones. Aeration happened either (a) in the tubes or (b) in a 10-litres-canister hanging 50 cm above the tubes. Air pressure was provided by an air pump (Motore Asincrono, No. G0225, Lafert Electric Motors Ltd. Cheshire, UK). The solution was circulated to the bottom of the tubes causing overflow at top. Draining solution was captured in a basin (length 1.3 m, width 0.38 m, height 0.17 m), then pumped (pump type 1250, Eheim, Deizisau, Germany) back into the canister through a tube (Super Tricoflex, Nobel Plastiques, Poissy Cedex, France; 1.25 cm inner \emptyset).

Table 2-1. Composition of nutrient solution (conductivity 39.1 mS cm⁻¹ at 19.3 °C)

Nutrients	g L ⁻¹	Micronutrients	mg L ⁻¹
NH ₄ Cl	0.16	MnCl ₂ ·4H ₂ O	1.19
Ca(NO ₃) ₂ ·4H ₂ O	0.94	H ₃ BO ₃	1.42
KNO ₃	0.40	ZnCl ₂	0.10
MgSO ₄	0.36	CuSO ₄ ·5H ₂ O	0.40
FeEDTA	0.04	Na ₂ MoO ₄ ·2H ₂ O	2.24
KH ₂ PO ₄	0.68	CoCl ₂ ·6H ₂ O	0.24

2.1.2 Measuring capacitance and resistance

Capacitance and resistance were measured with 1 Volt at 1 kHz frequency with an LCR Meter, either the MT4080D from Motech Industries (Tainan, Taiwan) or the Passive Component LCR Meter from Extech Instruments (Typ 130193, Waltham MA, USA). The advantage of the Extech LCR-meter was its ability to display capacitance and resistance simultaneously that facilitated the quick noting of both measures. The two test leads from the LCR meter were attached to the electrodes used to contact the plant or rooting substrate. The devices serving as plant electrodes were: stainless steel hypodermic needles (Fig. 2-2a; length 25 mm, 0.6 mm diameter, Terumo, Leuven, Belgium), alligator clips (Fig. 2-2b; Deltron, South Humberside, UK), hairclips (Fig. 2-2c; T10 silver, Boots, Nottingham, UK), strips of aluminium foil (Fig. 2-2d,e and h; breadth 4 ± 0.5 mm; 8-fold thickness), razor-blades (Fig. 2-2g) and battery clamps. Husk and dead leaves were removed, before capacitance was measured with a clamping or wrapping type of electrode, because they often prevented a satisfactory electrical connection. The substrate electrode was a stainless steel rod with a pointed end (Fig. 12f; length 16.5 cm, diam. 3 mm).

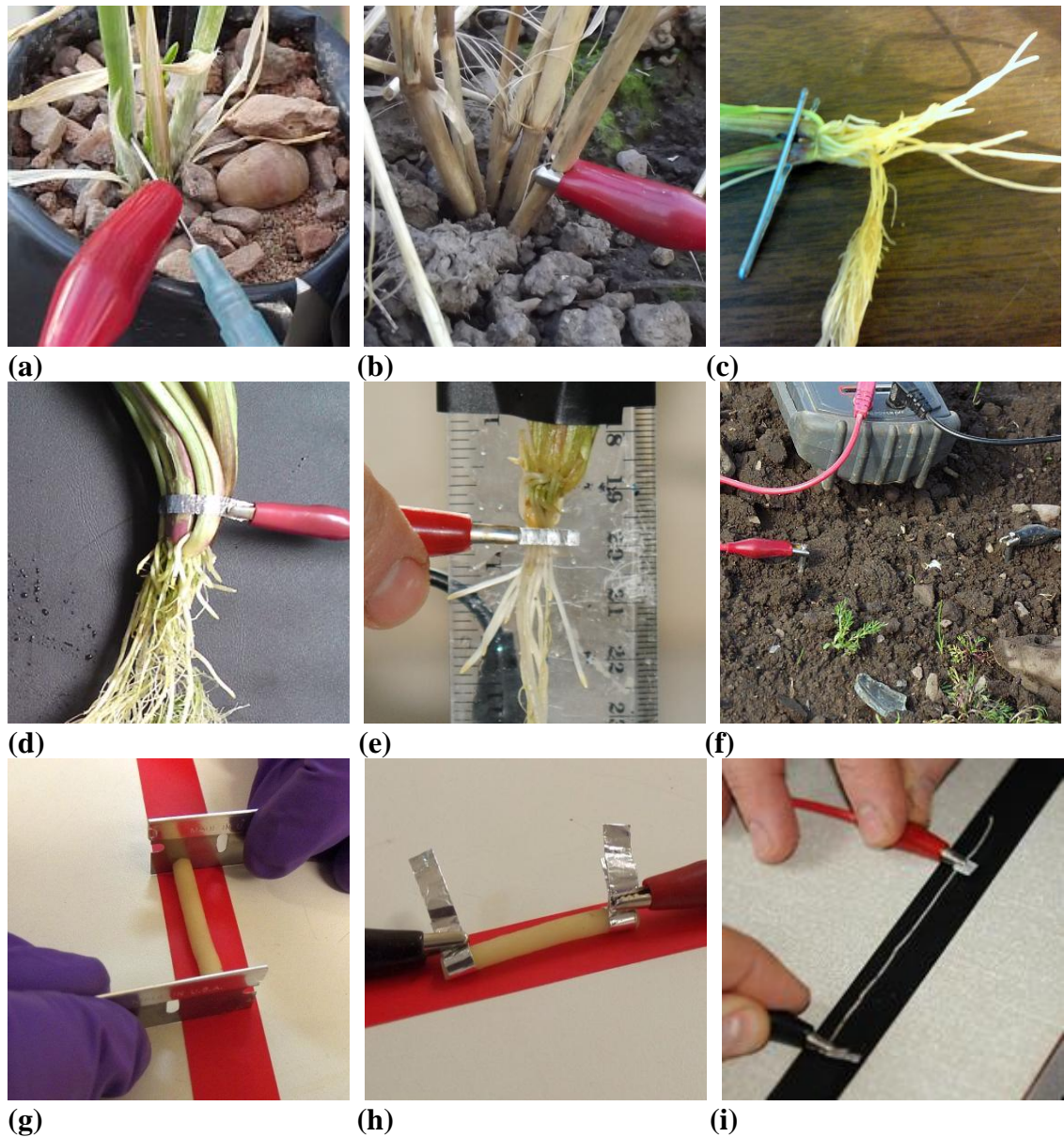


Figure 2-2. Measuring capacitance with different electrode types. Electrodes were horizontally attached to plant stems: (a) Needles pierced through the centre of one or of several stems; (b) clips were clamped at single stems; (c) the halves of a hairclip were gently bent open and laid around the shoot, before being slowly released (coating at the inner sides was filed away to ensure full electrical connection); and strips of aluminium foil were folded three times before being wrapped around (d) stems or (e) roots and then tightened by the clips of the LCR-meter. (f) substrate capacitance was measured by inserting two metal rods to 15 cm depth. Capacitance of plant parts in air was measured either (g) with two razor-blades held tight against the cutting edges of a piece of plant tissue, e.g. a cylindrical core of a potato tuber, or with strips of aluminium-foil wrapped around a piece of (h) shoot or (i) root.

Measuring capacitance in hydroponics – effect of electrode type

The development of capacitance with plant age was monitored for plants in hydroponics. The standard water regime (Fig. 2-1a) required plants to be transferred into an extra tube containing standard ionic solution before starting capacitance measurements. 12 cm of solution substrate electrode was submerged at the edge of the tube. Needles, hairclips or strips served as plant electrodes (Fig. 2-2). These were attached at the shoot (Fig. 2-2c, d) or the roots (Fig. 2-2e) at constant distance to the solution surface which was at least 5 mm. At distances less than 5mm to solution, neighbouring roots created a meniscus that could contact the electrode at shorter distances (Fig. 2-3). Such contact caused large increases in capacitance, possibly due to a short circuit between electrode and solution. A ruler of 50 cm length was attached to the plant and fixed with insulation tape at the shoot above the plant electrode to determine the distance between plant electrode and solution surface.



Figure 2-3. A root system submerged in hydroponic solution forms a meniscus.

When roots were removed from solution and measured with two plant electrodes the capacitance was significantly higher before they were surface-blotted than after. This suggests that moisture at the root surface served as a bypass and thus increased the capacitance reading. Equivalent results were obtained by monitoring the capacitance of root systems left to dry. In hydroponic experiments capacitance readings were repeated three times (technical replicates).

Measuring capacitance in solid media

Needles, clips, battery clamps and strips served as plant electrode (Fig. 2-2). Unless stated otherwise, soil electrodes were placed in 5 cm distance from a plant, because shorter distances bore the risk of root injury. Plant electrodes were attached to shoots either at 5, 10, or 15 mm height above flattened substrate surface. Height was determined with a sliding calliper (Somet, Rijeka, Croatia). The positions of plant electrode and rooting substrate were marked at the shoots with waterproof fine liner pens in different colours. Needles pierced a stem at the pen-mark, whereas clips and strips were attached such that their lower edges contacted the marks.

Measuring capacitance in air

The term “in air” describes capacitance measurements carried out with two electrodes on the plant material. This can, but need not include the removal of the plant from its rooting medium. When measured on a plant in the ground, one ground electrode was attached to the stem at the substrate surface with second plant electrode connected above.

2.1.3 Determination mass, plant dimensions and the soil water content

Mass was determined, either with a mobile balance (CS 5000E, Ohaus, Pine Brook, USA) *in situ* or in the laboratory. The mobile balance had a capacity of $5\text{kg} \pm 1\text{g}$ and was used for assessing the weight of compost-filled pots. Masses of soil and plant parts were determined with high-precision balances (LP 3200D, Sartorius, Göttingen, Germany or EP214, Ohaus, Pine Brook NJ, USA). Plant material was dried at 80°C (Hotbox oven size 2, Weiss Gallenkamp, Loughborough, UK), for 48h, soil at 105°C , for at least 72h.

Local plant dimensions, i.e. the cross-sectional area (A_c) and circumference (Φ) were derived from the diameter (\emptyset) which was determined with a graticule under the microscope (MZ75 or MZFIII, Leica Microsystems, Wetzlar, Germany). In the case of young barley stems which show a rather elliptic structure A_c and Φ were derived from major and minor axis. The cross-

sectional area of hollow stems derived from subtracting the inner from the outer cross-sectional areas. The total dimensions of a root system or an individual root, i.e. length, surface area and volume, were determined by an A3 desktop scanner (1640XL, Seiko Epson, Nagano, Japan) and analysis with WINRHIZO software (Regents Instruments, Quebec, Canada). Root systems were first disentangled and fanned out with a fine paint brush. To test the accuracy of WINRHIZO, diameters of thirty nodal roots were determined under the microscope and compared with the respective scan-data. There was a high proportionality found between the two measures.

The soil water content was determined with a theta-probe (ML 2x, AT Delta-T devices, Rotherham, UK) in combination with a theta-meter (HH2, AT Delta-T devices). The θ -meter was set to 'mineral soil' for field soil and 'organic soil' for potting compost. Rods were fully inserted into the soil with the central rod positioned at 5 cm distance from the plant.

2.1.4 Statistics

Average capacitance and resistance values were expressed as mean \pm standard deviation (SD). If not stated otherwise, the values resulted from three replicates or three repeated measurements (technical replicates). Technical replicates were necessary for and restricted to experiments in hydroponic systems, because lowering root systems into solution or lifting them out caused variations in the capacitance measurement. Such variations were probably caused by variations of surface-water menisci as mentioned previously. Regression analyses and t-tests were performed using Sigmaplot 11 or Sigmaplot 12 software (Systat Software, Inc. Chicago, IL, USA). Regression coefficients are expressed as mean \pm standard error (SE) from n determinations. Multivariate biplots, scatter plots matrixes and diagnostic residuals plots were realized with GenStat thirteenth edition (VSN International Ltd., Hemel Hempstead, UK).

2.2 Preliminary experiments

This section presents preliminary experiments that explored variation on root capacitance measurements for barley plants in hydroponics.

2.2.1 Introduction

The literature provides numerous findings of proportionality between capacitance and root mass and other root size parameters (Table 1-2). These were commonly interpreted with the model proposed by Dalton (1995); (Ch.1, S. 2). The literature also contains reports of correlations between capacitance and shoot mass (Pitre *et al.*, 2010) and yield (Chloupek *et al.*, 2010), respectively. In the latter article however correlations were significant only in a small proportion of the cases and the regression coefficients were small. Findings of proportionality between capacitance and root mass were often not consistent throughout the experiments (e.g. Kendall *et al.*, 1982; Chloupek, 1977; van Beem *et al.*, 1998; McBride *et al.*, 2008), sometimes non-linear (e.g. Preston *et al.*, 2004; Pitre *et al.*, 2010), or not observed at all (Blomme *et al.*, 2004). van Beem *et al.* (1998) found poor linear relationships between capacitance and mass when they combined the data of plants of different age. One explanation could be a change in proportionality constant between capacitance and root mass with increasing plant age, as was observed by Dalton (1995). The authors who reported these unexpected results concurred that they were caused either by (1) changing or different environmental conditions (Kendall *et al.*, 1982; Chloupek, 1977; Blomme *et al.*, 2004), (2) differences in measurement equipment (McBride *et al.*, 2008), or (3) plant-related changes due to development stage (Dalton, 1995; van Beem *et al.*, 1998; Preston *et al.*, 2004; Pitre *et al.*, 2010).

The aim of the preliminary experiments was to investigate variations in plant capacitance measurement for barley plants in hydroponics. Hydroponic systems promote easy access to the root system and avoid complications due to variations in the rooting medium. This allowed

manipulations of a root system under consistent conditions and capacitance measurement with various electrodes.

2.2.2 Material and methods

Three experiments (I to III) were conducted. The setups aimed at generating a wide range of root system sizes either by varying the available space (experiment I) or by measuring plants of different age (experiments II and III).

Plant growth

Barley caryopses were surface sterilized (Ch. 2, S. 1). After germination the seedlings were transferred either into a nursing-basin and subsequently into tubes, or directly into the tubes (Table 2-2).

Plants were harvested either at once (experiment I) or in quartets (experiment II & III) by chopping root material off the shoot base. The harvested material was stored between damp paper towel in sealed Petri dishes at 6 °C in a fridge.

Measuring capacitance, mass and root dimensions

Capacitance and resistance were measured with an LCR-meter either from Motech (experiments I & II), or Extech (experiment III) with hairclip-, needle- or strip-electrodes (Fig. 2-2) being attached 20 mm high above the solution surface (see Table 2-2).

The fresh mass of root and shoot material was determined within the first week after harvest.

Total dimensions of a root or root system were determined by scan-analysis with WINRHIZO-software, local dimensions, i.e. diameters at the solution surface position, by microscope (cf. Ch. 2, S. 1).

Table 2-2. Timelines of and, experimental conditions for, preliminary experiments (I – III)

Key: DAS: days after harvest, n: number of plants, C: capacitance

- * on harvest the selected plants were transferred into an extra tube for C-measurements to avoid injuries of neighbouring plants due to the handling.
- ** tubes were filled to 0.85 m height with rough, sterilized gravel
- *** the wire extended the clip-electrode 28 DAS onwards to ensure electrical contact with all tillers
- **** plant electrode was used as reference to the main, the strip-electrode.
- ***** 4 plants were replaced by reserve plants from the nursing basin 7 DAS and 28 DAS.
- ***** the fresh mass of 4 root systems was not determined, because material rotted due to fridge failure

	Experiment I DAS	Experiment II DAS	Experiment III DAS
Sowing date	25.12.2008	02.03.2009	28.05.2009
Transfer to basin	4	3	3
Transfer to tubes	6	3	6
C measurement	28	7, 10, 15, 19, 22, 25, 29, 32*	22-24, 26-30, 33-36, 38*
Solution replenished	17, 22, 27	6, 10, 14, 18, 21, 28	7, 14, 21, 25, 29, 32, 36
Harvest	28	22, 25, 29, 32	22-24, 26-30, 33-36, 38
Aeration	airstone	nutrient circulation	airstone
Container volume	tube long (1m); (1m + gravel**) or short (0.25m)	1m tube	1m tube
Plant electrodes	clips	clips, clips + wire***	clips****, strips, needles****
n	24	16*****	32*****

Treatments

In experiment I three groups were formed experiencing different growth conditions (see Table 2.2) and capacitance was measured on the plants in their tubes at harvest. In experiments II and III capacitance was measured on the plants in their tubes at different stages of development.

In all three experiments capacitance was first measured for a whole root system in solution and the origin positioned five millimetres above solution. Then individual roots were successively excised from the origin and capacitance remeasured after each excision. The procedure went on until all but one root were removed from the solution. Delta capacitance (Δ -C) that resulted from subtracting the capacitance measured after a root was excised from the capacitance

measured before the root excision was related to the mass of the excised root. In experiment III a random selection of excised, unbranched nodal roots underwent a further treatment: a strip-electrode was attached to a root's cutting edge, before the root was incrementally lowered into solution and capacitance measured for each increment.

2.2.3 Results and discussion

The results obtained are presented in the chronological order of the experiments.

Experiment I

Root systems grown in short tubes showed an average fresh mass of 1.65 g (± 0.106 g SE, n = 8), less than half of the mass of root systems grown in longer tubes (3.64 g ± 0.074 g SE, n=8) or in longer, but gravel-filled tubes (4.04 g ± 1.388 g SE, n=8). The lengths the longest root system axis however reflected the space availability better: Root systems in long tubes were on average 41% ($\pm 0.3\%$ SD) longer than those in short tubes and 214% ($\pm 1.4\%$ SD) longer than those in gravel. (Fig. 2-4a). No relationships were found between capacitance and root mass (Fig. 2-4b). Excision experiment: occasionally, good linear relationships between capacitance and root mass were found for root systems for the successive removal of roots from solution (Fig. 2-4c). However, correlations between capacitance and root number were often as close (Table. 2-3, Fig. 2-9a). Plotting Δ -C against the masses of individual roots yielded no relationship (Fig. 2-4d).

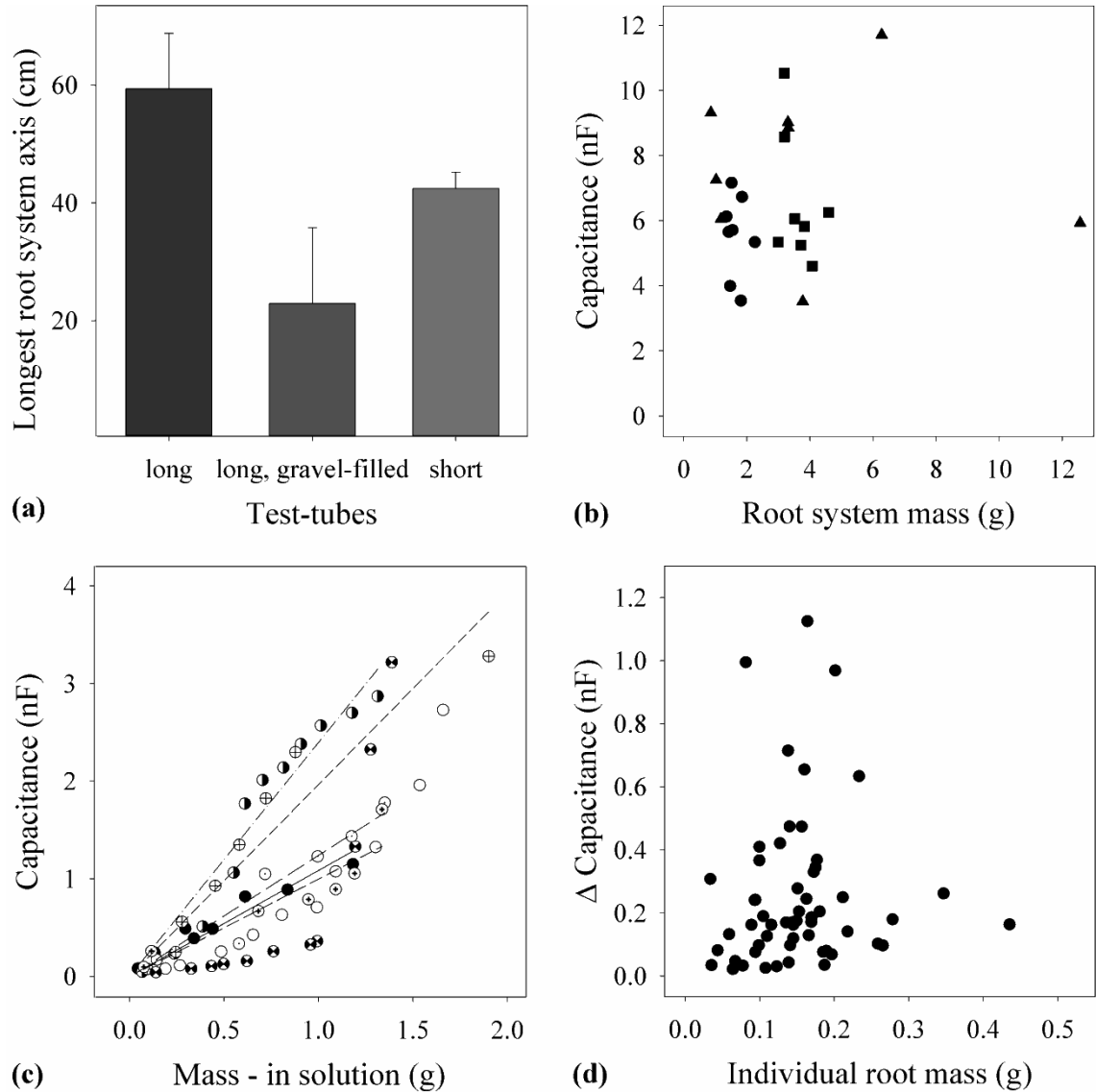


Figure 2-4. Results of experiment I: (a) Average lengths of the longest axis of a root system grown either in (●) short tubes (n=8), (■) long tubes (n=8), and (▲) long, gravel-filled tubes (n=8). (b) Relationship between capacitance and root system fresh mass. (c) Capacitance of plants from the ●-group measured for the successive removal of roots against the root mass in solution. (d) Relationship between change in capacitance following removal of an individual root (Δ capacitance) and its fresh mass (n = 56). Linear regressions see table (2-3).

Table 2-3. Linear regression equations for capacitance against root mass and number (Fig. 2-4c)

Key: C: capacitance (nF); M: root fresh mass in solution (g); N: number of roots at the solution surface

Plant symbol in Fig. 2-4c	filled		dotted		x-hair		crossed		semi-filled	
	solid		long dash		medium dash		short dash		dash-dot	
Line type in Fig. 2-4c										
Regression	M	N	M	N	M	N	M	N	M	N
R ²	0.907	0.922	0.907	0.869	0.857	0.905	0.904	0.872	0.929	0.941
gradient term	1.09	0.13	1.24	0.24	1.00	0.20	1.97	0.32	2.40	0.28
SE (gradient)	0.06	0.01	0.09	0.02	0.08	0.01	0.14	0.03	0.10	0.01

The lack of a linear relationship between capacitance and root mass for both whole root systems and individual roots is inconsistent with the Dalton (1995) model.

Occasionally capacitance decreased linearly with root mass in solution (Fig. 2-4c), although correlations between capacitance and root number were equally good (Table 2-3, Fig. 2-9a).

Experiment II

Capacitance increased non-linearly during the 25d-observation period (Fig. 2-5a,b). The increase in root mass with time was less clear, because plants were harvested on only four days. Capacitance showed a good linear relationship with root system mass (Fig. 2-5c) and an even better one with shoot mass (Fig. 2-5d, Fig. 2-9b). However, there was no relationship found between Δ -C and mass of 200 individual roots during root excision (cf. Appendix).

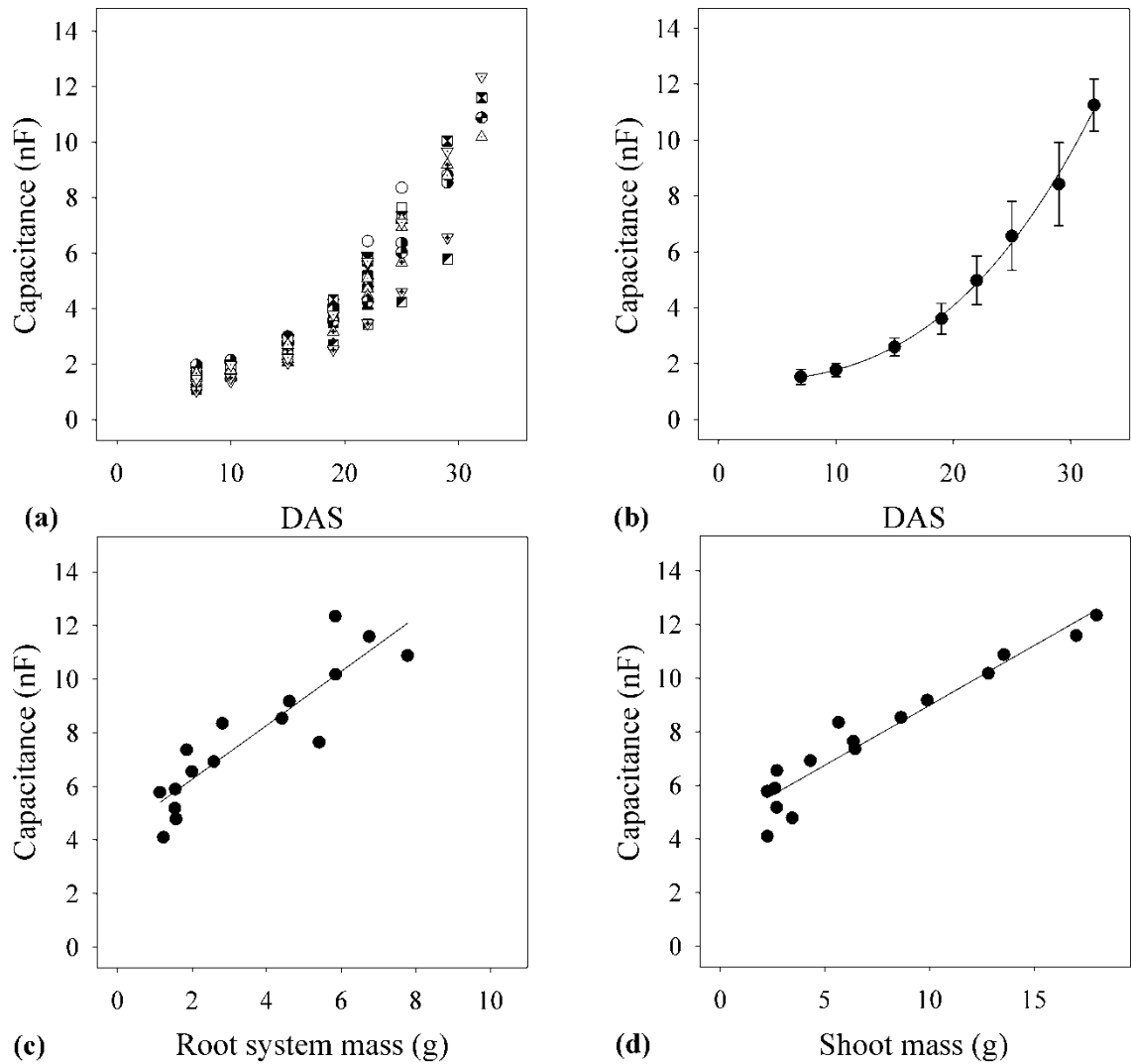


Figure 2-5. (a, b) Results of experiment II: Development of the capacitance of 16 plants with time. Relationship between the capacitance of the same plants and (c) root fresh mass and (d) shoot fresh mass. Data points in (b) represent all plants until 22 DAS. From then on the plant number is successively reduced by four due to harvest. Data points in (c) and (d) represent the mean \pm SD of three technical replicates. The power law regression was for (b) $C = 8 \times 10^{-4} (\pm 5 \times 10^{-4}) M^{2.72 (\pm 0.17)} + 1.36 (\pm 0.196)$ (mean \pm SE, $n = 7$, $R^2 = 996$). The linear regression was for (c) $C = 1.01 (\pm 0.13) M + 4.25 (\pm 0.54)$ (mean \pm SE, $R^2 = 0.808$) and (d) $C = 0.446 (\pm 0.035) M + 4.53 (0.314)$ (mean \pm SE, $R^2 = 0.922$).

Although a linear relationship was found between capacitance and root mass, there was no relationship between capacitance and root mass for individual roots, like in experiment I (Fig. 2-4d). The regression line also shows a positive intercept, as is quite common for capacitance

versus root mass regressions (e.g. Chloupek, 1977; Chloupek *et al.*, 2010; van Beem *et al.*, 1998; McBride *et al.*, 2008; Tsukahara *et al.*, 2009).

A similar relationship between capacitance and mass was observed by McBride *et al.* (2008) and Pitre *et al.* (2010), the latter authors tested suggesting a logarithmic rather than a linear relationship. It seems from these preliminary results that, whilst bigger plants have greater capacitance, there is often not direct proportionality.

Experiment III

The suitability of a strip-electrode for plant capacitance measurement was tested: Capacitances measured with a strip-electrode were compared with the capacitances measured with a clip-electrode and a needle-electrode, respectively. Capacitance measured with a strip-electrode was on average $220\% \pm 19\%$ (mean \pm SE, $n = 24$, 22 DAS) of capacitance measured with a clip-electrode. The strip-electrode gave readings approximately by $9\% \pm 0.04\%$ (mean \pm SE, $n = 8$, 25 DAS) higher than capacitance measured with a needle-electrode.

The observation period here ended one week later than in experiment II. In this week, capacitance showed an accelerated increase with time (Fig. 2-6a) and root mass (Fig. 2-6b). The surprisingly fast increase in capacitance during this last week was associated with three individual plants producing nodal roots that contacted the solution surface. This suggests that the presence of even short nodal roots that contact the solution surface can have a large effect on capacitance. As in experiment I and II there was no relationship found between the Δ -C and mass of 401 individual roots.

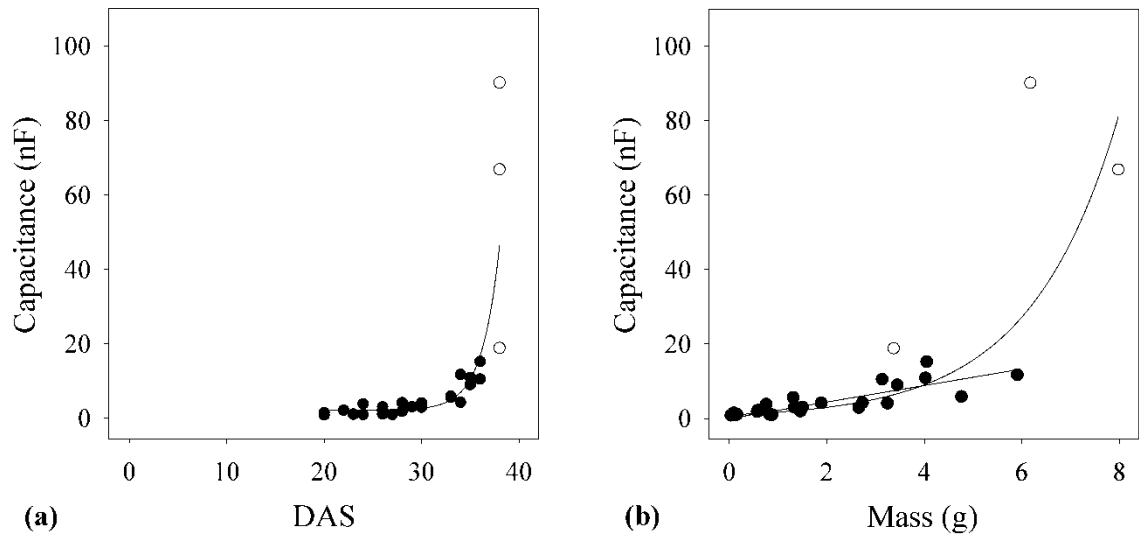


Figure 2-6. (a) Capacitance (C , nF) with time and (b) in relationship with root fresh mass (M , g) of 27 root systems. Hollow circuits show values of plants from 36 DAS onwards and are not used in the linear regression equation. Data represent the mean \pm SD of three technical replicates. The exponential regression was for (a) $C = 4.3 \times 10^{-11} (\pm 4.0 \times 10^{-10}) M^{0.73} (\pm 0.248) + 2.6 (\pm 2.47)$ (mean \pm SE, $n = 27$, $R^2 = 0.728$, $P < 0.0001$) and for (b) $C = 1^{0.55 \pm 0.279} \text{ DAS}$ (mean \pm SE, $n = 27$, $R^2 = 0.601$, $P < 0.0001$) and The linear regression for (\bullet) was $C = 2.22 (\pm 0.18) M$ (mean \pm SD, $n = 24$, $R^2 = 0.675$, $P < 0.0001$).

Strip-electrodes were judged superior to the other electrode types in that they can easily contact an increasing number of stems, and were non-invasive electrodes. Strip-electrodes gave the largest capacitance values, implying a better connection between electrode and plant than for the established clip- and needle-electrodes. Therefore, the strip-electrode was used in all subsequent experiments for barley grown in hydroponics.

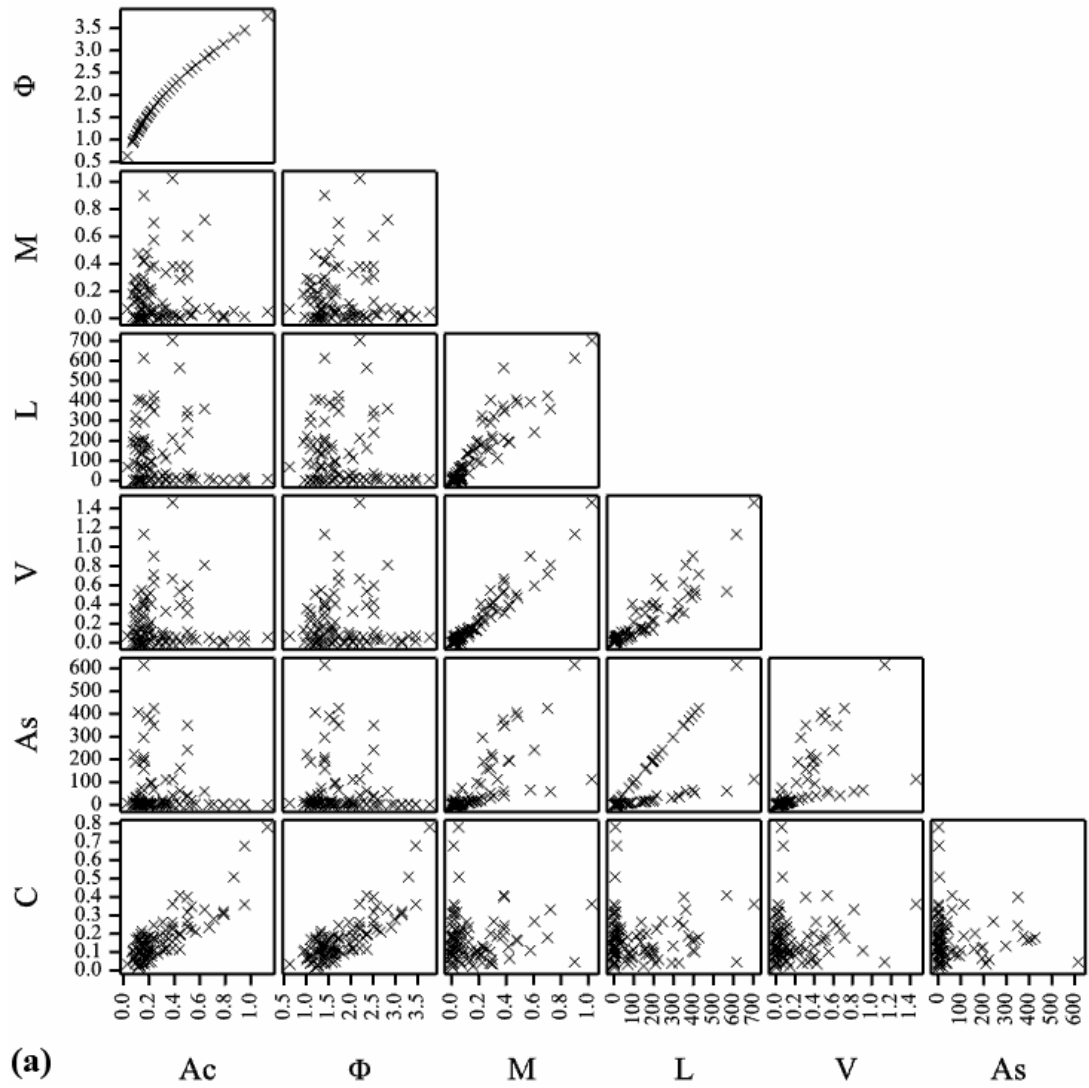
Root mass was much higher in experiment II, than in experiment III perhaps due to better growth conditions.

Successive root cutting

Only nodal roots were analysed, because seminal root systems were knotted together and could not be unravelled without tearing them apart. Capacitance was closely related to the root cross-sectional area (A_c) and total circumference (Φ), but not to the total dimensions mass, length, volume and surface area (Fig. 2-7a). Relationships between C and A_c (Fig. 2-7b) and Φ (Fig. 2-

7c) were magnified illustrating that the first is more linear than the second. The best fitting regression for C against Φ was a power relationship: $C = 0.007 \pm 0.0036$

$\Phi^{3.39 \pm 0.42} + 0.09 \pm 0.014$ (mean \pm SE, $n = 94$, $R^2 = 0.739$, $P < 0.0001$).



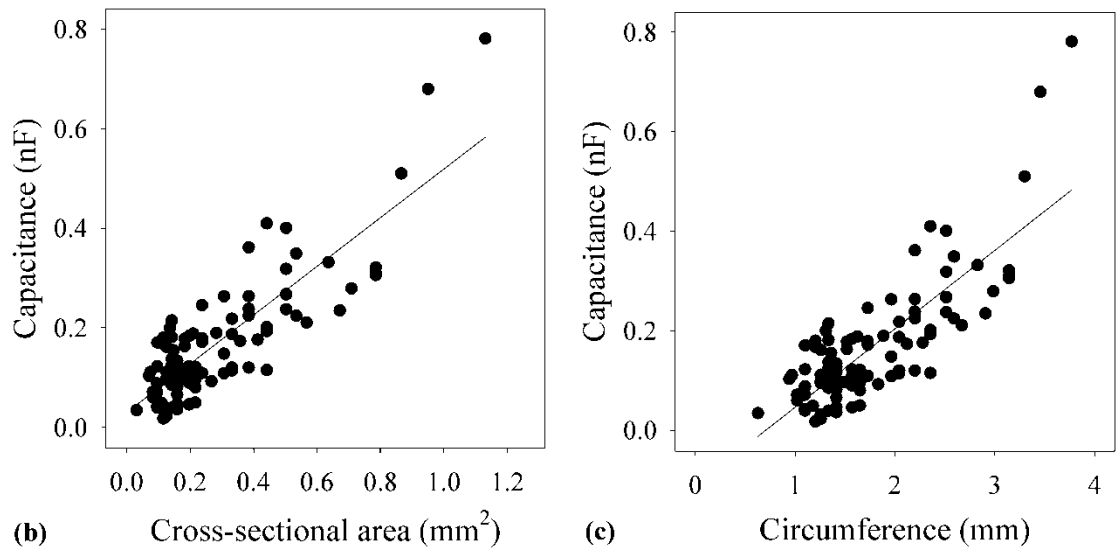


Figure 2-7. (a) A matrix scatter plot showing the relationships between capacitance (C , nF) and different root size factors (Table 2-4), i.e. root fresh mass (M , g), length (L , mm), volume (V , mm^3), surface area (A_s , mm^2), and the root cross-sectional area (A_c , mm^2) and circumference (Φ , mm) at the solution surface of 94 individual nodal roots excised from 11 root systems harvested at different days. The relationships between capacitance and (b) A_c and (c) Φ are shown as larger plots. The linear regression was for (b) $C = 0.489 (\pm 0.030) A_c + 0.03 (\pm 0.012)$ (mean \pm SE, $R^2 = 0.710$, $P < 0.0001$) and (c) $C = 0.158 (\pm 0.012) \Phi - 0.111 (\pm 0.023)$ (mean \pm SE, $R^2 = 0.645$, $P < 0.0001$). Data represent the mean \pm SD of three technical replicates.

Table 2-4. Mean parameters of 94 individual nodal roots from 11 whole root systems (Fig. 2-7)

Key: A_c = cross-sectional area, Φ = circumference, M = root fresh mass, L = length, V = volume, A_s = surface area, SE = standard error, WR = WHINRHIZO[®]

Parameter	C	A_c	Φ	M	L	V	A_s
Unit	nF	mm^2	mm	g	mm	mm^3	mm^2
Mean	0.17	0.30	1.82	0.16	118.55	0.19	65.74
SE	0.001	0.002	0.007	0.002	1.664	0.003	1.278
Area of validity	unknown	solution surface	solution surface	whole root	whole root	whole root	whole root
Determined by	LCR meter	microscope	microscope	WR	WR	WR	WR

Nodal root immersion

The incremental immersion of unbranched nodal roots resulted in a non-linear increase of capacitance with decreasing distance (D) between plant electrode and solution surface (Fig. 2-

8a). Capacitances measured at same distance varied little. Consistently good linear relationships were found when capacitance was plotted against the reciprocal of the distance (Fig. 2-8b).

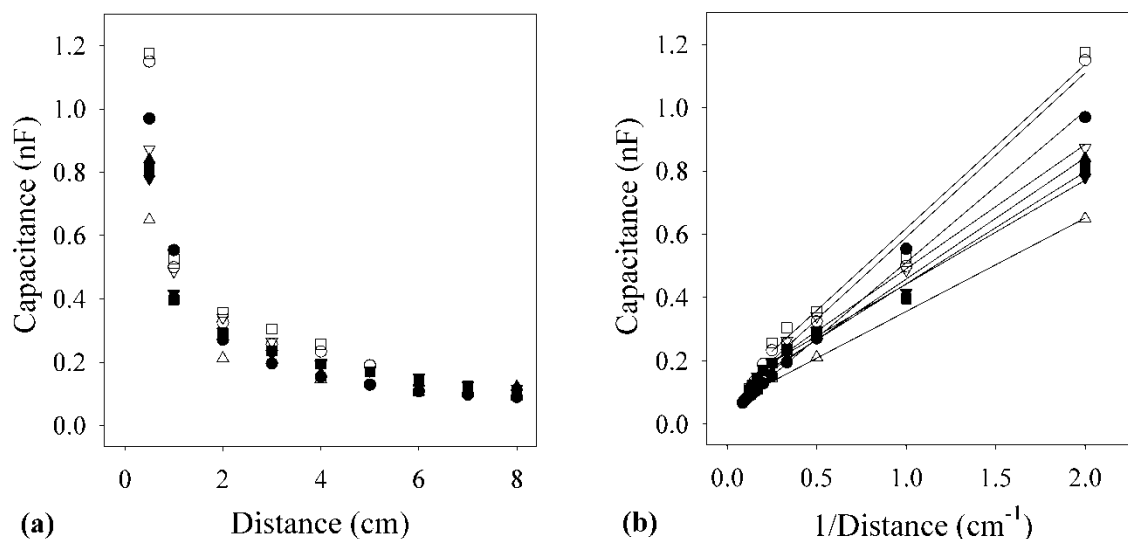


Figure 2-8. Relationship between capacitance (nF) and (a) distance (cm) and (b) the reciprocal of the distance between plant electrode and solution surface for eight unbranched nodal roots in hydroponics. Symbols represent different roots. Linear regressions are listed in Table 2-5.

Table 2-5. Linear regression equations for eight unbranched nodal roots from Fig. 2-8b

Symbol	n	R ²	a	SE _a	P _a	y ₀	SE _{y₀}	P _{y₀}
●	13	0.997	0.479	0.008	<0.0001	0.033	0.005	<0.0001
■	8	0.987	0.354	0.016	<0.0001	0.090	0.012	0.0002
▲	4	0.999	0.383	0.001	<0.0001	0.076	0.005	0.0008
▼	4	0.994	0.328	0.114	0.0001	0.014	0.014	0.0036
○	5	0.979	0.519	0.034	0.0001	0.072	0.033	0.0926
□	5	0.972	0.518	0.044	0.0013	0.101	0.046	0.1138
△	4	0.999	0.295	0.005	<0.0001	0.0614	0.005	0.0012
▽	8	0.989	0.393	0.016	<0.0001	0.0986	0.012	0.0001

Our preliminary data suggests that plant tissue between solution surface and plant electrode seems to influence the capacitance measurement: root material at the solution surface acts as though in parallel as the linearity between capacitance and root cross-sectional area shows (Figs 2-8b and 2-10c, d) while root material between solution surface and plant electrode act in series as Fig. 2-8b shows. This suggests considering plant material as dielectric between two electrodes with the solution surface being equivalent to a second electrode. This simple analogy implies that submerged root material has no influence on the capacitance reading which could explain the lack of proportionality between capacitance and total root size parameters (Figs 2-8a and 2-10c).

Multivariate analysis

Principal component analysis was applied with the intention to define a new set of meaningful variables summarising the total variation among the original variables allowing comparisons between the correlation between three and more dimensions. Separate principal component analyses were run for each experiment. Data were used from the experiments I, II and III to display the relationship between three or more variables always including capacitance, but also shoot mass, root number, and various root dimensions (Table 2-4). Each principal component is a linear combination of the original variables so that the new axes represent a rotation of the original axes.

The resulting biplot for experiment I shows that the capacitance of individual roots is more closely correlated with root number, than root mass (Fig. 2-9a); the biplot for experiment II that capacitance of whole root systems and shoot mass are closer correlated with each other, than with root mass (Fig. 2-9b); the biplot for experiment II that the capacitance of individual roots is related to the root dimensions at the solution surface, A_s and Φ , and not to the total root dimensions mass (g), volume (mm^3), length (mm), or surface area (mm^2) (Fig. 2-9c).

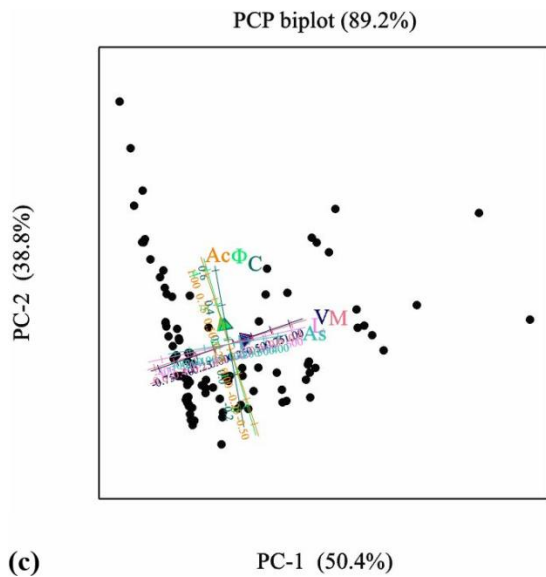
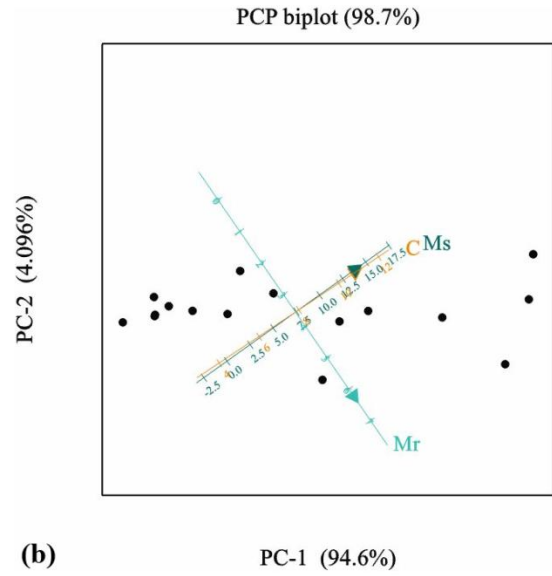
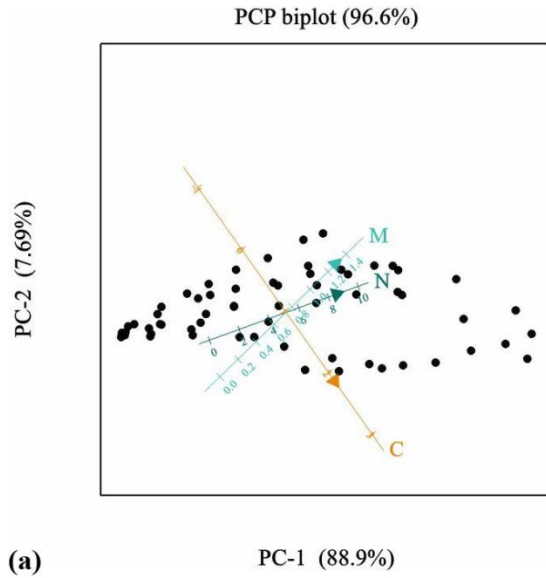


Figure 2-9. Interpolative biplots of the dimensions (a) capacitance (C, nF), root mass (M, g), and root number (N) of 61 individual barley roots from experiment I (Table 2-3); (b) C, root system mass (M_r , g) and shoot mass (M_s , g) of 16 barley plants from experiment II (Fig. 2-4b); (c) C, M, root volume (V , mm^3), root surface area (A_s , mm^2), root circumference at the solution surface (Φ , mm), and root cross-sectional area at the solution surface (A_c , mm^2) of 94 individual barley roots from experiment III; and (d) C, Φ , A_s of the same roots as in (c). Circles represent the scores that replace the original values, lines the original variables. Lines in the same direction indicate positive correlation; lines at right angles indicate no correlation. The percentage variance explained by the each principal component displays how much of the total variation in the data the component accounts for.

2.2.4 Conclusions

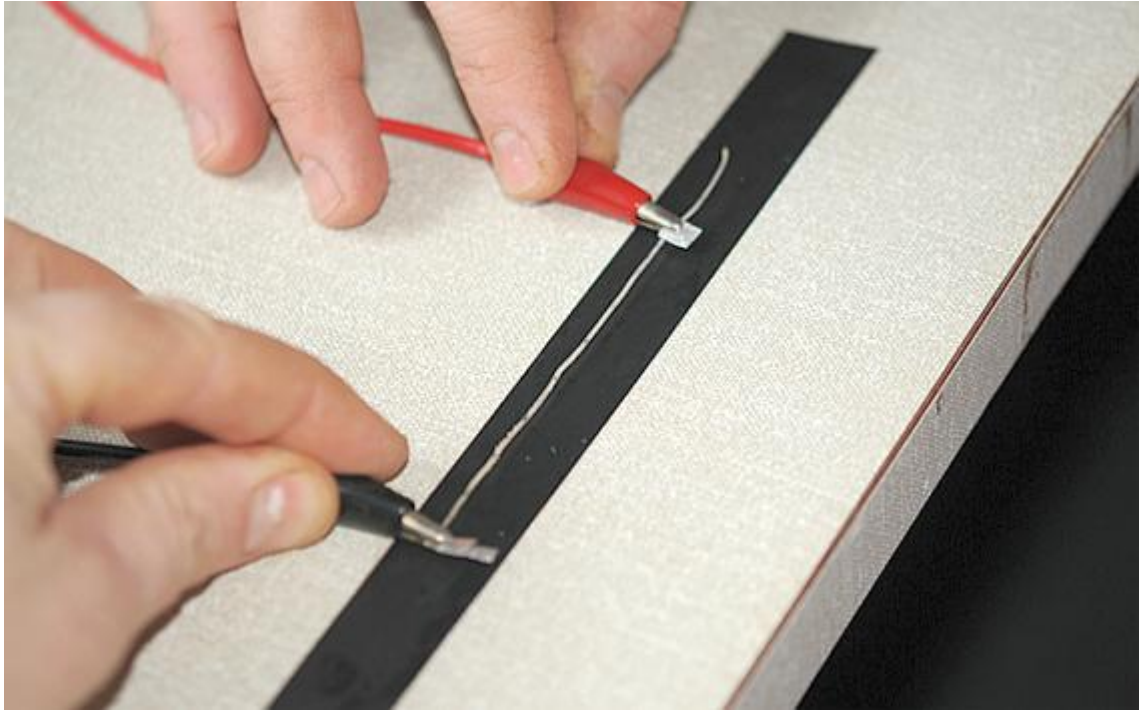
The preliminary experiments have shown that although linear correlations of capacitance and root system mass can be achieved, this is not always the case (e.g. Fig. 2-4b, d). The work suggests that good correlations can be achieved between root system mass and the root total cross-sectional area at the solution surface: Correlations between capacitance and root mass were only found for whole root systems (Fig. 2-5c), and not for individual roots (e.g. Figs 2-4d and 2-10c). Their capacitances were more closely correlated with root dimensions at the solution surface than with any parameter for the total root size (Fig. 2-9a, c). These findings cannot be explained with the Dalton (1995) model, but might be consistent with a simple analogy of the plant material between solution surface and plant electrode being equivalent to a dielectric material between two electrodes, the second electrode being the solution surface. The analogy could explain why (1) unbranched roots acted more similarly to capacitors in serial connection along the root axis (Fig. 2-8), (2) multiple roots as capacitors in parallel connection (Table 2-3), and (3) root dimensions in solution were not related to the capacitance at all (Fig. 2-9c).

The strip-electrode gave larger capacitance values than needle- or clip-electrodes and ensured good contact between electrode and each tiller at all growth stages. Furthermore it is a non-invasive device allowing capacitance measurements at even very early stages of development where a needle would be more destructive.

A thorough re-evaluation of the capacitance technique is necessary. This requires further investigations that aim to answer the following questions

- Does root material provide capacitance equally?
- How does root material in solution, at the surface, and out of solution influence the capacitance measurement?
- Does the capacitance of the solution influence the capacitance measurement, as well?

The next chapter presents a series of experiments that aims to answer these questions for barley growing in hydroponics.



3 TESTING THE DALTON MODEL OF CAPACITANCE FOR BARLEY IN HYDROPONICS

The experiments in this chapter test the Dalton (1995) model for barley plants in hydroponics, using a range of treatments that included: raising roots out of solution, cutting roots at positions below the solution surface, and varying the distance between plant electrode and the solution surface. The results of these tests proposed a re-evaluation of the physical basis for the electrical capacitance of plants in hydroponics. This chapter forms the basis of a paper in the format of the *Journal of Experimental Botany*, and is kept largely in the same format (Dietrich *et al.*, 2012).

3.1 Introduction

The most widely-accepted model to explain the capacitance of plant root systems was put forward by Dalton (1995). He proposed a simple resistance–capacitance model (Fig. 3-1) to describe the underlying electrical pathways between an electrode in the root substrate and an electrode inserted into the base of the shoot. The model considers roots to be equivalent to cylindrical capacitors. It suggests that the plasma membranes of root cells serve as dielectrics (Dvořák *et al.*, 1981) separating the soil solution from the inner solution and generating capacitance. Accordingly, the boundary layers between the plasma membranes of root cells and these solutions are seen as equivalent to capacitor plates. Thus, the capacitance of a root system would be linearly related to its size, analogous to the addition of capacitors when they are connected in parallel (Eqn 2). Dalton's model (1995) has gained wide acceptance, because the linear relationship between the capacitance and the size of a plant root system it predicts has been found for many different plant species in many different substrates (Table 1-2). Dalton (1995) surmised that the suberized plant tissue of fully developed endodermis would act as an

insulator. Hence, according to Dalton, the root capacitance would be provided predominantly by “active” apical parts of the root. The model equates xylem and phloem vessels with wires that conduct the current to the plant electrode aboveground. Thus, Dalton (1995) concluded that root-C would provide information about both the mass and the physiological “activity” of roots. Dalton (1995) observed what he called a “hyperbolic decrease of capacitance” with increasing distance between the shoot electrode and the soil surface and explained this by a network of resistance–capacitance elements in the shoot connected in series. When capacitors are connected in series, the effective plate separation increases and the total capacitance (C_{total}) is then less than that of the smallest capacitor (Eqn 13). The substrate (soil, sand, water, etc.) around the roots also provides capacitance, and the root system and substrate can be considered as two capacitors connected in series (Rajkai *et al.*, 2005). Hence, an accurate estimation of the capacitance of a root system requires either that the capacitance of the substrate is substantially higher than that of the root system or that it is known: this criterion is met, at least in fine sandy subsoil at 1 kHz for sunflower root, according to Rajkai *et al.* (2005).

Although Dalton’s (1995) key prediction of a linear relationship between capacitance and root mass is supported by a number of studies (Table 1-2), there are several examples of apparent failures of the model. For example, the best fitting regressions are not always linear functions, but can be quadratic (Preston *et al.*, 2004) and, even when a linear regression fits, the intercept often deviates from zero (e.g. van Beem *et al.*, 1998; McBride *et al.*, 2008). To evaluate Dalton’s (1995) model more fully, we devised a series of tests using a hydroponic system to minimise complications resulting from the soil component of the electrical pathway. These tests included: (1) using roots and root systems of different sizes and ages, (2) comparisons of nodal and seminal roots, (3) removal of parts of submerged roots and root systems, (4) changing the depth of submergence of roots and root systems, (5) varying the location of the plant electrode, and (6) measuring roots and root systems in air.

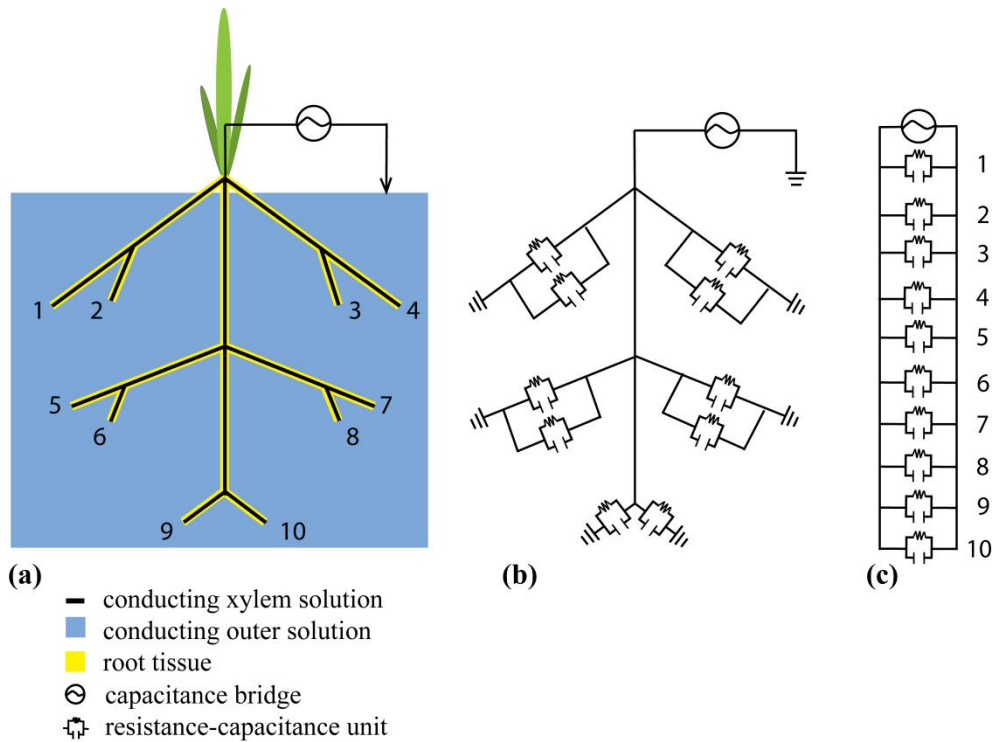


Figure 3-1. Resistance-capacitance (RC) circuits according to the Dalton (1995) model: (a) diagram of a plant root system with ten root tips showing the tissue separating the xylem solution from the nutrient solution, (b) electrical equivalent network of the root system showing the location of the RC components, and (c) the equivalent circuit for the root system. Note that the individual RC components can have different values.

3.2 Material and methods

Plant material

Barley caryopses were surface sterilised by soaking in a saturated 2% calcium hypochlorite solution for 15 minutes, then rinsed three times in distilled water. The caryopses were germinated on paper towel moistened with sterile distilled water in a sterile Petri dish in the dark at 16°C for four days. Five days after sowing (DAS) 20 seedlings at similar stages of development were transferred to a 10 L basin in a controlled environment room. Plants were illuminated for 18 hours daily with a photon irradiance (PAR; 400–700 nm) of $320 \mu\text{mol m}^{-2} \text{s}^{-1}$ at plant height. The day/night temperature regime was 18°C/12°C. The basin was filled with

nutrient solution (Table 2-1) and aerated through eight porous stones (Hagen Inc., Toronto, Canada). Air pressure was provided by an air pump (Motore Asincrono, No. G0225, Lafert Electric Motors Ltd., Cheshire, UK). Ten DAS₁ seedlings were transferred to plastic tubes of 50 mm diameter, 1 m length and two litres volume (Fig. 3-2). Each seedling grew in a separate tube containing a gently-bubbling, aerated, nutrient solution. Losses of water by evaporation and transpiration were replaced daily. The nutrient solution was replaced weekly and on the day before harvest.

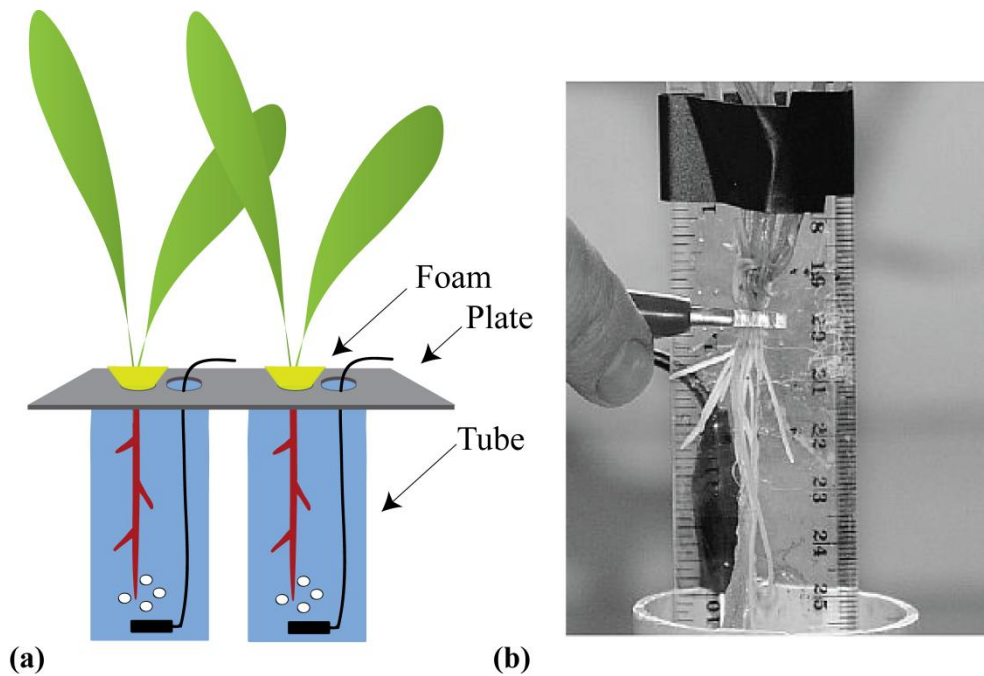


Figure 3-2. Experimental apparatus: (a) plants supported in foam within plastic tubes (50 mm diameter \times 1 m length) containing aerated nutrient solution (not to scale), (b) capacitance measurement with one electrode (a stainless steel rod) submerged in the solution and the other (a strip of aluminium foil) wrapped around either a single root or the whole root system.

Measurement of capacitance

Capacitance measurements were made on plants between 22 and 37 DAS to create root systems of a wide range of sizes. For these measurements, foam, husk and dead leaves were removed, and plants were placed in tubes filled with fresh nutrient solution. In the case of whole root systems, nodal roots that were too short to enter the solution surface by more than 2–3 mm were excised at the plant base. This was necessary, because root tips that just touched the solution surface caused large variations in capacitance. Capacitance was measured at 1kHz and 1V with an LCR-meter (Passive Component LCR Meter, Extech Instruments, Massachusetts, USA) connected to a ‘solution’ electrode and a ‘plant’ electrode via alligator clips. The solution electrode was a stainless steel rod (length, 165 mm; diameter 3 mm) placed at the edge of the tube, of which 12 cm was submerged. The capacitance readings were insensitive to electrode depth or position. The plant electrode was a strip of aluminium foil (breadth 4 ± 0.5 mm; 8-fold thickness) wrapped around the plant tissue and clamped with the alligator clip. In a preliminary experiment the foil strip was found to be the gentlest and most flexible way of attaching the electrode to a plant when compared with subcutaneous needles (Dalton, 1995; Ozier-Lafontaine and Bajazet, 2005; Chloupek, 1977; Tsukahara *et al.*, 2009; Blomme *et al.*, 2004), with wires (Preston *et al.*, 2004) or with clamping devices (Rajkai *et al.*, 2005; Kendall *et al.*, 1982; van Beem *et al.*, 1998) which injured the plant. The use of foil also gave more reproducible C-values (data not shown). The capacitance measurements performed are shown in Figure 3-3.

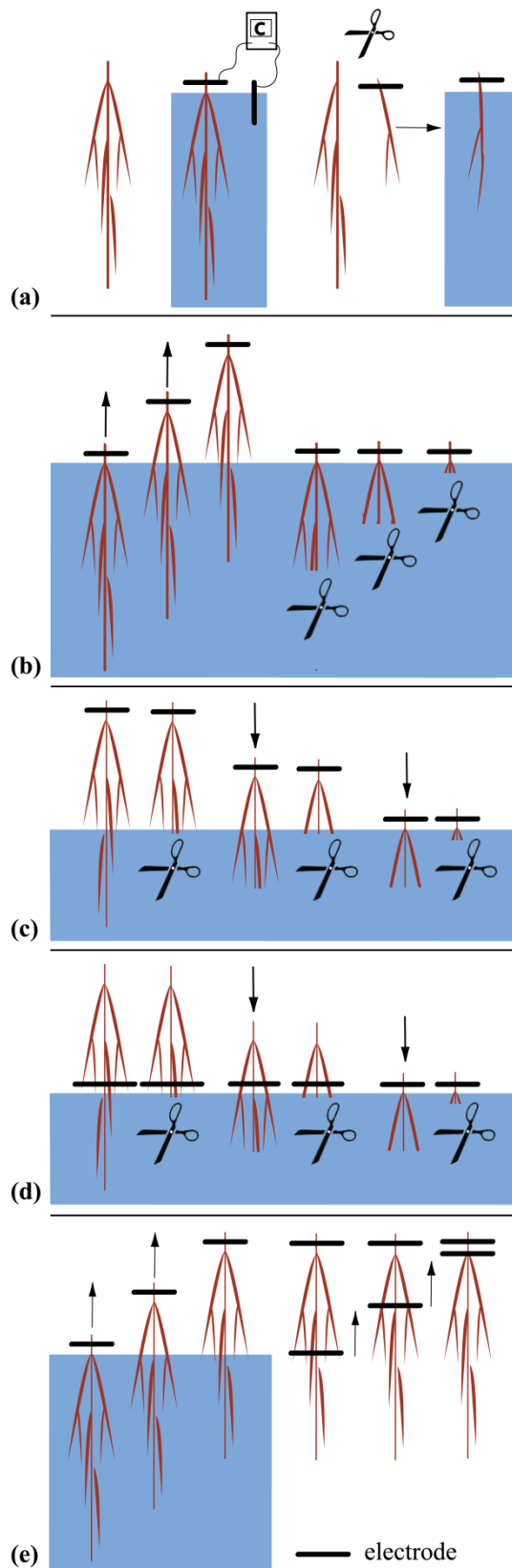


Figure 3-3. Capacitance measurements performed on whole root systems and single roots: (a) Plant electrodes were attached to the top of the root system, roots were submerged to 5 mm from the plant electrode, and the capacitance measured. Then, similar measurements were made with single excised roots. (b) Plant electrodes were attached to the top of the roots, roots were submerged to 5 mm from the plant electrode, and the capacitance measured. Then, roots were raised incrementally and capacitance was measured after each increment. After this, roots were trimmed incrementally from the bottom and, after the removal of each increment, the remaining root was resubmerged to 5 mm from the plant electrode and capacitance measured. (c) Roots were removed from the solution and plant electrodes were attached to the top of the roots. Roots were partially submerged and capacitance measured. Roots were then trimmed 1–2 mm below the solution surface and the capacitance remeasured. This procedure was repeated incrementally by further submergence and trimming until no root remained. (d) Roots were removed from the solution and partially resubmerged. Then the plant electrodes were attached to roots 5 mm above the solution and capacitance measured. Roots were trimmed 1–2 mm below the solution surface and the capacitance remeasured. This procedure was repeated incrementally by further submergence and trimming until no root remained. (e) Plant electrodes were attached to the top of the roots, roots were submerged to 5 mm from the plant electrode, and the capacitance measured. Roots were then raised incrementally and capacitance was measured after each increment until the entire root was removed from the solution. The root was then blotted with a damp paper towel and the alligator clip formerly attached to the solution electrode was clamped directly on to the root at different positions and the capacitance measured at each position.

Root mass and diameter

After capacitance measurement, roots were stored for up to 20 d in damp paper towel sealed within Petri dishes placed in a fridge at 6 °C. Root fresh mass (FM) was measured and root diameters determined using a microscope with eyepiece graticule (MZ75, MZFIII, Leica, Solms, Germany). Root cross-sectional areas (A_c) and circumferences (Φ) were calculated assuming a circular geometry.

Statistics

Capacitance data are expressed as mean \pm standard deviation (SD) from three repeated measurements (technical replicates). Regression analyses and t-tests were performed using Sigmaplot 11 or Sigmaplot 12 software (Systat Software Inc., Chicago, IL, USA). Regression coefficients are expressed as mean \pm standard error (SE) from n determinations.

3.3 Results and discussion

The relationships between capacitance and mass for submerged roots (Fig. 3-3a)

The finding of first experiments (Fig. 3-3a left) was a significant correlation between capacitance and mass across sixteen completely-submerged whole root systems of different ages and thus sizes (Fig. 3-4). Dalton's model (1995) predicts a linear relationship between capacitance and mass of roots submerged. The linear regression line intercepts the y-axis at 221 ± 0.024 nF (mean \pm SE, n = 16).

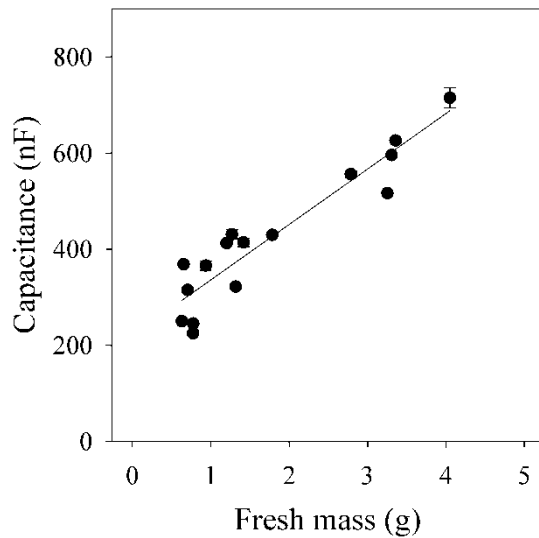


Figure 3-4. Relationship between capacitance (C , nF) and fresh mass (M , g) of 16 whole root systems of different ages submerged with 5 mm distance remaining between solution surface and plant electrode. Linear regression: $C = 0.115 (\pm 0.012) M + 0.221 (\pm 0.024)$ (mean \pm SE, $R^2 = 0.869$, $P < 0.0001$). Data represent the mean \pm SD of three repeated measurements.

In contrast to the results obtained for entire root systems (Fig. 3-4), when individual excised seminal and nodal roots were examined (Fig. 3-3a right), there was little relationship between capacitance and root mass (Fig. 3-5a). This does not concur with the model of Dalton (1995). Significant linear relationships were obtained between capacitance and root cross-sectional area at the solution surface for both seminal and nodal roots (Fig. 3-5b). The gradient of this relationship was 4.3-times steeper for seminal than for nodal roots. Thus, seminal roots provided more capacitance per unit area than nodal roots. This might be due to differences in the anatomy or morphology of seminal and nodal roots (Esau, 1977). As apparent in figure 3-5b, the cross-sectional area at the solution surface of seminal roots was generally less than that of nodal roots.

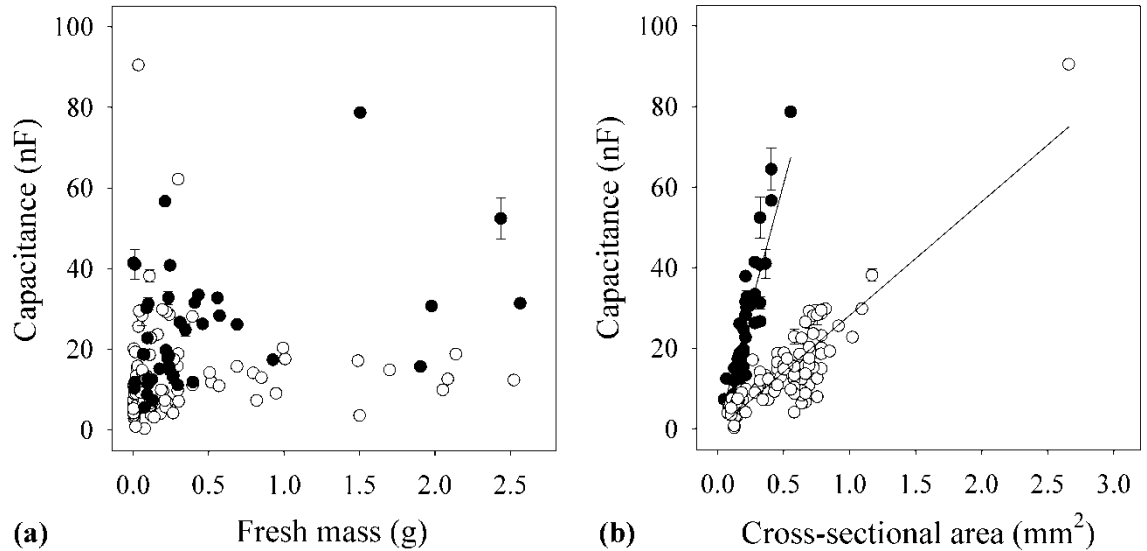


Figure 3-5. Relationships between capacitance (C , nF) and (a) fresh mass (mg) and (b) the sum of cross-sectional areas at the solution surface (A_c , mm²) for (●) 48 seminal and (○) 103 nodal roots after excision from eight plants. The roots were submerged with 5 mm between solution surface and plant electrode (see Fig. 3-3a). There was no significant correlation between C and fresh mass for seminal roots or nodal roots. Linear regressions were forced through the origin and were for the relationships between C and A_c $C = 121 (\pm 4.4) A_c$ ($R^2 = 0.806$, $P < 0.0001$) for seminal roots and $C = 28.2 (\pm 0.88) A_c$ ($R^2 = 0.771$, $P < 0.0001$) for nodal roots (mean \pm SE). Data represent the mean \pm SD of three repeated measurements.

Further evidence that capacitance is not linearly related to the root mass submerged (Figs 3-3b, 3-3c, 3-3d)

When roots were raised incrementally out of solution (Fig. 3-3b, left), capacitance decreased nonlinearly with each increment (Fig. 3-6a). In the same experiment, capacitance increased nonlinearly with increasing root mass submerged (Fig. 3-6b). These results do not agree with any model predicting a simple linear relationship between capacitance and mass of roots submerged. It suggests that root tissues close to the plant electrode contribute disproportionately to the measured capacitance. Equivalent data were obtained when plant electrodes were attached to the top of the roots and roots were lowered incrementally into solution (Fig. 3-3c; Fig 3-7a). There was an approximately linear relationship between measured capacitance and the reciprocal of the distance between the plant electrode and the

solution surface (Fig. 3-6c), which is that expected for capacitors connected in series along the root axis (Eqn 13).

Trimming roots (Figs 3-3b right and 3-3c) did not affect capacitance (Figs 3-6d and 3-7b): linear regressions between capacitance before and after trimming did not differ significantly from a 1:1 relationship. Again this is inconsistent with the model of Dalton (1995), which suggests that capacitance is determined by submerged root mass or the “active” apical parts of the root. Similar insensitivity to root excision was found for capacitance measurements by Matsumoto *et al.* (2001) and Kendall *et al.* (1982) and resistance measurements by Cao *et al.* (2010).

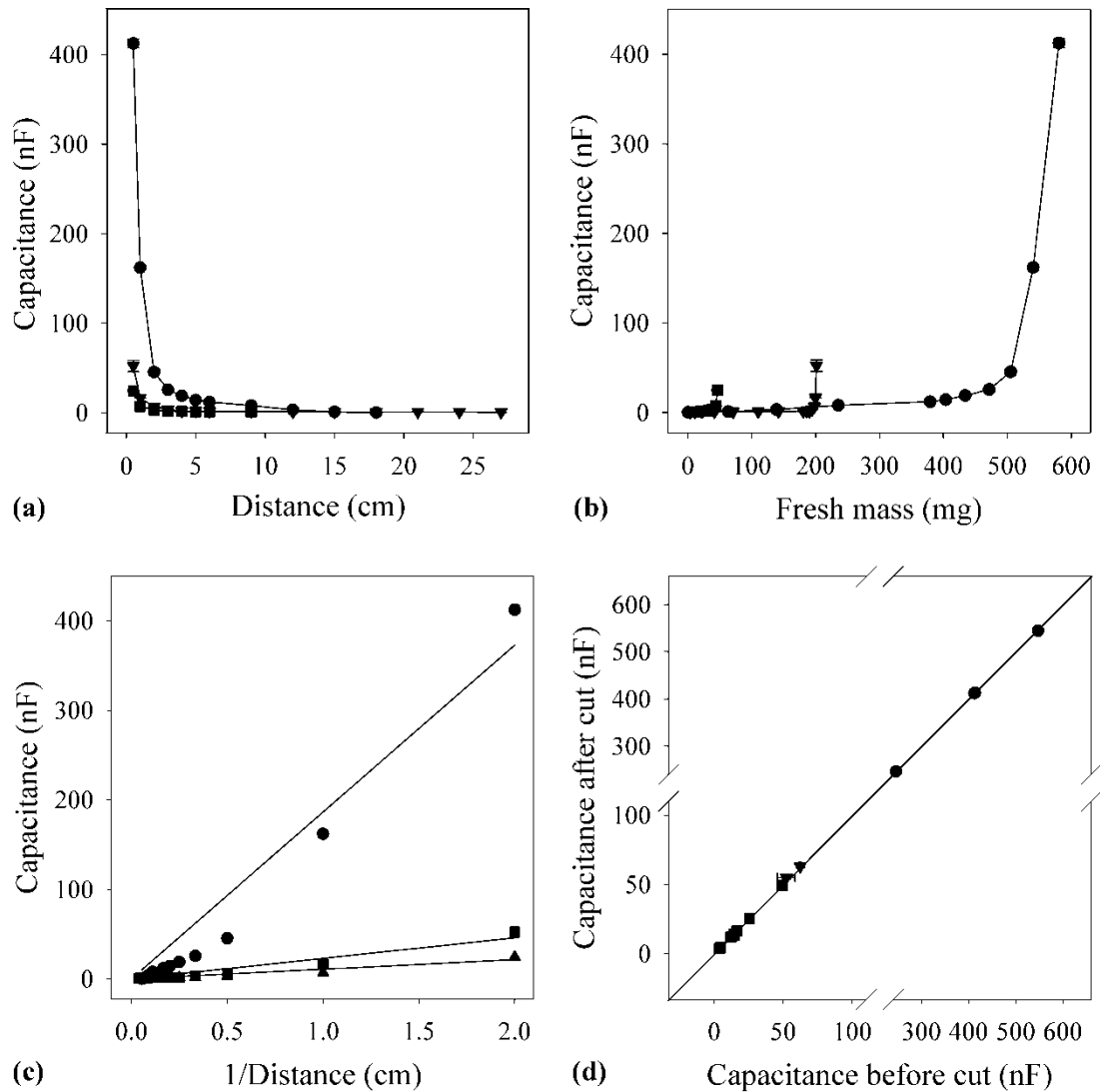


Figure 3-6. Examples of relationships between capacitance (nF) and (a) the distance (D , cm) between the plant electrode and the solution surface and (b) the fresh mass (mg) of submerged root tissue when roots were raised incrementally out of solution (Fig. 3-3b left). Data are shown for a whole root system (circles), an excised seminal root (triangles) and an excised nodal root (squares) from a survey of four whole root systems and 10 individual roots. (c) The relationship between capacitance (C) and the reciprocal of the distance ($1/D$) between plant electrode and solution surface. The linear regression was forced through the origin and was for the root system $C = 186.43/D \pm 12.02$ (mean \pm SE, $n = 11$, $R^2 = 0.949$, $P < 0.0001$), for the seminal root system $C = 22.96/D \pm 1.48$ (mean \pm SE, $n = 14$, $R^2 = 0.936$, $P < 0.0001$), and for the nodal root $C = 10.82/D \pm 0.96$ (mean \pm SE, $n = 8$, $R^2 = 0.925$, $P < 0.0001$). (d) The relationship between capacitance measured after (C_a) and before (C_b) complete trimming of the submerged root (Fig. 3-3b right). The linear regression was $C_a = 0.997 \pm 0.002 C_b + 0.323 \pm 0.364$ (mean \pm SE, $n = 14$, $R^2 = 1.000$). Data are shown for four whole root systems (circles), two excised seminal roots (triangles) and eight excised nodal roots (squares). Data represent the mean \pm SD of three repeated measurements.

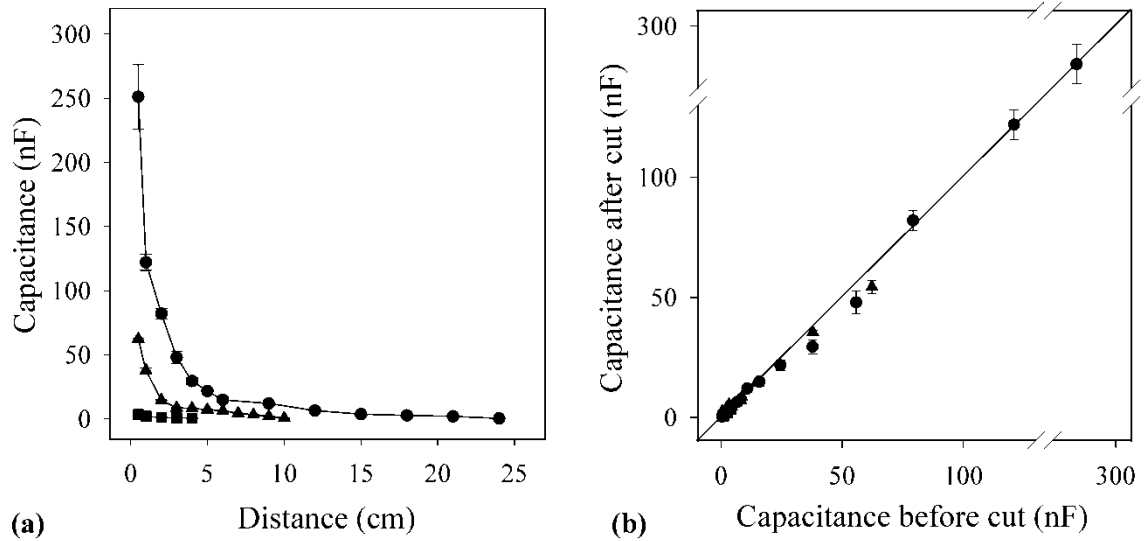


Figure 3-7. (a) Relationship between capacitance and the distance between the plant electrode and the solution surface, when roots were lowered incrementally into solution (Fig. 3-3c). (b) The relationship between capacitance measured after (C_a) and before (C_b) trimming of the submerged root (Fig. 3-3c). The linear regression for the combined data was $C_a = 1.008 \pm 0.01 C_b - 1.47 \pm 1.17$ (mean \pm SE, $n = 29$, $R^2 = 0.998$). Points represent the mean \pm SD of 3 repeated measurements. Data are shown for a whole root system (circle), an excised seminal root (triangle) and an excised nodal root (square). Capacitance was measured at increments of 1 cm for the first 6 cm and in increments of 3 cm thereafter.

Capacitance depends strongly on root cross-sectional area at the solution surface (Fig. 3-3d)

Capacitance was measured at different positions on an individual root or root system, in each case with the electrode 5 mm above the solution surface (Fig. 3-3d). Complex relationships were observed between capacitance and position (Fig. 3-8a). Maximal capacitance occurred in both whole root systems and seminal roots where the number of secondary roots was greatest. In general, young whole root systems had greater capacitance than young seminal roots which in turn had greater capacitance than nodal roots. Trimming roots (Fig. 3-3d) did not affect capacitance ($P > 0.1$; data not shown). Total root cross-sectional area at the solution surface varied in the same way as capacitance with position (Fig. 3-8b). The relationship between capacitance and cross-sectional area at the solution surface was linear for any individual root or root system (Fig. 3-8c; Table 3-2). This confirms the previous observation that capacitance was linearly related to cross-sectional area at the top of the root when fully submerged (Fig. 3-5b).

The slopes of these relationships were greater for whole root systems and branched seminal roots than for unbranched nodal roots (Table 3-2). There were large differences between slopes for individual seminal roots. The regressions between capacitance and cross-sectional area at the solution surface usually passed through the origin, though intercepts were occasionally found (intercepts not shown; there were very few such cases and no obvious characteristics of roots with intercepts were observed). The R^2 values for regressions of capacitance against sum of circumferences of individual roots at the solution surface and against the total cross-sectional area at the solution surface were not consistently different (Table 3-2). Therefore it is unclear as to which relationship is stronger.

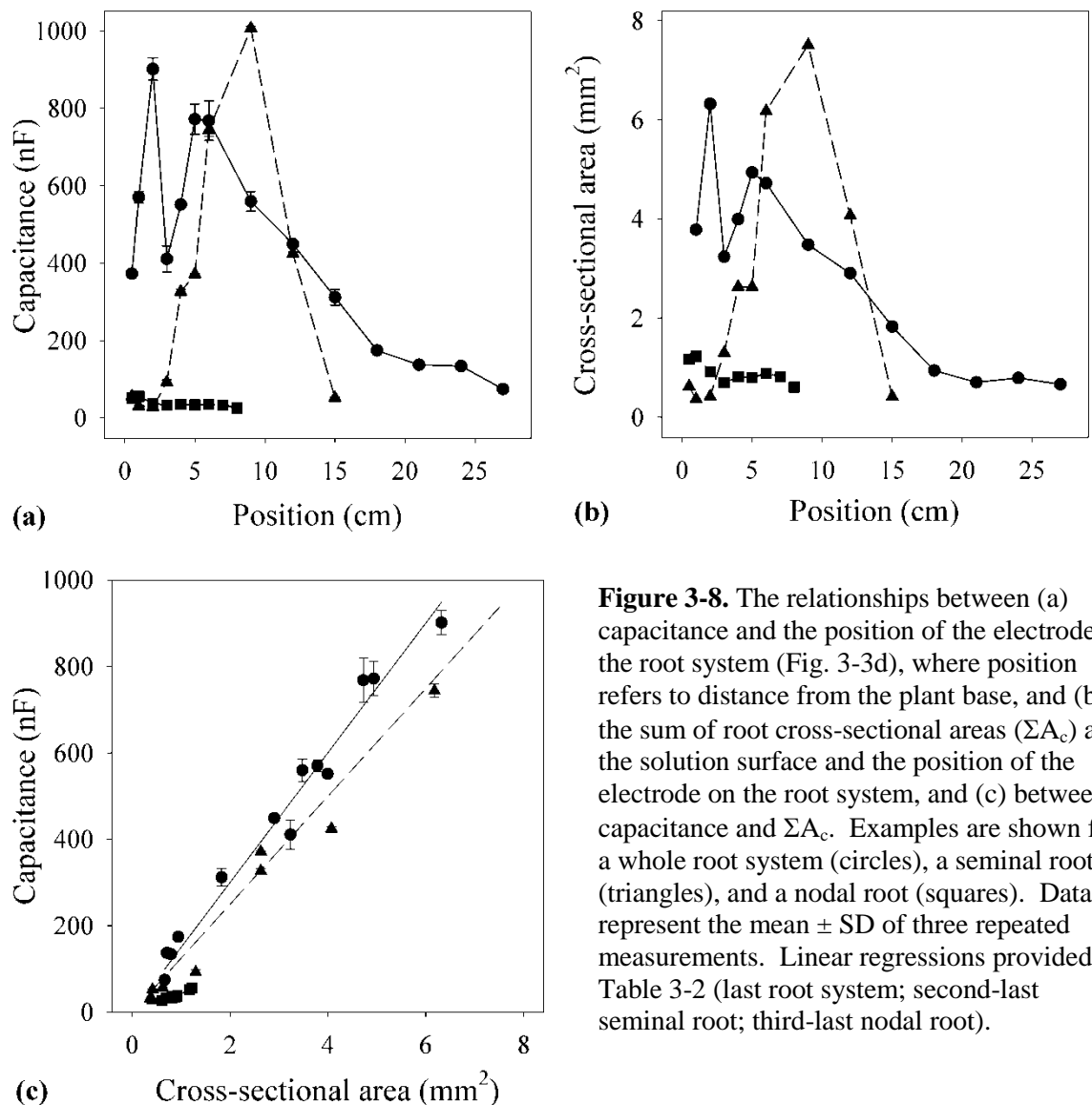


Figure 3-8. The relationships between (a) capacitance and the position of the electrode on the root system (Fig. 3-3d), where position refers to distance from the plant base, and (b) the sum of root cross-sectional areas (ΣA_c) at the solution surface and the position of the electrode on the root system, and (c) between capacitance and ΣA_c . Examples are shown for a whole root system (circles), a seminal root (triangles), and a nodal root (squares). Data represent the mean \pm SD of three repeated measurements. Linear regressions provided in Table 3-2 (last root system; second-last seminal root; third-last nodal root).

Table 3-1. Linear regressions forced through the origin for capacitance against the root cross-sectional area and sum of circumferences of individual roots at the solution surface. P values were <0.0001 for all regressions.

Key: DAS: days after sowing, C: Capacitance (nF), A: cross-sectional area (mm²), Σκ: sum of circumferences of individual roots (mm), SE(b): Standard error of coefficient

Root type	DAS	n	C = b.A			C=b.Σκ		
			b	SE(b)	R ²	b	SE(b)	R ²
root system	22	11	103	2.8	0.967	9.09	0.84	0.567
root system	22	13	190	11.4	0.853	13.6	0.64	0.906
root system	22	12	208	17.0	0.759	17.9	0.61	0.950
root system	24	14	145	5.6	0.923	14.2	0.62	0.900
seminal root	22	12	265	16.5	0.929	16.6	0.60	0.977
seminal root	27	9	165	10.7	0.930	10.7	0.73	0.922
seminal root	28	9	109	5.9	0.954	12.9	0.69	0.955
seminal root	30	13	146	7.1	0.940	9.46	0.64	0.887
seminal root	32	11	72	3.1	0.946	4.54	0.23	0.926
seminal root	34	7	80	4.6	0.952	6.83	0.41	0.948
seminal root	37	11	92	8.2	0.837	25.5	1.95	0.879
seminal root	37	9	144	4.2	0.989	11.1	0.32	0.989
seminal root	37	10	125	4.2	0.980	12.0	1.04	0.876
seminal root	37	9	82	4.3	0.965	9.13	0.44	0.971
nodal root	28	6	27	0.9	0.941	6.76	0.56	0.632
nodal root	29	13	55	4.7	0.341	12.5	0.41	0.895
nodal root	29	13	36	1.1	0.780	9.06	0.28	0.780
nodal root	37	9	53	2.0	0.857	12.9	0.63	0.757
nodal root	37	9	43	0.8	0.953	11.6	0.55	0.673

Capacitance of roots out of solution (Fig. 3-3e right)

The capacitance measured in plants in air, when electrodes were placed at the base of the shoot and at any point on the root system (Fig. 3-3e), equalled the capacitance measured in the hydroponic system when the root system was raised out of solution to the same point (Fig. 3-9). These values followed a 1:1 line. This confirms that the root below the solution surface has negligible effect on the measured capacitance, which depends only on the material between the plant electrode and the solution surface.

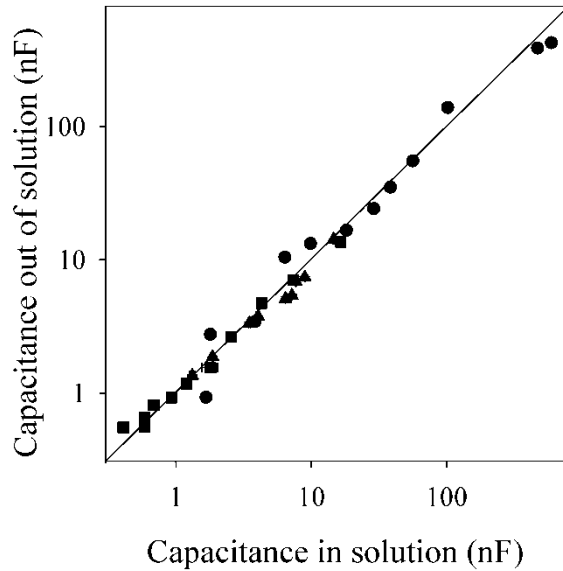


Figure 3-9. Relationship between the capacitances of roots measured in solution against capacitance measured at an equivalent separation of electrodes in roots removed from solution (Fig. 3-3e). Examples are shown for a whole root system (circles), a seminal root (triangles), and a nodal root (squares). Data represent the mean \pm SD of three repeated measurements. The line indicates a 1:1 relationship.

Towards a new model for root capacitance

The model of Dalton (Fig. 3-1) is consistent with the initial observations reported here (i.e. the linear correlation between capacitance and root mass; Fig. 3-4), but it cannot explain the other observations herein (Figs 3-5 to 3-9). The observation that root capacitance is dominated by the capacitance of the tissue between the solution surface and the plant electrode has led us to formulate an alternative model (Fig. 3-10); this has some similarities to the one proposed by Cao *et al.* (2011).

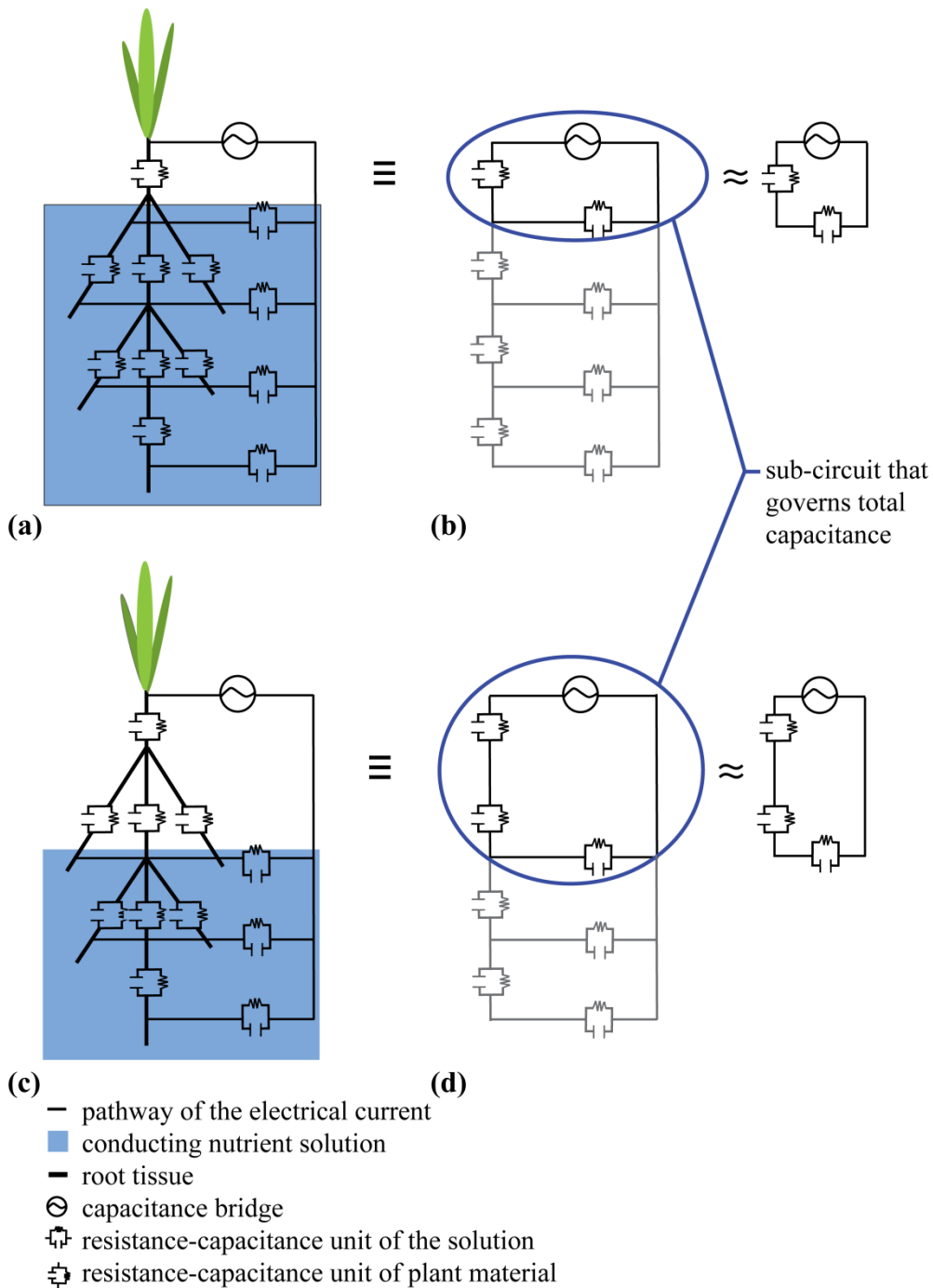


Figure 3-10. Resistance–capacitance (RC) circuits according to the revised model: (a,c) diagrams of barley plants with five root tips, (b,d) electrical equivalent networks of the root systems showing the location of the RC components, (a,b) RC circuits for a completely submerged root system, (c, d) RC circuits for a partly submerged root system. The sub-circuit that largely determines the capacitance is ringed to emphasise its importance. Note that the individual RC components can have different values.

The basics of the new model are as follows. (1) The capacitance of the solution is much greater than the capacitance of the plant tissue (preliminary experiments suggest that this is also the case in soil at field capacity). (2) The capacitances of tissues along an unbranched root can be considered as connected in series. (3) The capacitances of multiple unbranched root sections comprising the whole root system act in parallel, but reduce to the equivalent of a single capacitor. (4) The capacitances of individual roots are directly proportional to their cross-sectional area or circumference (Fig. 3-5b; Table 3-2), though different constants of proportionality may apply to different roots.

The new model is consistent with all of the observations. For example: A linear correlation between capacitance and root mass (Fig. 3-4) is explained in the new model by the capacitance being proportional to root cross-sectional area at the solution surface. The positive intercept for the relationship between capacitance and root mass (Fig. 3-4) is due to the substantial contribution to the measured capacitance of the plant material between the solution surface and the plant electrode. The lack of correlation between the capacitance of individual roots and their fresh mass shown in the experiments (Fig. 3-5a) occurs because the root cross-sectional area at the solution surface varies independently of root mass. The non-linear relationship between capacitance and the distance between the plant electrode and solution surface (Figs 3-6a, 3-7a) fits a reciprocal relationship which is that expected of a series of capacitors along the root axis. The lack of effect of trimming roots below the solution surface (Figs 3-6d, 3-7b) is explained by root of below the solution surface having negligible effect on the measured capacitance, which implies that the material between the plant electrode and the solution surface dominates measured capacitance. This is also consistent with the 1:1 relationship between the capacitance measured in plants in air, when electrodes were placed at the base of the shoot and at any point on the root system, and the capacitance measured in the hydroponic system when the root system was raised out of solution to the same point (Fig. 3-9). The complex relationship

between capacitance and electrode position on the root (Fig. 3-8a, b) can be explained by the variation in root cross-sectional areas with position. This effect can be incorporated into the model by correcting the capacitance estimate through weighting the values according to the variation in cross-sectional area. This can be achieved by calculating capacitance according to the following equation:

$$C \propto \left[\sum_{i=1}^n \frac{\Delta d_i}{A_i} \right]^{-1} \quad (7)$$

where, A_i is the cross-sectional area of the i^{th} segment of root of length Δd , where the summation is along n segments of root. An example of this relation is given in Figure 3-11, using data recalculated from Figure 3-8, where A is in mm^2 , and Δd is in cm.

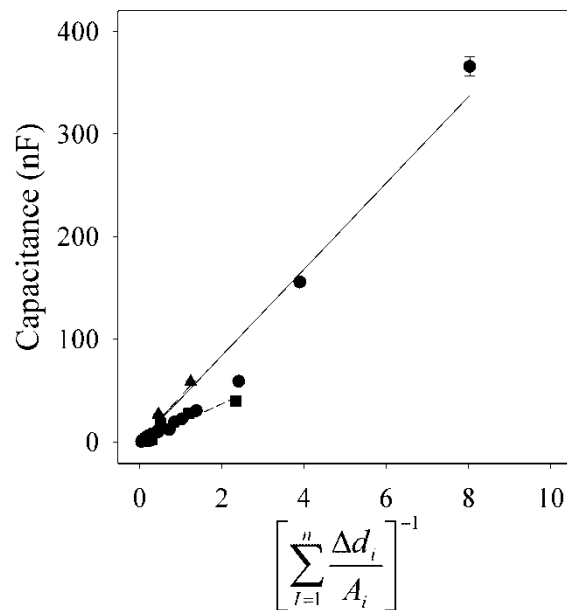


Figure 3-11. The relationships between capacitance and the reciprocal of cumulative distance/area $\left[\sum_{i=1}^n \frac{\Delta d_i}{A_i} \right]^{-1}$ (Eqn 7) for a whole root system (circles), a seminal root (triangles) and an unbranched nodal root (squares). The linear regression coefficients for the relationship

were $C = 491.3 \left[\sum_{i=1}^n \frac{\Delta d_i}{A_i} \right]^{-1}$ ($R^2 = 0.964$, $P < 0.0001$, $n = 13$) for the whole root system, $C =$

$281.6 \left[\sum_{i=1}^n \frac{\Delta d_i}{A_i} \right]^{-1}$ ($R^2 = 0.964$, $P < 0.0001$, $n = 10$) for the seminal root and $C = 48.46$

$\left[\sum_{i=1}^n \frac{\Delta d_i}{A_i} \right]^{-1}$ ($R^2 = 0.989$, $P < 0.0001$, $n = 9$) for the nodal root. Values were calculated from

data presented in Figure 3-8 (where A is in mm^2 , and Δd is in cm), and represent the mean \pm SD of three repeated measurements.

Remaining questions include: (1) Why is the linear relationship between capacitances and root cross-sectional area good for individual roots, but differs between roots? This might be related to differences in anatomy, for example, between nodal and seminal roots. (2) What is the underlying physical basis for the good relationship between measured capacitances and root cross-sectional area (or circumference)? One possible analogy is to consider the plant tissue as a homogenous dielectric material of dielectric constant ϵ , of cross-sectional area A and thickness d . The capacitance would then be given by Equation 4. (3) How do the measurements made in hydroponics relate to measurements made in other growth media? In the new model the measured capacitance is dominated by the total cross-sectional area of root near the solution surface and its distance from the plant electrode. Thus, the measured capacitance can provide an estimate of the number of roots at the solution surface if these two variables are related, thereby allowing capacitance to “measure” the developmental stage and growth rate and the size of a plant’s root system. The location of the interface between root and soil solution will have a great influence on the measured capacitance. Indeed, the new model explains why the measured capacitance is lower in dry soil than in wet soil (c.f. Dalton, 1995; Kendall *et al.*, 1982). This arises because there is less effective contact between the plant and the root–soil solution menisci distributed along the root surface.

3.4 Conclusions

In conclusion, the measurements of electrical capacitance of barley roots were inconsistent with the model of Dalton (1995) in many respects. This necessitated a new model for the underlying electrical pathways (Fig. 3-10); this new model was consistent with all observations herein. It approximates the root tissue as a continuous dielectric and, therefore, root capacitances can be calculated according to established physical principles. Root capacitance is dominated by the tissue between the plant electrode and the solution surface and closely related to the cross-sectional area (or circumference) of the root at the solution surface. Measurements of root capacitance are applicable to studies of root development, although the data obtained should be interpreted in the context of the new model. This cautions that the results will be dominated by only a small fraction of the total plant root tissue.

Chapter 4 describes series of experiments to investigate the capacitance of wheat and barley plants grown in compost, soil, and sand. Water regime within the rooting substrate is varied systematically, in a manner analogous to the experiments in Chapter 3.



4 ELECTRICAL CAPACITANCE OF PLANTS IN SOLID MEDIA

This chapter describes results of experiments to investigate the capacitance of cereal plants in compost, sand and in field soil. The effects of water distribution, the role of aboveground plant material, and the role of the plant electrode were investigated. The results described have been submitted as an article in the Journal of Applied Botany and this is based largely on the content of this paper.

4.1 Introduction

Many studies have reported good correlations between root mass and electrical capacitance, measured between an electrode inserted at the base of the stem and an electrode in the rooting substrate (e.g. Dalton, 1995; Ozier-Lafontaine and Bajazet, 2005; Chloupek, 1977; van Beem *et al.*, 1998; McBride *et al.*, 2008; Preston *et al.*, 2004; Tsukahara *et al.*, 2009). Linear relationships between root mass and electrical capacitance have been interpreted using an electrical model proposing that roots behave as cylindrical capacitors and their capacitances can be added together as though wired in parallel (Dalton (1995). This model was tested in hydroponics (Ch. 3) finding that the capacitance of barley (*Hordeum vulgare* L.) appeared to be determined, not by the mass of their root system, but by the cross-sectional area of roots at the solution surface. It was also observed (a) that capacitance was not linearly related to the mass of roots in solution when root systems were partly submerged and (b) that excising the root below the solution surface had negligible effect on the capacitance measured. These observations are inconsistent with the model of Dalton (1995). The new model for plant capacitance was proposed in Chapter 3 suggesting that plant tissue behaves as a continuous dielectric and, provided the capacitance of the tissue is much smaller than that of the rooting

substrate, the capacitance measured in hydroponics is dominated by tissue between the solution surface and the electrode attached to the plant. The new model suggests that the measured capacitance will be inversely proportional to the distance between the plant electrode and the solution surface. This model remains to be tested in solid rooting substrates, where both the capacitance of the substrate and the contact between roots and solution are likely to be smaller than in hydroponics and will vary with the water content of the rooting substrate. In this chapter, the ability of the new model to explain capacitance measurements made on cereals growing in sand or in compost in the glasshouse, or in a sandy-loam soil in the field, was tested under various water regimes.

4.2 Material and methods

Experiment 1: Capacitances of compost and soil

The capacitances of compost and soil were measured using an LCR Meter (Extech 130193; Extech Instruments, Waltham, MA, USA) in the laboratory at a range of water contents, using 16.5 cm long stainless steel rods (diameter 3 mm) as parallel electrodes separated by up to 40 cm. Compost (approx. 0.85 v/v peat, 0.1 v/v sand, 0.05 v/v vermiculite) contained 1 kg m⁻³ of cellulose-based water management additive (Celcote, Certis, Wiltshire, UK), 2.5 kg m⁻³ of a 1:1-calcium-magnesium limed mix, and 4.25 kg m⁻³ of NPK-fertilizer (Osmocote “Exact Hi Start, 5-6M”, Scotts, Baulkham Hills, Australia). Soil was collected from East Loan Field (latitude 56.4560°N, longitude 3.0800°W), The James Hutton Institute (JHI), Dundee, UK. Compost or field soil was placed in a plastic container (60 cm long × 40 cm wide × 11 cm deep) with drainage holes and irrigated with tap water to a water content approaching field capacity. Nine rod electrodes were inserted into the compost or soil in a line. The compost or field soil was then allowed to dry for 65 days and capacitance and water content were measured periodically at five locations in the substrate. The volumetric water content of the compost or

soil was measured using a theta probe (ML2x, Delta-T Devices, Cambridge, UK). Soil capacitance was also measured in the field as a function of electrode separation using steel rod electrodes, at a soil water content of $0.223 \text{ cm}^3 \text{ cm}^{-3}$, 30 min after rain.

Experiment 2: Wheat (Triticum aestivum L.) grown in sand in the glasshouse

Grains of forty cultivars of winter wheat were imbibed for 3 to 5 hours in water and then sterilized in a solution of 2% calcium hypochlorite for 15 minutes. Sterilised grains were rinsed in distilled water and placed between sheets of moist filter paper in Petri dishes. The Petri dishes were covered with aluminium foil and incubated at a temperature of 4°C for 7 days. Seedlings with similar leaf development were selected and transferred on 24th October 2008 to vertically aligned plastic tubes (1 m length, 5 cm diameter) lined with heavy duty black plastic sheeting and filled with a gravel–grit–sand mixture (40:40:20 by volume, 6:7:4 by weight) over 0.1 m^3 gravel. The bottom of each tube was covered with 0.5 mm pore size nylon mesh.

The tubes were arranged in 42 rows and 12 columns in a compartment of a Cambridge-type glasshouse at JHI, Dundee, UK (latitude 56.4566°N , longitude 3.0708°W). Four rows constituted a block. The experimental plants were completely surrounded by guard plants (cv. Hereward) occupying all tubes in rows 1 and 42 and columns 1 and 12. Individuals of each of forty cultivars were randomly assigned to one of forty tubes in each block. The compartment was set to maintain temperatures of 20°C by day and 15°C at night using automatic vents and supplementary heating. Daylight was supplemented by artificial lighting (MASTER SON-T PIA Green Power; Philips, Guildford, UK) to maintain an irradiance greater than 200 W m^{-2} for 16 h each day.

Prior to the transfer of seedlings, all tubes were flushed with water delivered at 9 mL/min through drip feeders using a HortiMaX Irrigation Computer (Aqua 500; HortiMaX, Pijnacker, The Netherlands). Following the transfer of plants to tubes, each tube was fertigated daily at 03:00 am for 3 to 6 min with a mineral solution containing 4.359 mM K^+ , 2.1 mM Ca^{2+} , 2.0 mM

NH_4^+ , 0.75 mM Mg^{2+} , 10.0 μM FeNaEDTA, 1.0 μM Mn^{2+} , 1.0 μM Zn^{2+} , 0.25 μM Cu^{2+} , 4.2 mM Cl^- , 4.0 mM NO_3^- , 1.75 mM SO_4^{2-} , 0.307 mM H_2PO_4^- , 12.5 μM H_2BO_3 and 0.25 μM MoO_4^{2-} , and weekly for 1 to 2 min with a solution of 2.1 mM CaCl_2 , both delivered at 9 mL/min using a HortiMax GPS Irrigation Computer. Solutions were supplied to the fertigation system through a Dosatron (DI 16; Dosatron International, Bordeaux, France).

Vernalisation was achieved by moving tubes containing plants on 19th November 2008 to a growth chamber supplying 12 hours light daily, running at 4 °C. Whilst plants were in the growth chamber all tubes were placed in containers containing a pool 1 cm deep of water. Plants were removed from the growth chamber and returned to the glasshouse on 7th January 2009 and fertigation was resumed. Plants were harvested at commercial maturity, between 18th and 27th May 2009, when the grain moisture content approximated 8–10 % fresh mass.

At harvest, shoots were cut at the surface of the sand, and the base of the shoot plus roots remained in the sand. Selected sand columns were then irrigated with tap water until it flowed from the bottom of the tubes. Approximately 30 minutes after irrigation, when no water was pooled on the surface of the sand, a 16.5 cm long stainless steel rod electrode (diameter 3.2 mm) was inserted approximately 10 cm into the sand about 2.5 cm away from the base of a shoot. A second electrode, made from a stainless steel needle (NN-2325R, 0.6 x 25 mm Terumo, Leuven, Belgium), was inserted through the bases of the main stem and tillers. Electrodes were then connected to an Extech LCR Meter using the test leads supplied by the manufacturer.

Capacitance was measured by applying 1 V at a frequency of 1 kHz. No difference was found in the relationships between root mass and capacitance measurements between LCR meters.

Capacitance measurements were made on 1 to 5 replicate plants of 35 cultivars of winter wheat (A50-03, Alchemy, Avalon, Batis, Brompton, Caphorn, Claire, Cordiale, Deben, Dover, Einstein, Enorm, Flanders, Gatsby, Gladiator, Gulliver, Hereward, Isengrain, Lynx, Malacca, Maris Widgeon, Mascot, Monopol, Ochre, Opus, PBIS, Petrus, Rialto, Riband, Robigus, Scorpion 25, Soissons, Sokrates, Solstice, Zebedee). Roots were washed free of sand and their

fresh mass was determined. Root material was dried at 70°C in an oven for 3 days before their dry mass was determined.

Experiment 3: Barley (Hordeum vulgare L.) grown in compost in the glasshouse

Caryopses of barley (cv. Optic) were surface sterilised using a solution of 2% calcium hypochlorite for 15 min. Sterilised caryopses were sown into plastic pots (height 20.5 cm, volume 2.97 l) each filled with 1.9 kg of the compost mixture described in Experiment 1 at a depth of 3 cm. Pots were placed in a glasshouse compartment at JHI on 31st September 2010 and watered daily. A polyethene mesh (9.5 threads mm⁻¹, Tildenet, Bristol, UK) was used to retain the compost in the pots during inversion.

Capacitances of 43 plants were determined between 43 and 45 days after sowing (DAS). Capacitances were first measured using an Extech LCR Meter between a needle electrode inserted into the stem about 3.3 mm above the surface of the compost and a steel rod electrode in the compost. The capacitance of the stem tissue was then determined. To achieve this, the compost surface position was first marked on the stem of each plant with a waterproof pen. Then, stems were cut about 2 cm below the compost surface and removed from the compost. The capacitance was measured between an electrode contacting the stem at the compost surface mark and the original needle electrode site. The diameter of all tillers was determined. Shoot circumference and cross-sectional area of the hollow stems were calculated from perpendicular diameters of inner and outer surfaces at the position of the plant electrode and the soil surface. Calculations took into account that mature shoot pieces were elliptic and hollow. Thus the cross-sectional area was calculated by $A = \pi ab$ with a as the semi-major and b as the semi-minor axis. Compost was washed off the root material, which was dried with a paper towel and weighed (EP214, Ohaus, Pine Brook NJ, US).

Watering was suspended for a further 70 plants from 45 DAS. Capacitance measurements were made on these plants between 65 and 75 DAS before, during, and after the various controlled

water treatments described in Fig. 4-1. The average height of the plant electrode above the compost was 5 mm. The position of the transition between wet and dry compost was observed using a snake camera (Model no. 8803AL, Goscam, Shezhen, China) in 14 pots that were furnished with a clear, scaled plastic tube (20 cm length, 5 cm diameter) for this purpose.

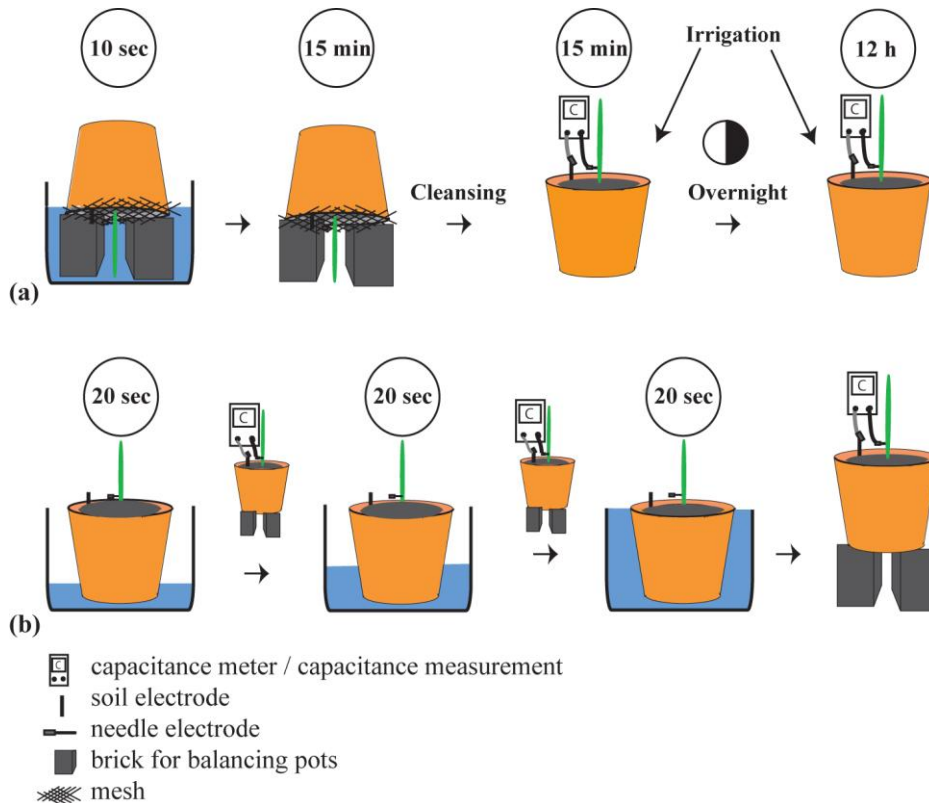


Figure 4-1. Controlled irrigation treatments performed in Experiment 3. Watering of compost-filled pots containing barley plants was suspended from 45 DAS and, 65 to 75 DAS, the pots were randomly split into two groups. (a) One group of 35 pots were turned upside down and placed in a water-filled basin for 10 s. Bricks in the basin served as supports and ensured that only the first centimetre of the top soil was wetted. Pots were then removed from the basin and placed upside down on bricks to drain for 15 min. Plants were then turned upright again and any compost adhering to the shoot was removed. Capacitance was then measured using an Extech LCR Meter between a needle electrode inserted into the stem of plants about 5 mm above the surface of the compost and a steel rod electrode in the compost. The pots were irrigated from above twice in the evening and once in the morning to a water content approaching field capacity. Capacitance was then remeasured. (b) The second group of 35 pots were placed in a basin which was then filled with water to a depth of 4 cm. After 20 s the pots were taken out and capacitance was measured using an Extech LCR Meter between a needle electrode inserted into the stem of plants about 5 mm above the surface of the compost and a steel rod electrode in the compost. Pots were returned to the basin, which was filled with water to a greater depth. After 20 s pots were removed from the basin and capacitance was remeasured. This procedure was repeated until the water in the basin was level with the surface of the compost.

Experiment 4: Barley grown in soil in the field

Winter barley (cv. Siberia) was grown in the field at JHI in 2010 and 2011. Caryopses were sown in East Loan Field (latitude 56.4560°N, longitude 3.0800°W) on 6th October 2009 and in East Pilmore Field (latitude 56.4577°N, longitude 3.0718°W) on 25th September 2010.

Capacitance measurements were performed between 26th July and 14th August 2010, and on 20th August 2011. In 2010 and 2011, capacitance was measured using an Extech LCR Meter between a needle electrode inserted into one or more tillers of a barley plant 1.5 cm above the ground and a steel rod electrode in the soil. The soil around the shoot was then irrigated with 10 cm³ of water and capacitance was measured 20 s later. This procedure was repeated until 100 to 200 cm³ water had been added to the soil. In 2011, two steel rod electrodes were inserted in the soil close to pairs of neighbouring plants after irrigating the soil around each of the two plants with 100 cm³ water and the soil between the two plants with 100 cm³ water. The capacitance was then measured between different combinations of needle electrodes inserted in the tillers (either 3 mm or 15 cm above the soil surface) or the steel rod electrodes in the soil, as will be described in the Results section. This experiment was conducted on five plant pairs.

Statistics

Regressions were performed using Sigmaplot 12 software (Systat Software, Chicago, IL, USA). Data and regression coefficients are expressed as mean \pm standard error (SE) from n determinations. In linear regressions, when the intercept did not differ significantly from zero, the regression was forced through the origin.

4.3 Results

Capacitances of compost and soil increase with water content

When measured with an electrode separation of 10 cm, the capacitances of both compost and field soil increased with increasing water content (Fig. 4-2a, b). This is consistent with previous studies (e.g. Robinson et al. 2005; Kizito et al. 2008; Wu et al. 2011). When capacitance was measured in compost at a water content of $0.447 \text{ cm}^3 \text{ cm}^{-3}$, it decreased with increasing electrode separation (Fig. 4-2c). When capacitance was measured in soil in the laboratory at a water content of $0.263 \text{ cm}^3 \text{ cm}^{-3}$ or in the field at a water content of $0.223 \text{ cm}^3 \text{ cm}^{-3}$, it also decreased with increasing electrode separation (Fig. 4-2c). Soil capacitance, measured in the field appeared to be inversely proportional to electrode separation (Fig. 4-2d).

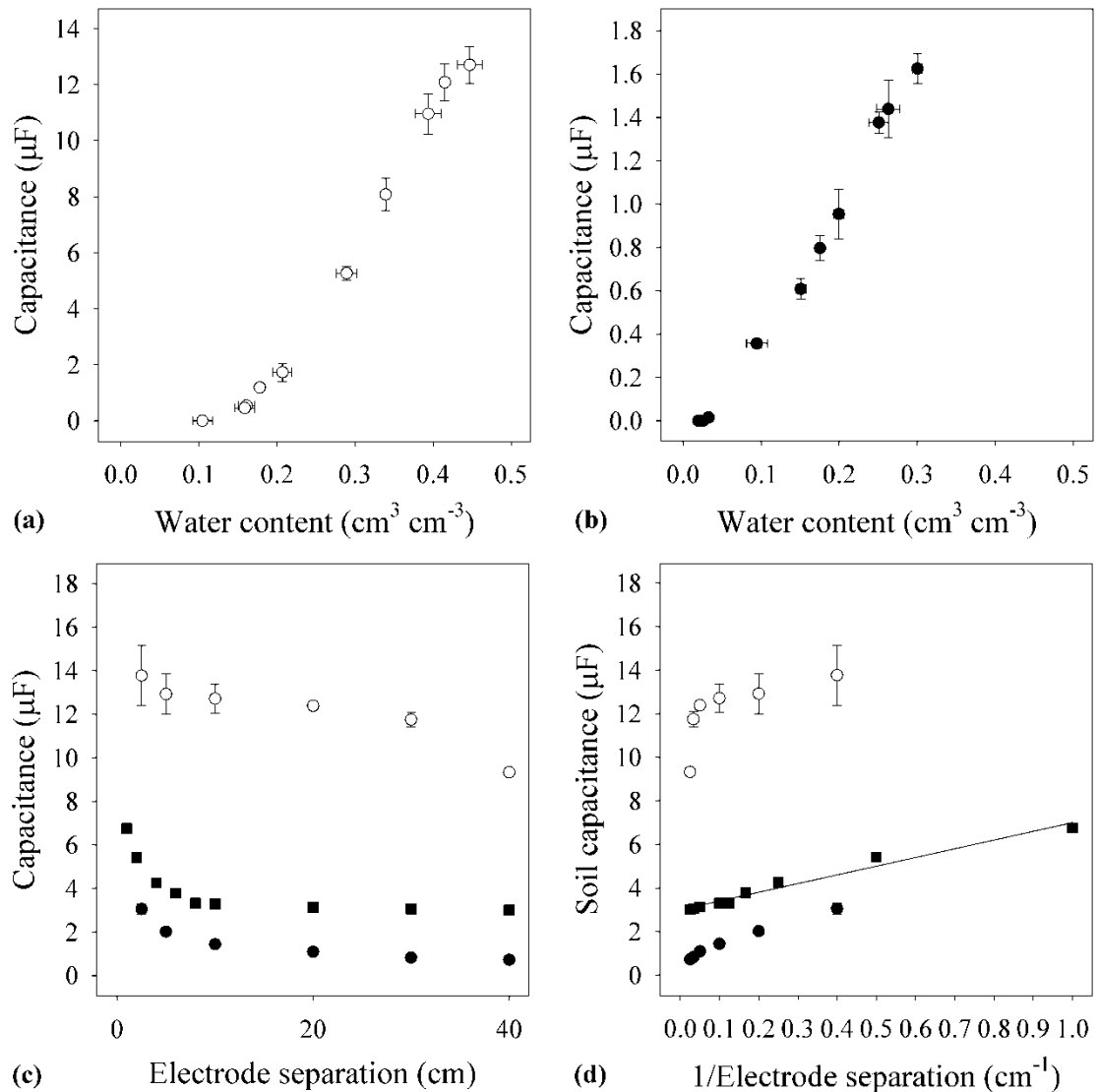


Figure 4-2. (a) Relationship between the capacitance of compost and its water content measured with an electrode separation of 10 cm. (b) Relationship between the capacitance of soil and its water content measured in the laboratory with an electrode separation of 10 cm. (c) Relationships between the capacitance of compost (\circ), of soil measured in the laboratory (\bullet) and of soil measured in the field (\blacksquare) and electrode separation. (d) Relationships between the capacitance of compost (\circ), of soil measured in the laboratory (\bullet) and of soil measured in the field (\blacksquare) and the reciprocal of electrode separation. In panels (c) and (d) capacitances were measured at water contents of $0.447 \text{ cm}^3 \text{ cm}^{-3}$ for compost, $0.263 \text{ cm}^3 \text{ cm}^{-3}$ for soil measured in the laboratory, and $0.223 \text{ cm}^3 \text{ cm}^{-3}$ for soil measured in the field. Data for panels (a) and (b) represent means \pm SE of 5 independent measurements of capacitance and water content. Data for panels (c) and (d) represent means \pm SE of up to 5 independent measurements of capacitance. The linear regression in panel d is $y = 4.00x + 3.00$ ($R^2 = 0.967$, $n = 8$ electrode separations).

Capacitance is correlated with root system mass in wheat grown in sand columns

In the sand-column study (Experiment 2), a close linear relationship was found between the capacitance of wheat plants of different cultivars and root dry mass (Fig. 4-3). These data show that a linear relationship between capacitance and root mass can be obtained across many cereal genotypes in a sand culture system. However, it is possible that this relationship arises because of allometric relationships between root mass, cross sectional area of roots near the surface of the sand, and plant tissue between the surface of the sand and the electrode attached to the plant.

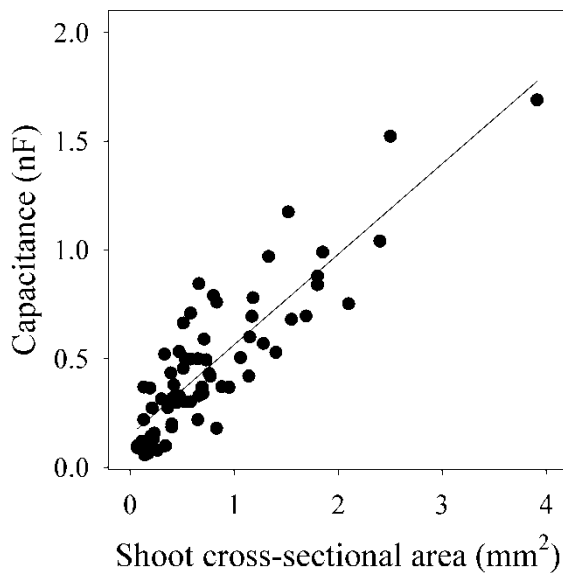


Figure 4-3. Relationship between the capacitance of wheat plants of different cultivars grown in sand columns and their root dry mass. The linear regression was $y = 0.416x + 0.149$ ($R^2 = 0.753$, $n = 67$ stems).

Maximal capacitance of barley plants requires local wetting of substrate around the base of the stem

The capacitance of barley plants growing in dry substrate was much smaller than in wet substrate (Fig. 4-4). Wetting either the top centimetre of the compost (Experiment 3; Fig. 4-1a) or the soil immediately around the shoot base with 1.0–2.5 cm³ water (Experiment 4) sufficed to increase the capacitance to the values recorded in fully wetted soil (Fig. 4-4). Further wetting

had only marginal effects on the capacitance. This is consistent with recommendations in the literature to perform capacitance measurements on plants in wet substrate (Dalton, 1995; Kendall *et al.*, 1982; Chloupek, 1977; van Beem *et al.*, 1998; McBride *et al.*, 2008). Raising the water table in compost (Fig. 4-1b) had little effect on the capacitance of barley plants until the water table reached within 1–2 cm of the compost surface (Fig. 4-5a). Thus, wetting the substrate locally around the stem base is both necessary and sufficient to record the maximum plant capacitance.

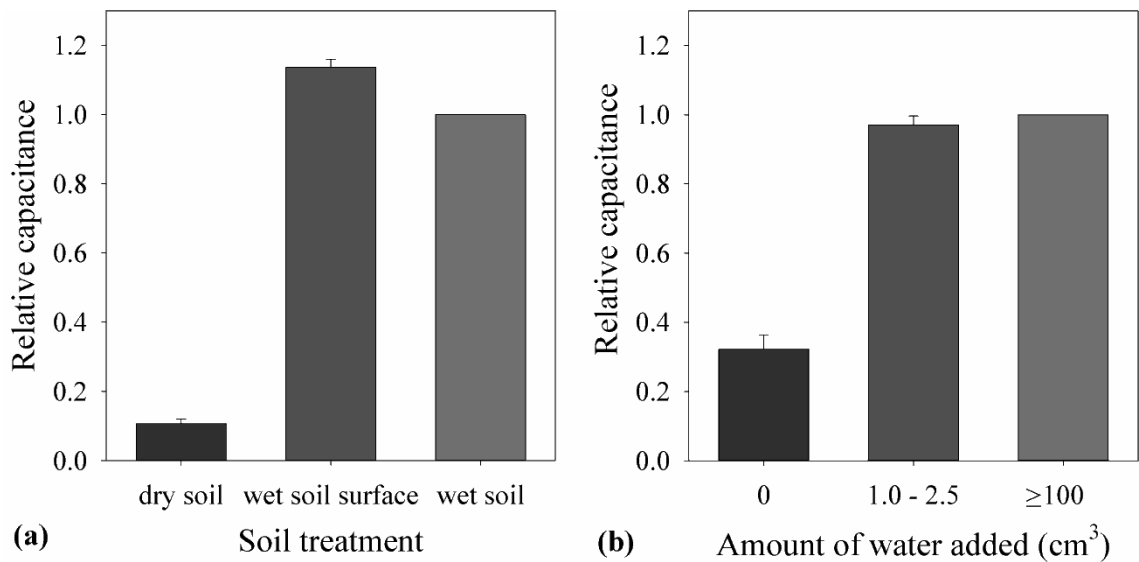
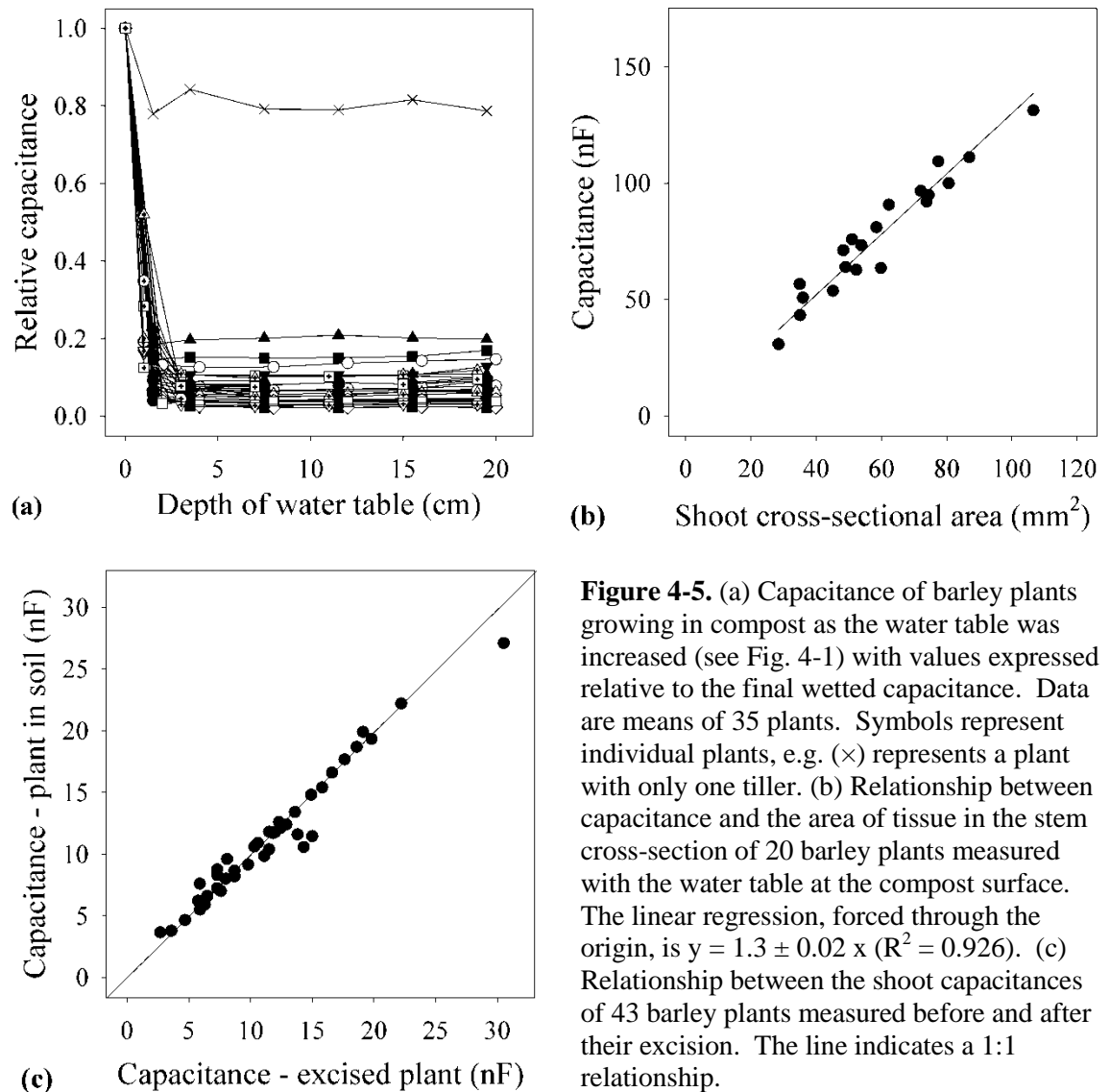


Figure 4-4. (a) Capacitance relative to fully wetted compost for barley plants in dry compost, compost wetted at the surface, and thoroughly wetted compost. Data are expressed as mean \pm SE ($n = 35$ plants). (b) Capacitance relative to fully wetted soil of tillers of barley plants growing in the field to which zero, 1.0 - 2.5 cm³ or ≥ 100 cm³ of tap water was added around the stem base. Data are expressed as mean \pm SE ($n = 8$ plants).

When the water table was at the compost surface (Fig. 4-1b), the capacitance of plants was linearly related to the area of tissue in the stem cross-section (Fig. 4-5b). This suggests that plant capacitance was determined by the dimensions of plant tissues close to the soil surface. When the shoot was excised, the capacitance of the tissue that had been between the compost surface and the original electrode inserted into the plant was almost identical to the capacitance

measured for whole plants growing in compost (Fig. 4-5c). This implies a negligible contribution of roots to the observed capacitance.



Capacitances of plant and soil components combine in series

Dietrich *et al.* (2012) have proposed that capacitances of plant tissues and rooting substrate combine according to standard electrical circuit theory. They consider plant tissue above the soil surface and the soil itself as individual components of the circuit. Their model predicts that the capacitance measured between two electrodes combines as the component capacitors wired

in series, with capacitances of individual tillers of a plant attached to the same electrode acting in parallel (Fig 4-6a). This model was tested on pairs of neighbouring plants in the field following rain. Data were collected for five pairs of neighbouring plants (Fig. 4-6b). The predicted capacitance (C_{pred}) was estimated from an equation of the form:

$$\frac{1}{C_{pred}} = \frac{1}{(C_{T1} + C_{T2})} + \frac{1}{(C_{T3} + C_{T4})} + \frac{1}{(C_S)} \quad (8)$$

where C_{T1} and C_{T2} were the capacitances of two tillers of one plant, C_{T3} and C_{T4} were capacitances of two tillers of another plant and C_S was the capacitance of the soil between the two plants. There was good agreement between the measured capacitances and the capacitances predicted by Equation 9 (Fig. 4-7).

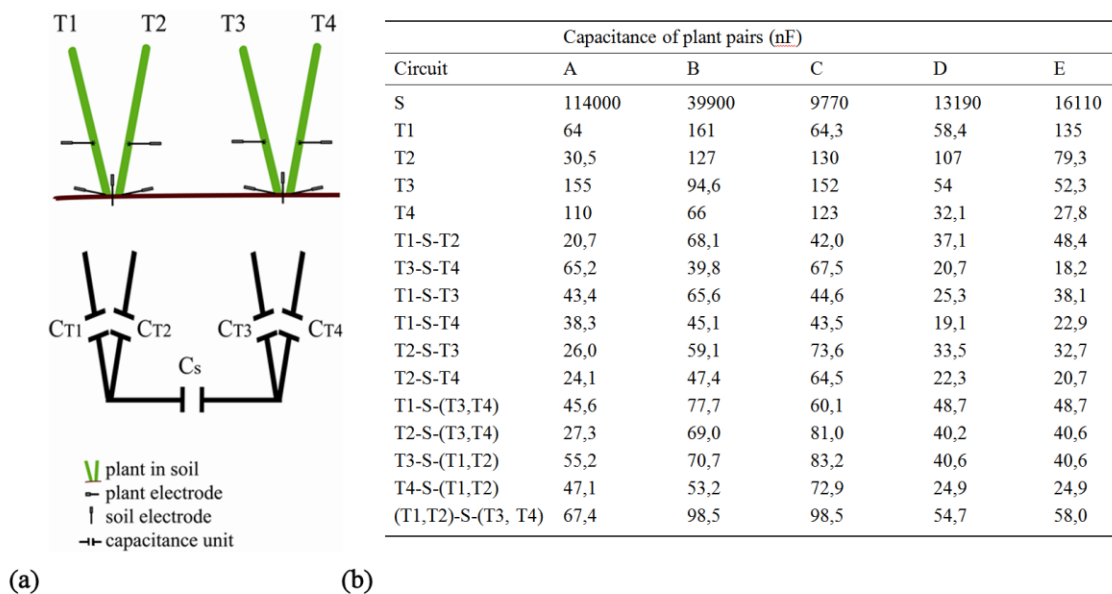


Figure 4-6. (a) Illustration showing the position of insertion of electrodes in tillers of neighbouring barley plants and in soil, with the equivalent electrical circuit diagram below. (b) Capacitance measured between two electrodes in the soil (S), electrodes inserted at the base and at a height of 1 cm in an individual tiller (T1, T2, T3, T4), electrodes attached to individual tillers of the same plant (T1-S-T2, T3-S-T4), to individual tillers of neighbouring plants (T1-S-T3, T1-S-T4, T2-S-T3, T2-S-T4) or to multiple combinations of tillers.

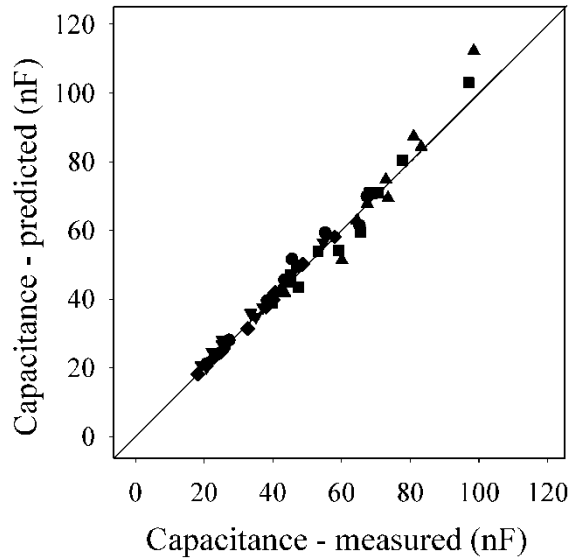


Figure 4-7. Relationship between the measured capacitance (C_m) and the capacitance predicted (C_p) using Equation 9 for the combination of tillers described in Figure 4-6. The linear regression is $C_p = 1.02 \pm 0.008 C_m$ ($R^2 = 0.978$, $n = 54$ combinations).

4.4 Discussion

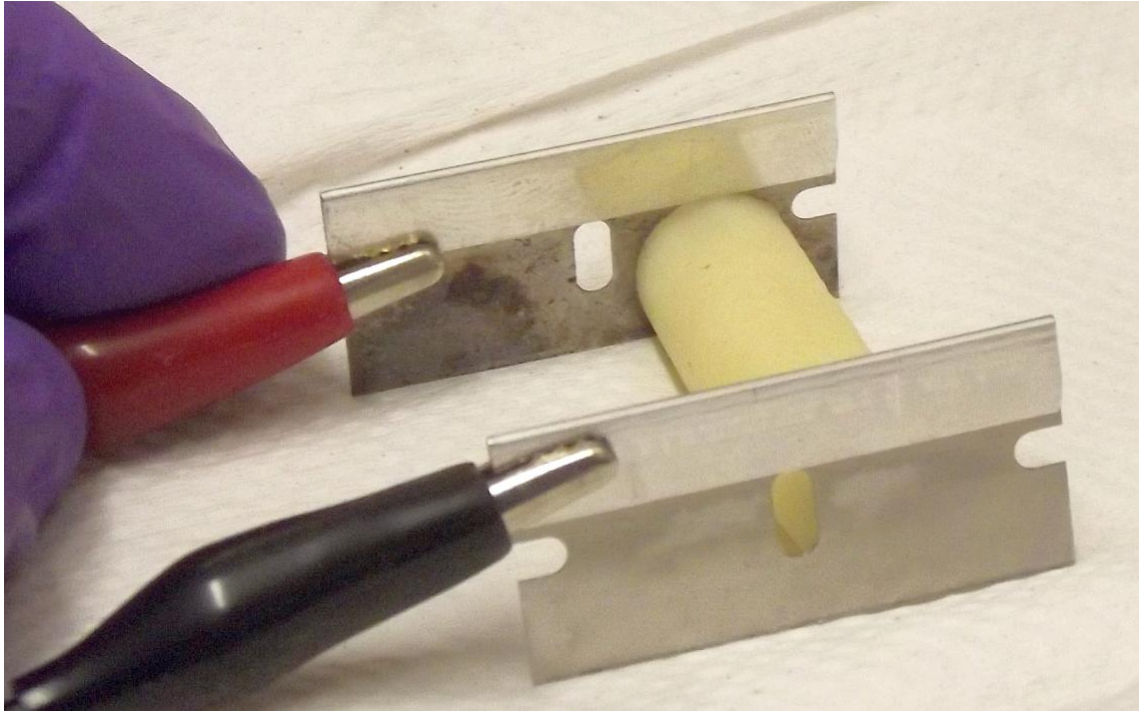
The capacitances of compost and soil increased with increasing water content (Fig. 4-2), as observed in previous studies (e.g. Wu *et al.*, 2011; Robinson *et al.*, 2005; Kizito *et al.*, 2008). When the substrates had water contents approaching field capacity, their capacitances were at least an order of magnitude greater than capacitances measured for plant tissue. Thus, the capacitance measured between an electrode in the rooting substrate and one inserted at the base of the stem would be dominated by plant tissue according to the model proposed by Dietrich *et al.* (2012). Wetting the substrate locally around the stem base was both necessary and sufficient to record maximum plant capacitance (Figs 4, 5a). This is consistent with the hypothesis that capacitance is dominated by tissue between the solution surface and the electrode attached to the plant, and that the bulk of the root system makes a negligible contribution to the measured capacitance (Dietrich *et al.*, 2012). Indeed, when the shoot was excised, the capacitance of the

tissue that had been between the compost surface and the original electrode inserted into the plant was almost identical to the capacitance measured for plants growing in compost (Fig. 4-5c). Capacitance was linearly related to the area of tissue in the stem cross-section when the water table was at the compost surface (Fig. 4-5b). Thus, the model proposed by Dietrich et al. (2012) could explain the variation in capacitance measurements made on cereals growing in solid substrates under various irrigation regimes. In addition, there was good agreement between the capacitances measured on pairs of neighbouring plants in the field and the capacitances predicted by Equation 9 (Fig. 4-7). This states explicitly that the capacitance measured between two electrodes combines as the component capacitors (plant tissue or solid substrate) wired in series, with capacitances of individual tillers of a plant connected to the same electrode acting in parallel.

4.5 Conclusion

All the findings presented in this paper are consistent with the model for plant capacitance developed in Chapter 3. Substrate capacitance and plant capacitance combine according to standard physical laws. Wetting the substrate locally around the stem base is both necessary and sufficient to record maximum capacitance. Under these conditions, plant tissue capacitance is much smaller than soil capacitance and, when these components are combined in series, the capacitance measured is largely determined by the tissue between the wet soil surface and electrode attached to the plant. Whilst the measured capacitance might, in some circumstances, be correlated with root mass, it is not a direct measure of root mass.

In Chapter 5 the effect of the plant tissue geometry is considered in relation to capacitance, and RC circuits analogous to plant–substrate systems are investigated.



5 EFFECT OF PLANT TISSUE GEOMETRY AND CONNECTION SCHEME ON CAPACITANCE, USING POTATO PARENCHYMA AND ELECTRICAL ANALOGIES

This chapter presents the results of a series of experiments conducted on cores taken from potato tubers and electrical circuit components. The aim was to study the effects of plant tissue geometry and circuit connection scheme on capacitance.

5.1 Introduction

The previous chapters tested capacitance for cereal plants in hydroponics (Ch. 3) and in solid media (Ch. 4) as an estimate of root mass, leading to a new model for plant capacitance. The basics of the new model were (1) the capacitances of the plant tissue and the rooting medium are in series; (2) the capacitances of tissues along an unbranched root or stem can be considered as connected in series; (3) the capacitances of multiple unbranched roots comprising the whole root system or multiple stems comprising the shoot, act in parallel; (4) the capacitances of individual roots or stems are directly proportional to their cross-sectional area, though different constants of proportionality may apply to different plant tissues.

Experiments in this chapter used a simplified system based on cores taken from potato tubers as a source of more homogeneous plant tissue. Cutting cylindrical cores of potato tuber tissue allowed accurate definition of the dimensions of a plant sample. Furthermore, potato tubers provide relatively large volumes of tissue allowing comparisons between different types of potato tissue. Experiments reported in Section 5.3.1 explored (i) tissue- and (ii) electrode-related differences in the measurement of capacitance and presents results of experiments were

potato tissue was submerged in water or placed on wet paper towel. The second result-section (S. 5.3.2) presents electrical analogies of the preceding cereal and potato experiments constructed with electrical components on an electrical breadboard using the same LCR-meter.

5.2 Material and methods

5.2.1 Potato tuber experiments

Plant material

Tests with potato tubers (*Solanum tuberosum* L.), stored previously at 4 °C, of the cultivars Maris Piper and Sterling were conducted during January 2011, and February 2012. A selection of large tubers (11.3 cm (\pm 1.9 cm SD) length \times 6.9 cm (\pm 2.4 cm SD) width) washed with tap water and left to dry for at least ten minutes, before cylindrical cores were cut. A range of nine sizes of stainless-steel borers (Borer Rexaloy cork, R & L Enterprises, Leeds, UK) was used (Table 5-1). If not stated otherwise, cores were cut longitudinally from the stem end to the bud end (Fig. 5-2) before vascular tissue at the periphery was removed. The cross-section of a core was either uniform along its length (Fig. 5-1a) or changed in steps along the core as indicated in Fig. 5-1b.

Table 5-1. Bore-sizes of potato tuber cores

Key: \emptyset : Diameter; Φ : Circumference, A_c : Cross-sectional area

Bore-size	1	2	3	4	5	6	7	8	9
\emptyset (mm)	4.8	6.0	7.2	8.4	9.6	10.8	12.0	13.2	14.4
Φ (mm)	15.1	18.8	22.6	26.4	30.2	33.9	37.7	41.5	45.2
A_c (mm ²)	18.1	28.3	40.7	55.4	72.4	91.6	113.1	136.8	162.9

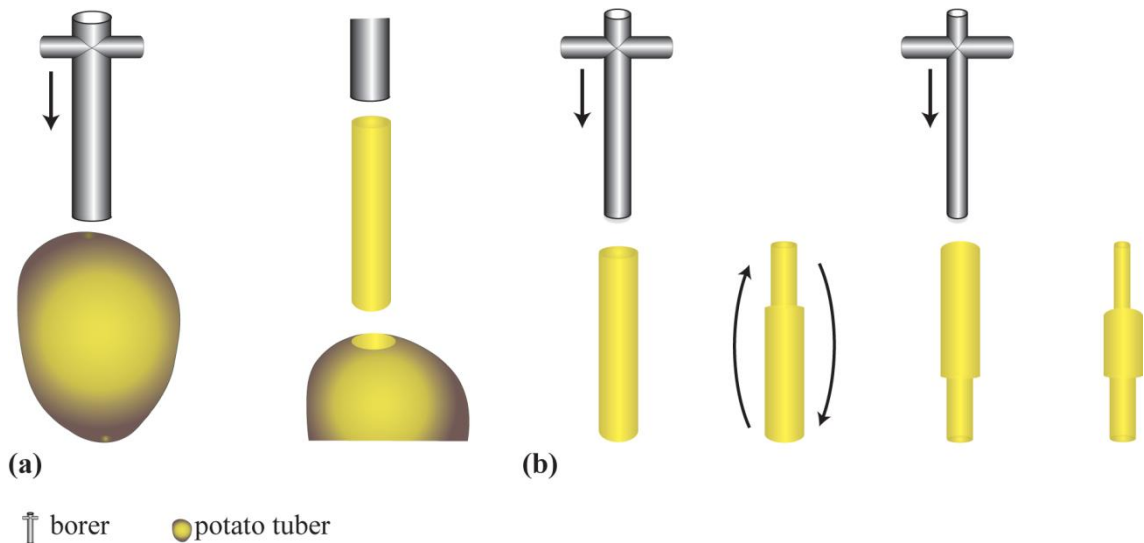


Figure 5-1. Cutting potato tuber cores with (a) even and (b) stepped cross-section. (a) First a core with a uniform cross-section was cut. (b) Then, a smaller borer cut a section of 2.75 cm length from one core pole before an even smaller borer cut a section from the other core pole up to a distance of 2 cm from the opposite section.

Techniques

Capacitance and impedance were measured with 1 Volt at 1 kHz frequency with the Extech LCR-meter. Each meter-lead was connected to an electrode. Two plant electrodes were attached to potato cores in parallel alignment. Distance information refers to the space between two electrodes or between an electrode and a water surface. Razor-blades (Fig 2-2g), strips of aluminium foil (ca. 5 mm \pm 1 mm breadth, Fig.2-2h), and hypodermic needles (Fig. 2-2a) served as plant electrodes. Blade-electrodes were pressed gently in parallel alignment against the flat cut edges of a potato core. Strips were wrapped around a core and held tight by the crocodile clips of the meter-leads. Needles penetrated a core perpendicular to its longitudinal axis. Solution-electrodes were razor-blades (Fig. 5-5a) and disks of aluminium foil stamped out with the borers used for cutting cores (Fig. 5-6a, b). Plant electrode position and water level were marked on the cores with a waterproof

pen. Fresh mass was taken with a balance (LP3200D, Satorius, Göttingen, Germany) within 1 min after capacitance measurement. Lengths were measured with digital callipers. Cross-sectional area and circumference (Φ) were calculated from the inner diameter (\emptyset) of the borers.

Experiments

(i) *Effect of plant different plant tissues on capacitance*

Potato tuber tissues could easily be discriminated by eye (Fig. 5-2a). Thin tuber sections were cut, stained and then studied under the microscope (BX50F-3, Olympus Optical Co. LTD., Tokyo, Japan) to confirm the distribution and orientation of tracheid elements in a tuber: One tuber was cut in both longitudinal and cross-sectional directions. Slices were cut and then rinsed with tap water before being submerged into an acid fuchsine-solution (conc.: 0.5 $\text{C}_{20}\text{H}_{17}\text{O}_9\text{S}_3\text{Ca mg}^1\text{L}^{-1}$, dye content: 85%) so that the dye could infiltrate the opened tracheid elements. After five minutes the slices were removed from solution, rinsed again with water, and examined under the microscope. Dye had coloured the tracheid elements as described by Lulai (2005) so that they could be discriminated from the surrounding parenchyma. Based on observation three zones could be distinguished (Fig. 5-2b): an inner pith zone showing no tracheid elements, a middle perimedullary zone showing relatively sparse concentrations of tracheid elements, and an outer cortex/vascular ring zone showing dense concentrations of tracheid elements.

For the first experiment (Expt *i-1*), cores (1cm length, bore-size 2; Table 5-1) were cut from all three zones of a fresh potato tuber and their capacitances measured with blade-electrodes. Half of the cores containing cortex tissue including the vascular bundles were bored along the bundles, the other half across the bundles. For the second experiment (Expt *i-2*) capacitance was measured in partly in tap water submerged whole potato tubers before (Fig. 5-3a) and after peeling (Fig. 5-3b,c). Furthermore the capacitance of the skin was measured on eight samples of 0.5 mm^2 area.

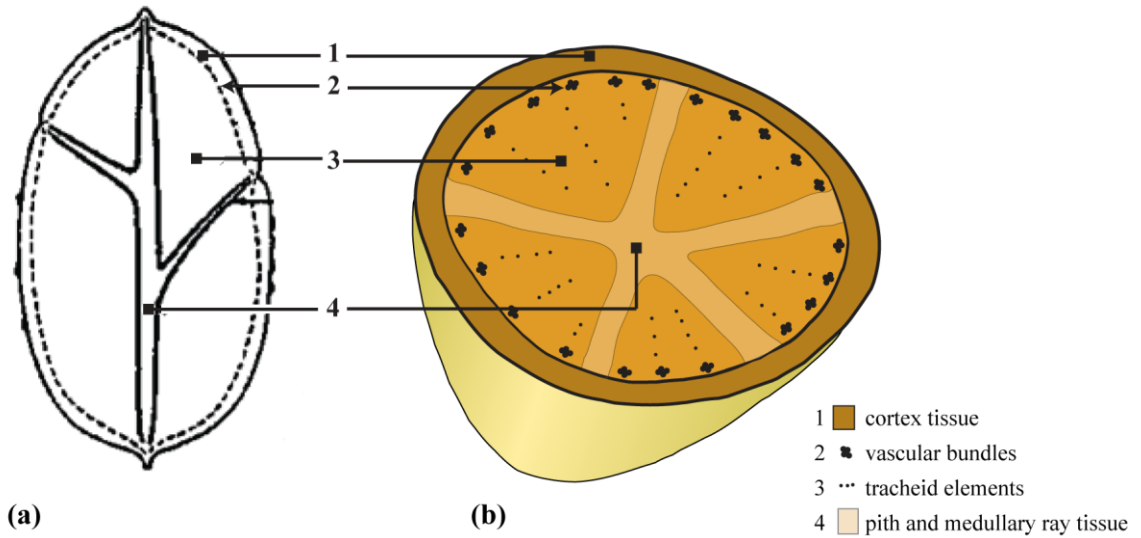


Figure 5-2. (a) Scheme of a longitudinal section through a potato tuber after Rastovski & Van Es (1981). (b) Annotated drawing of a transverse section through a tuber. Longitudinal cores were cut from (1, 2) the periphery of the tuber containing cortex and vascular ring tissue; (3) the perimedullary zone; and (4) the centre (pith). Transverse cores were cut from (1, 2).

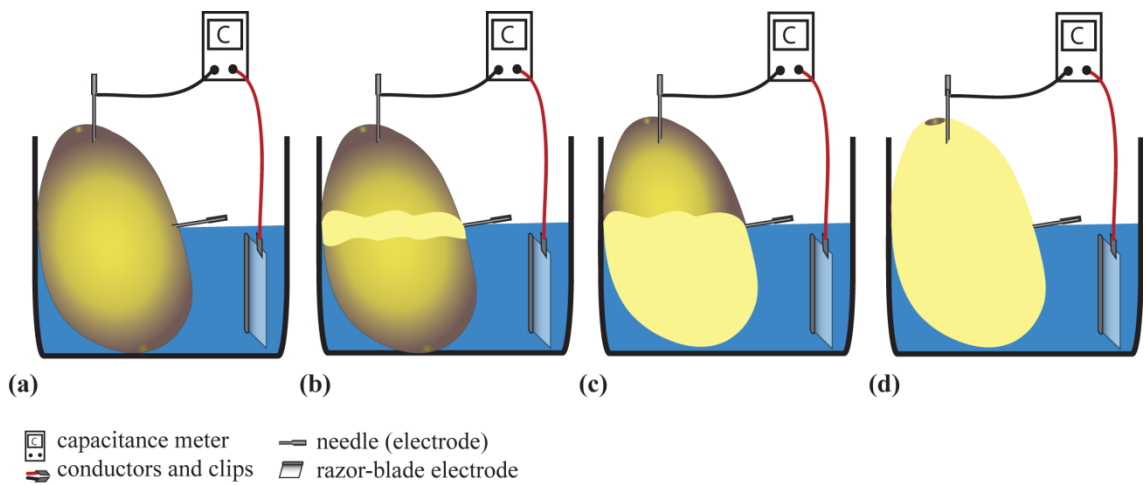


Figure 5-3. Measuring capacitance of whole potato tubers in tap water. (a) Tubers were placed in stable position into a 500ml-beaker. The beaker was filled with tap water until circa half of the tuber was submerged. Water height was marked at the tuber by inserting a subcutaneous needle filled with acid fuchsine solution. A needle-electrode was inserted vertically for 1 cm into the top tuber part, a razor-blade electrode was submerged and capacitance measured. (b) Tubers were then removed from the beaker and the skin was peeled off at the transition zone between wet and dry surface (D119, Tupperware, Orlando, FL, USA). Tubers were subsequently transferred back into the basin, the water height adjusted to the mark, and capacitance remeasured. (c) Again, the tubers were removed from the water to peel all the submerged tuber part. Tubers were transferred back into the basin, water height adjusted, and capacitance remeasured. (d) The plant electrode being removed the remaining skin was peeled off and capacitance measured accordingly after the plant electrode was reinserted.

(ii) *Effect of electrode connection schemes on capacitance*

In Expt *ii-1* different *electrode types* were used to measure the capacitance of freshly cut potato cores of various bore-size (Table 5-1) for different electrode separations (range: 0.5 – 6 cm). In Expt *ii-2* capacitance was measured with blade-electrodes on freshly cut cores of various bore-size and length (range: 0.1 – 9 cm). Care was taken to measure capacitance with consistent and minimal pressure, because it was been observed that capacitance increased with pressure against the electrodes. Expt *ii-3* capacitance was measured with blade-electrodes on cores of various bore-size and 1 cm length before and after the core surface was gently dried by briefly rolling it between two layers of dry paper towel. In Expt *ii-4* capacitance was measured for cores of various bore-size and 2 cm lengths after cores were surface-dried. In Expt *ii-5* capacitance was measured with a combination of different electrode types (Fig. 5-4a - f) for cores of bore-size 3 and 2 cm length.

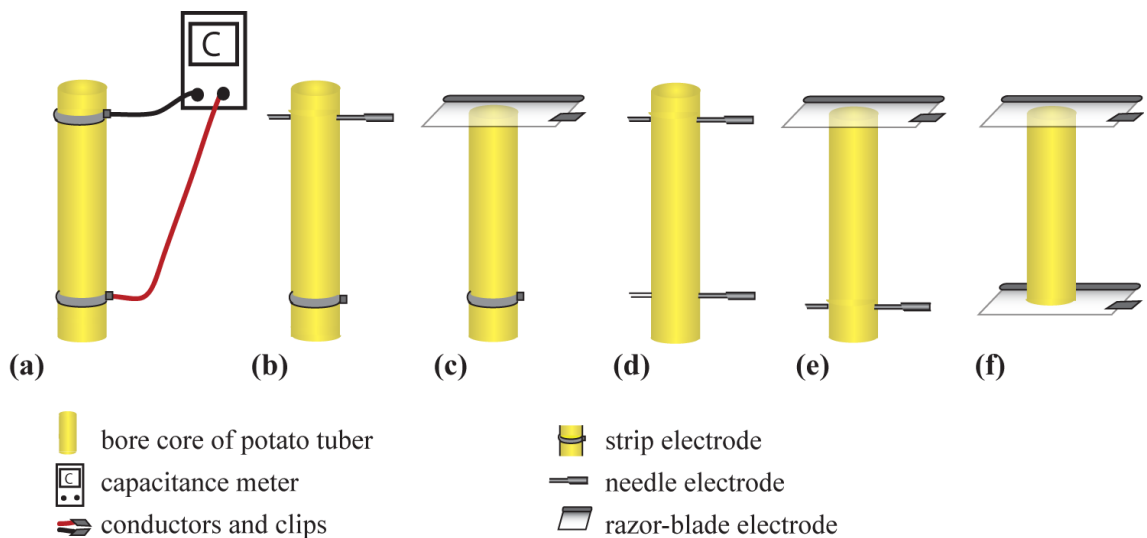


Figure 5-4. Measuring the capacitance with electrodes of the same and of different type. Cores of all 9 bore-sizes (Table 5-1) were cut from potato tubers. Capacitance was measured with (a) two strip-electrodes, (b) one strip-, one needle-electrode, (c) one strip-, one blade-electrode, (d) two needle-electrodes, (e) one needle-, one blade-electrode, and (f) two blade-electrodes at an electrode-separation of 1cm.

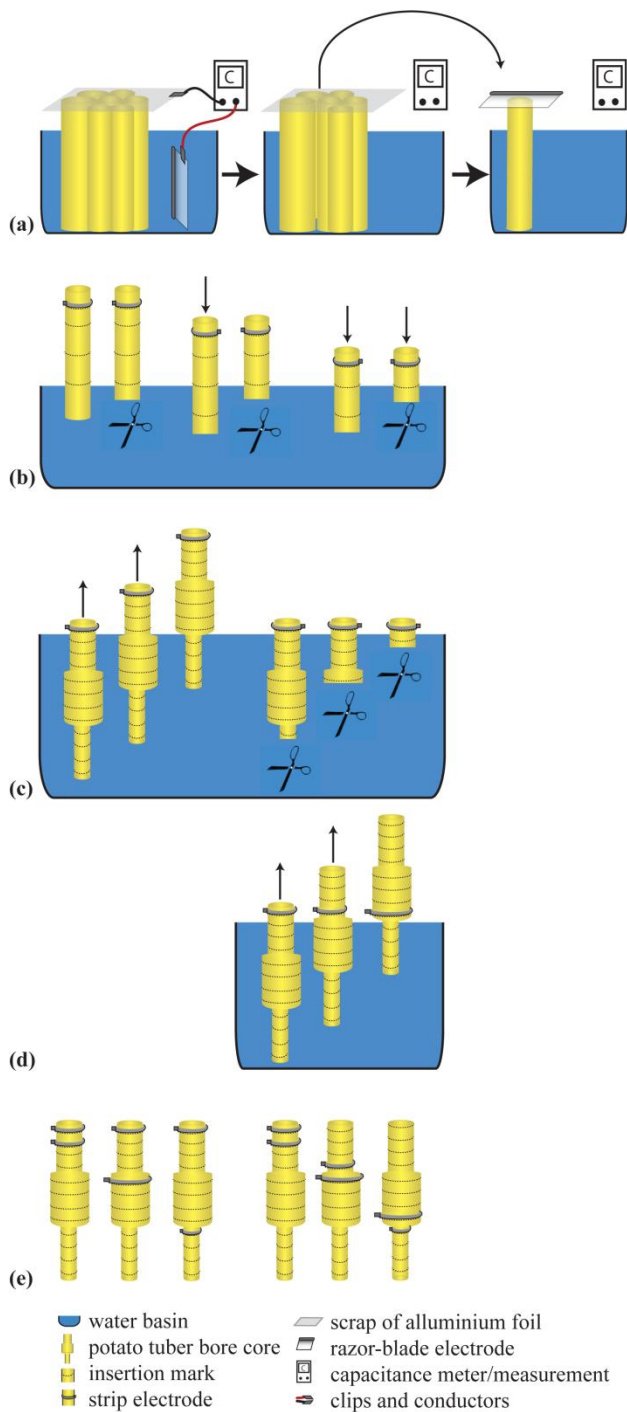


Figure 5-5. Potato core submersion experiments analogous to the barley roots and root systems in nutrient solution (Fig. 3-3): The cores had (a, b) even or (c – e) stepped diameters. (a) Multiple cores of same lengths were vertically submerged to 5 mm from the plant electrode. Left: A piece of folded aluminium foil served as plant electrode. It was gently pressed on the top of the cores and capacitance measured. Middle: Cores were then successively removed from the water and capacitance measured after each removal, until one core remained in the water. Right: Each of the cores were individually submerged and capacitance measured with a blade-electrode hold horizontally on top. A core of either (b) even or (c – e) stepped diameter was furnished with a strip-electrode on one end. (b) The core was incrementally submerged and capacitance measured for each increment before and after the submerged part was excised 5 mm below the water surface. The procedure was repeated until no plant material remained for excision. (c) The core was submerged to 5 mm from the plant electrode and capacitance measured. It was then incrementally lifted out of the water and capacitance measured for each increment until the core was out of water completely. Subsequently, the core was resubmerged, the increments successively excised and capacitance measured after each excision, until all increments were excised. (d) The core was submerged to 5 mm from the plant electrode and capacitance measured. It was then incrementally raised out of solution, the plant electrode reattached 5 mm above the water surface, and capacitance measured. The procedure was repeated for each increment until no plant material remained in the water. (e) Left: A second strip-electrode was attached to the core at various positions and capacitance measured. Right: Two strip-electrodes at 1 cm separation were incrementally moved along the core and capacitance measured.

(i) *Simulating barley experiments in hydroponics (Fig. 3-3) and field soil (Fig. 4-6)*

The effect of partly immersing and emerging potato cores in water was studied, in a manner analogous to the experiment performed in Chapter 3 for barley (Fig. 3-3). Experiments with barley plants in hydroponics (Fig. 3-3) were simulated with potato tuber cores in tap water:

A capacitance experiment with field barley plants (Fig. 4-6) was simulated with tuber cores on wet paper towel. Cores represented barley tillers, a wet paper towel field soil. The capacitance of two cores with different diameters was measured with two blade-electrodes (Fig. 5-4f). The capacitance of the paper towel was measured with two disk placed on the towel (Fig. 5-6a).

Then both cores were connected to a wet paper towel and the total capacitance measured (Fig. 5-6b). Layers of one, three and six sheets of wet paper towels were tested for their suitability to represent field soil. Proportionality between capacitance (C , nF) and the reciprocal of electrode separation (d , cm), as observed for field soil (Fig. 4-2d), was found for the use of one sheet only (Linear regression: $C = 36.5 (\pm 0.91) / d$ (mean \pm SE, $n = 11$, $R^2 = 0.990$ $P < 0.0001$). Thus, only one layer of wet paper towel was used in the test.

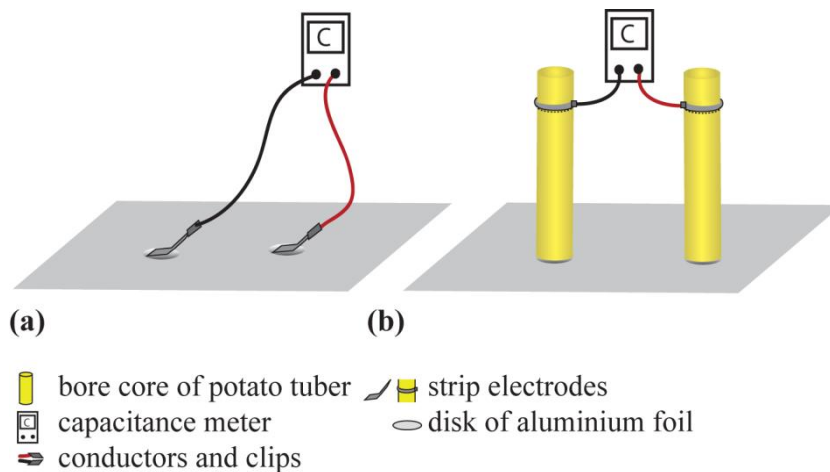


Figure 5-6. Simulating field barley experiments (Fig. 4-6) with two potato tuber cores on a wet paper towel. A thoroughly wetted paper towel drained for 1 min on a grid, before being unfurled on a level, non-conductive plate. Two disks of aluminium foil were stamped out with the borers for cutting tuber cores and placed onto the towel. (a) The capacitance of the paper towel was measured with two strip-electrodes connected to the disks. (b) The electrodes were then removed from the disk and each attached to the top of a core which were placed on to the free disk and capacitance was measured.

5.2.2 Electrical analogies

The meter

Capacitance

The Extech LCR-meter offers capacitance measurements at two frequencies (f ; 120 Hz and 1 kHz) and in two modes, one for parallel (PAL) and the other for series (SER) equivalent circuits. The capacitance accuracy of both modes was tested with a capacitor box that allowed adjustment of capacitance. Initially the box was set to 0.1 nF and capacitance measured in SER-mode at 1kHz and 120 Hz, respectively. The box-capacitance was then successively increased by the tenfold up to 1 μ F and capacitance measured for each setting. The procedure was repeated with capacitance measurements in PAR-mode at 1kHz and 120 Hz, respectively. The outcome was that the meter-capacitance was on average by 1.8% ($\pm 0.011\%$ SE, $n = 20$) lower than the box-capacitance.

Resistance

The meter provides two readings for resistance (R_1 and R_2). The user's guide explains the different R-readings as follows: "the mode defines the R loss of a (...) capacitor as a series loss or a parallel loss". This was understood as reference to different equations for calculating impedance in a parallel and series RC circuits, respectively. Impedance (Z, Ω) is calculated as magnitude in terms of Ohm's resistance (R, Ω) and reactance (X_c, Ω) for series RC circuits (Z_s) by

$$Z_s = \sqrt{R^2 + X_c^2} \quad (9)$$

and for parallel RC circuits (Z_p) by

$$Z_p = \frac{RXc}{\sqrt{R^2 + X_c^2}} \quad (10).$$

It was tested whether Z_p and Z_s calculated with the two equations would match with the two R-readings. The resistance was put up by resistors. The reactance follows from the capacitance (Eqn 5). Capacitance was measured for one resistor connected to the capacitor box in parallel and in series, respectively. The resistances of the resistors used were 1 Ω , 10 Ω , 100 Ω , 1 k Ω , 3.3 k Ω , 4.7 k Ω , 5.6 k Ω , 7.9 k Ω , 10 k Ω , 22 k Ω , 27 k Ω , 39 k Ω , 0.1 M Ω , 0.50 M Ω , 1M Ω , 1.5M Ω , and 10 M Ω . The box-capacitance was set to 1 nF, 10nF, 0.1 μ F and 1 μ F. The R-values were read in PAL-mode when the resistor was connected in parallel, and in SER-mode when connected in series to the box. The findings were:

The meter failed to display capacitance in PAL-mode, when capacitance was set to 1 nF and to display R_1 -values when the resistance was 10 Ω or less. When measured in SER-mode R_1 -values showed an almost 1:1 relationship with Z_s (Linear regression: $R_1 = 1.01 (\pm 0.01) Z_s$: mean \pm SE, $n = 39$, $R^2 = 0.993$ for the combined f -data). When measured at 1 kHz R_2 -values showed an almost 1:1 relationship to Z_p , although they were measured in SER-mode (Linear regression: $R_2 = 0.93 (\pm 0.03) Z_p$: mean \pm SE, $n = 20$, $R^2 = 0.982$). When measured at 120 Hz, there was no obvious relationship found between R_2 and Z_p . At relatively high resistances the LCR-meter failed to display the set capacitance values (Fig. 5-23).

To avoid that capacitances were not displayed, capacitance and impedance were measured in SER-mode. To ensure that the displayed impedance followed established electrical laws, measurements were conducted at 1 kHz.

Tests with electrical components were conducted on an electrical breadboard (Model 488-618, RS Components, Corby, UK) with ceramic capacitors (ECKA series, Panasonic, Osaka, Japan) and aluminium electrolytic capacitors (EEA-GA series, Panasonic, Osaka, Japan). The

breadboard consisted of two bus-strips (Fig. 5-7a: A, L) with 40 interconnected clips and 47 clip cores of five interconnected clips. Fig. 5-7c illustrates how an RC circuit (Fig. 5-7b) was constructed.

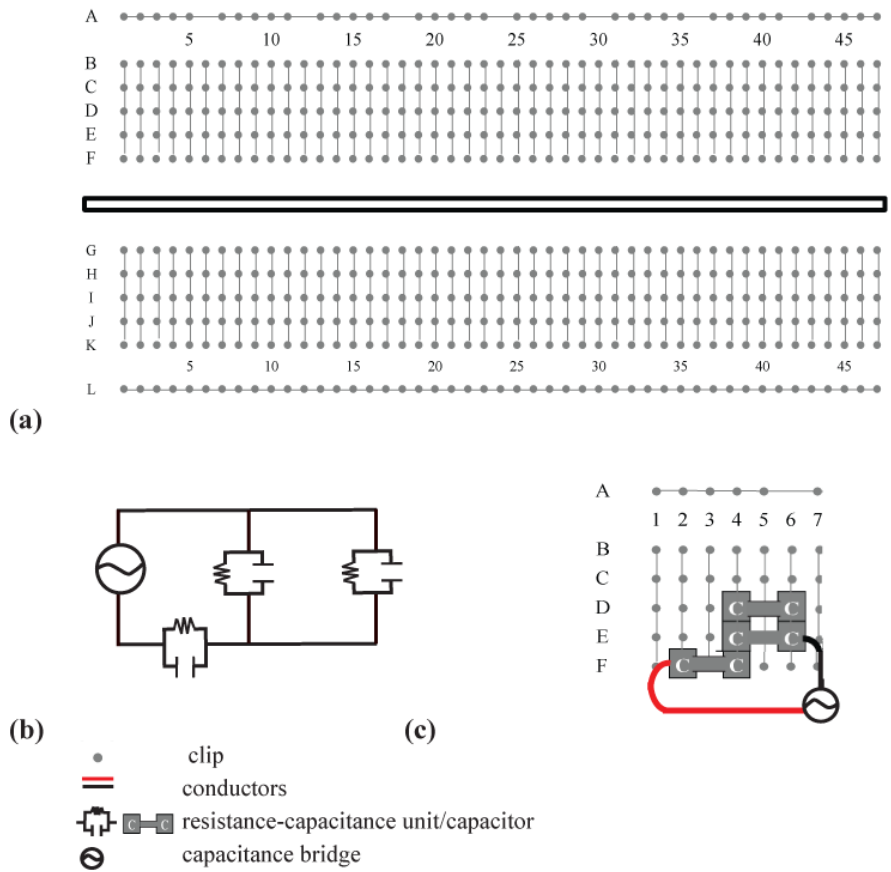


Figure 5-7. (a) Scheme of the electrical breadboard, (b) an exemplary RC circuit consisting of one resistor-capacitor-unit (RC units) being connected in series to two RC units in parallel connection to each other, and (c) the schematic illustration of this RC circuit on the breadboard.

5.3 Results and discussions

5.3.1 Plant tissue- and electrode-related effects on capacitance and the simulation of plant experiments

(i) *Capacitance of different tuber tissues*

Expt i-1. Capacitance was greater for cortex and vascular tissue

Capacitance was measured on potato cores of same size that differed in their composition of tissue. The highest average capacitance was measured for cores including cortex tissue and vascular bundles (see Fig. 5-2b). The capacitance of cores cut in longitudinal orientation to the vascular bundles (408 nF \pm 48 nF SD) did not differ significantly ($df = 46$, $P = 0.65$) from the capacitance of cores cut in transversal orientation (400 nF \pm 67 nF SD). Significantly smaller capacitances were measured for cores containing tissue of the perimedullary zone (260 nF \pm 71 SD, $df = 94$) and of the pith (271 nF \pm 62 nF SD). Tissue from both the pith and the perimedullary zone was predominately parenchyma. Although the pith tissue was more translucent and contained about double the amount of starch grains as the perimedullary zone, this did not significantly affect the capacitance.

The orientation of the vascular bundles had no effect on the capacitance suggesting the plant tissue can be a continuous dielectric. It was observed however that the capacitance was greater for regions of increased concentrations of plant vessels. It is possible that the water content in the tissue affects the dielectric constant (ϵ) and hence its capacitance, but water content was not measured in this experiment.

Expt i-2. Suberized periderm acts as an insulator lowering the capacitance reading

Peeling potato tubers at water level height (Fig. 5-3b) increased the average capacitance significantly from 100 nF (\pm 25 nF SD) to 149 nF (\pm 23 nF SD, $df = 14$, $P = \leq 0.001$). Having the whole submerged part peeled (Fig. 5-3c) increased the average capacitance significantly

further to 189 nF (± 33 nF SD, $df = 14$, $P = 0.02$). However, having tuber parts peeled above water level (Fig. 5-3d) had negligible effect on the capacitance. The average capacitance of potato skin was with 0.4 nF cm^{-2} (± 0.04 nF SD) relatively small in comparison with the intern tissue of the tuber.

The increase in capacitance induced by peeling is consistent with the potato skin being connected in series with the water and the intern of the tuber. Adapting Equation 1 gives:

$$\frac{1}{C_{total}} = \frac{1}{C_p} + \frac{1}{C_w} + \frac{1}{C_s} \quad (11)$$

where C_p is the capacitance of the inner potato tissue, C_w the capacitance of the water, and C_s the capacitance of the skin. As $C_s \ll C_p$ and C_w , the capacitance of the skin will dominate the capacitance reading.

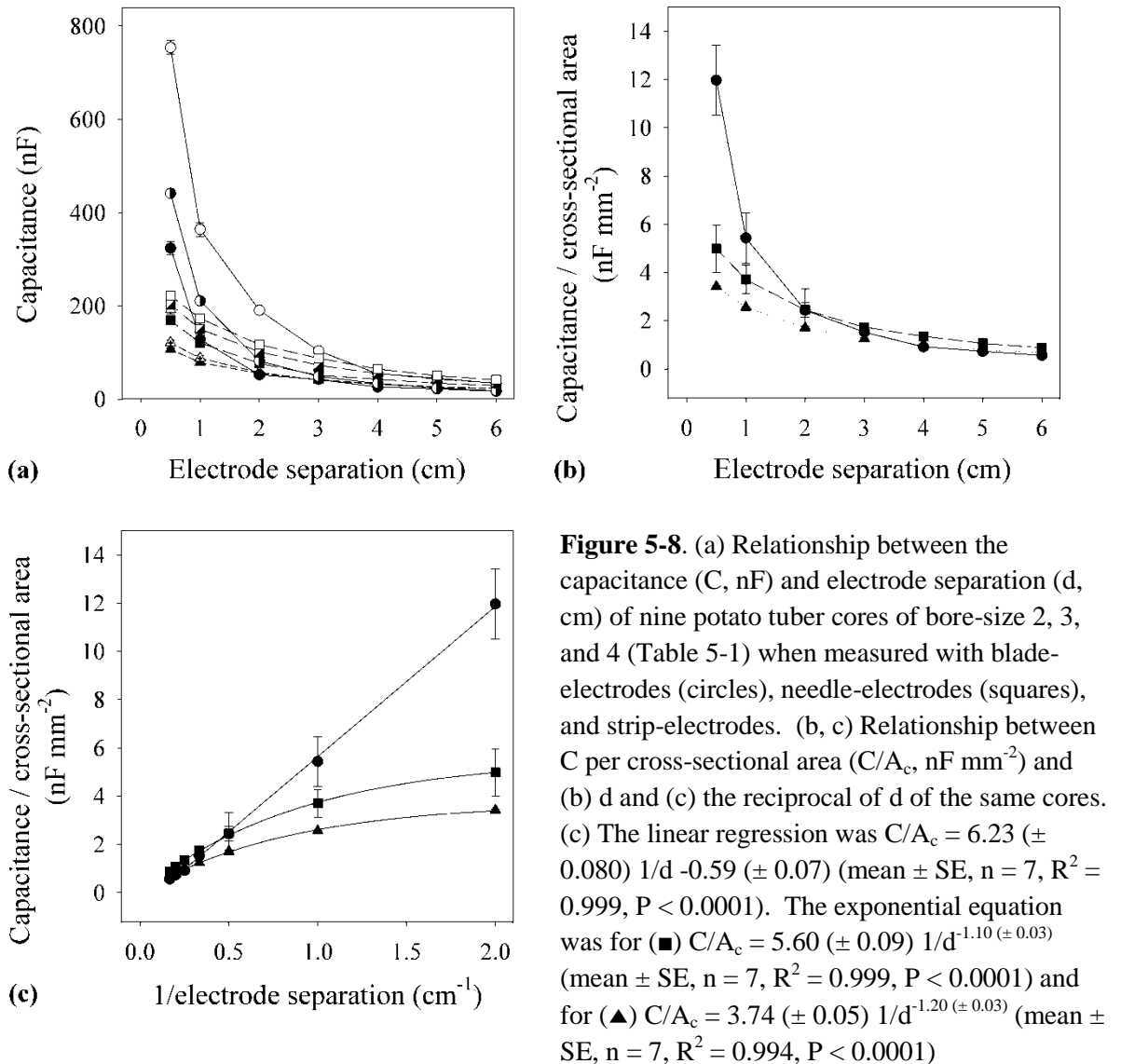
Peeling of tuber parts outside the solution had no effect on the capacitance, presumably because the plant electrode was directly connected with the inner potato tissue.

(ii) *Effect of electrode on capacitance*

Expt ii-1. Various electrode types measured different values of capacitance

Capacitance of potato tuber cores was measured with different electrode types: strip-, needle-, and blade-electrodes (Fig. 2-2). All electrodes measured a non-linear increase in capacitance with decreasing electrode separation (Fig. 5-8a). When capacitance was normalized by the core cross-sectional area (Fig. 5-8b) highest capacitances were measured with blade-electrodes up to an electrode separation (d) of 2 cm. From there on, needle-electrodes measured the highest values. Blade-electrodes measured the lowest capacitance from 4 cm d onwards, as it decreased steeper with d , than the capacitances of the other electrodes. Plotting the normalized

capacitance against the reciprocal of d (Fig. 5-8c) yielded a linear relationship for the use of blade-electrodes and exponential relationships for needle- and strip-electrodes.



The outcome that blade-electrodes measured the highest capacitance, at least at short distances, was probably due to the full electrode-coverage of the core cross-section. The reason why strip-electrode and needle-electrode recorded less capacitance was possibly, because the contact area between electrode and plant tissue was smaller (Fig. 5-9). However, with increasing electrode separations the capacitance of blade-electrodes decreased faster than the capacitance measured

with different electrode types. The reason for this may have been associated with a boundary effect of the outer cut tissue, or because of the different electrical fields generated within the potato tissue (Fig. 5-9).

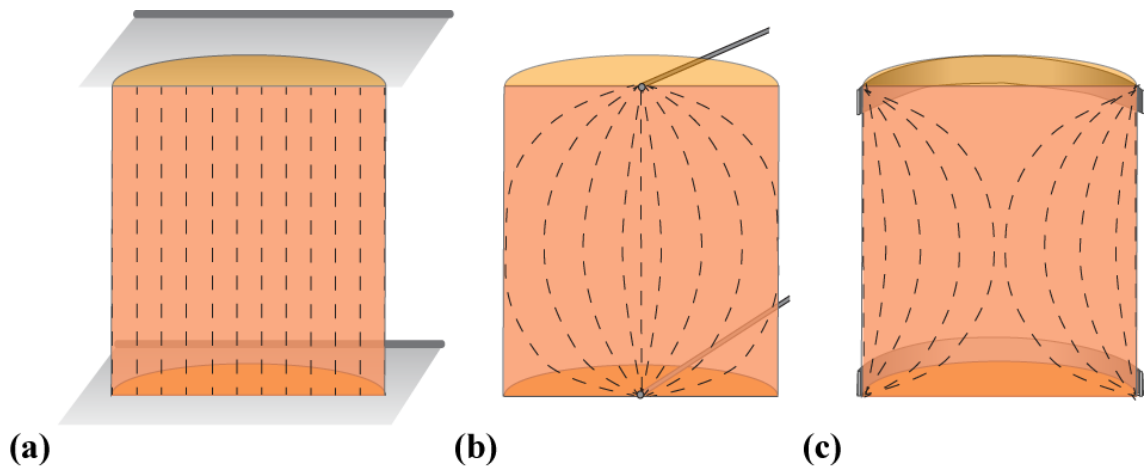


Figure 5-9. Hypothesised electrical fields in plant tissue for (a) blade-electrodes, (b) needle-electrodes, and (c) strip-electrodes.

Expt ii-2. Capacitance correlated with cross-sectional area and circumference, and inversely with electrode separation

Capacitance was measured with blade-electrodes for wider range of core dimensions than in test *ii-1*. Again, capacitance decreased non-linearly with electrode separation (Fig. 10a) and values followed the core diameters being highest for the thickest and lowest for thinnest cores.

Capacitance normalised by cross-sectional area showed a less close linear relationship with the reciprocal of the electrode separation (Fig. 5-10b) than capacitance normalised by the circumference (Fig. 5-10c).

The better fit for capacitance normalised by Φ and electrode separation, rather than capacitance normalized by the cross-sectional area, is surprising. A possible explanation for test *ii-1* results is that the solution on the core surface might have served as electrical bypass of plant tissue. This may also explain the results achieved in test *ii-2*, because a bypass along the core surface would increase the capacitance and might strengthen the correlation between capacitance and circumference.

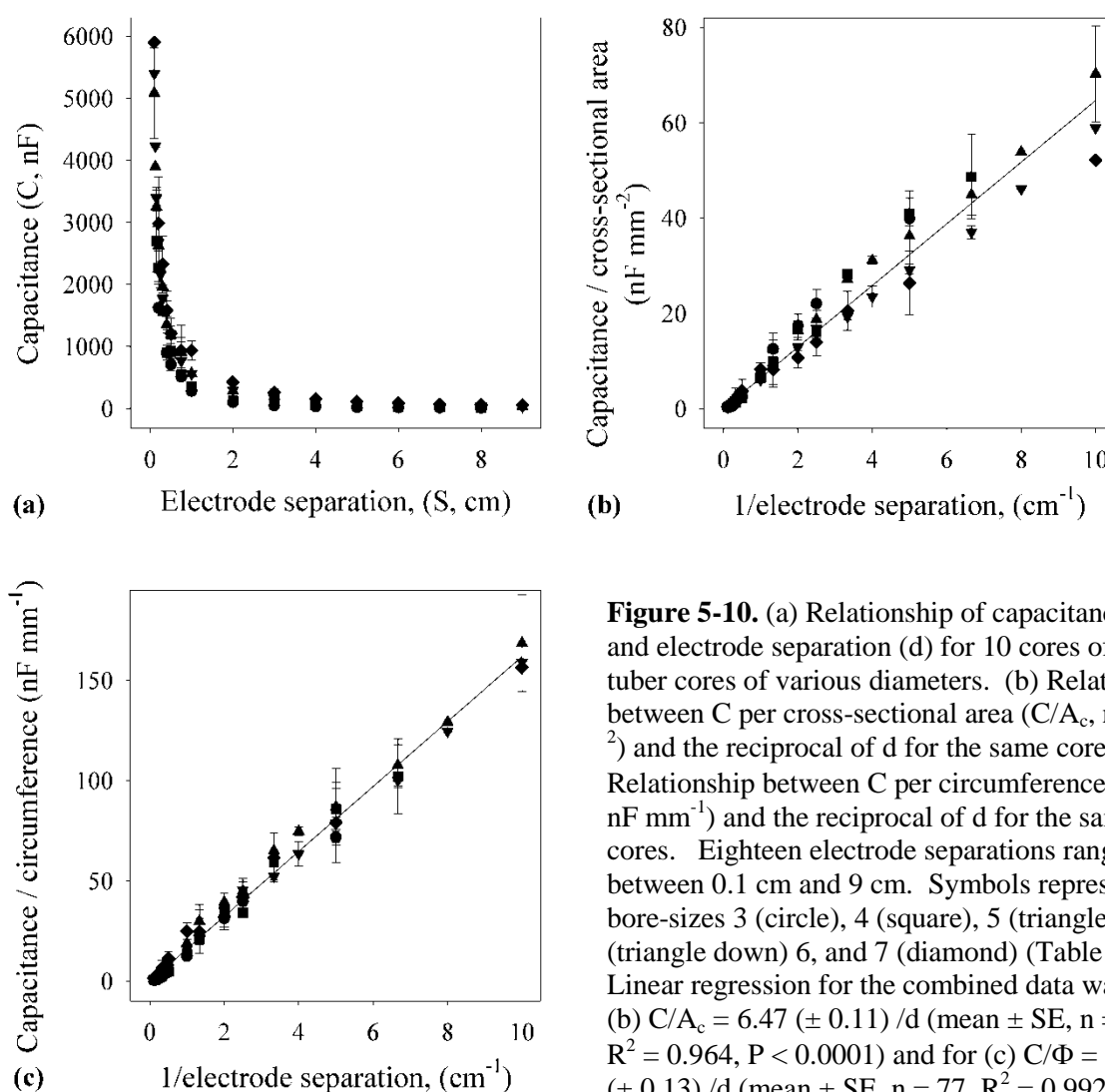


Figure 5-10. (a) Relationship of capacitance (C) and electrode separation (d) for 10 cores of potato tuber cores of various diameters. (b) Relationship between C per cross-sectional area (C/A_c , nF mm^{-2}) and the reciprocal of d for the same cores. (c) Relationship between C per circumference (C/Φ , nF mm^{-1}) and the reciprocal of d for the same cores. Eighteen electrode separations ranged between 0.1 cm and 9 cm. Symbols represent the bore-sizes 3 (circle), 4 (square), 5 (triangle up), 6 (triangle down), 6, and 7 (diamond) (Table 5-1). Linear regression for the combined data was for (b) $C/A_c = 6.47 (\pm 0.11) / d$ (mean \pm SE, $n = 77$, $R^2 = 0.964$, $P < 0.0001$) and for (c) $C/\Phi = 16.20 (\pm 0.13) / d$ (mean \pm SE, $n = 77$, $R^2 = 0.992$, $P < 0.0001$).

Expt ii-3. Capacitance is decreased by surface drying of freshly cut potato cores

Test *ii-3* investigated the effect of solution on the surface of potato cores on the capacitance. Drying the core surface halved the average capacitance ($\pm 19\%$ SD, $n = 50$) while decreasing the average mass by only 2.6% ($\pm 1.2\%$, $n = 50$). Before cores were blotted dry capacitance (nF) was more closely linearly related to the core circumference (mm) than to the cross-sectional area (mm^2): $C = 11.6 (\pm 1.2) \Phi$ (mean \pm SE, $n = 5$, $R^2 = 0.767$) and $C = 2.6 (\pm 1.00) A_c + 127 (\pm 96.6)$ (mean \pm SE, $n = 5$, $R^2 = 0.596$, $P = 0.078$). After they were blotted dry both relationships were improved and equally good ($C = 4.9 (\pm 0.15) \Phi$ (mean \pm SE, $R^2 = 0.967$, $P < 0.0001$) and $C = 1.0 (\pm 0.09) \pm 64.2 (\pm 8.98) A_c$ (mean \pm SE, $R^2 = 0.967$, $P = 0.0017$).

The solution that collected on the surface of potato cores after being cut from the tubers therefore increased the capacitance.

Expt ii-4. Capacitance was linearly correlated with the cross-sectional area of dried potato cores

As the number of data points was relatively small in test *ii-3*, a greater range of core dimensions was used in test *ii-4*. There, a close linear relationship was found between C and A_c (Fig. 5-11a) and a power relationship between C and Φ (Fig. 5-11b).

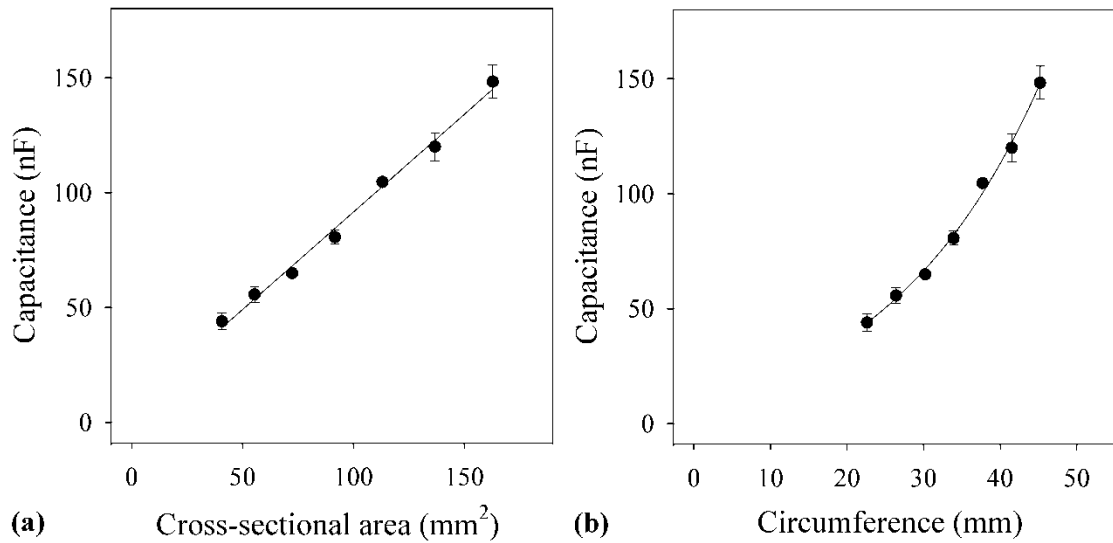


Figure 5-11. Relationship of capacitance and (a) cross-sectional (A_c , mm²) and (b) circumference (Φ , mm) for surface-dried potato cores of different diameter (bore-size 1-9, Table 5-1). The linear regression for (a) was: $C = 0.908 (\pm 0.015) A_c$ (mean \pm SE, $n = 7$, $R^2 = 0.987$, $P < 0.0001$). The exponential regression for (b) was $C = 17.7 (\pm 10.0) \Phi^{0.05 (\pm 0.01)} - 8.9 (\pm 19.7)$ (mean \pm SE, $n = 7$, $R^2 = 0.994$, $P < 0.0001$). Data represent the mean \pm SD of three replicate measurements.

The linear relationship between capacitance and the cross-sectional area of blotted-dry potato cores (Fig. 5-10c) suggests that solution collected at the cut surface of plant tissue had indeed increased the capacitance and strengthened the correlation between capacitance and circumference (see Fig. 5-10).

Expt ii-5. Effect of electrode type on capacitance

Capacitance was measured with two electrodes of different kind on potato cores, before capacitance was measured with pairs of electrodes of the same kind (Fig. 5-4). The capacitance measured with two unequal electrodes laid in between the values measured with equal electrodes (Fig. 5-12a). In fact, it showed almost a 1:1 relationship to the average capacitance of the capacitances measured with the respective electrodes of same type (Fig. 5-12b).

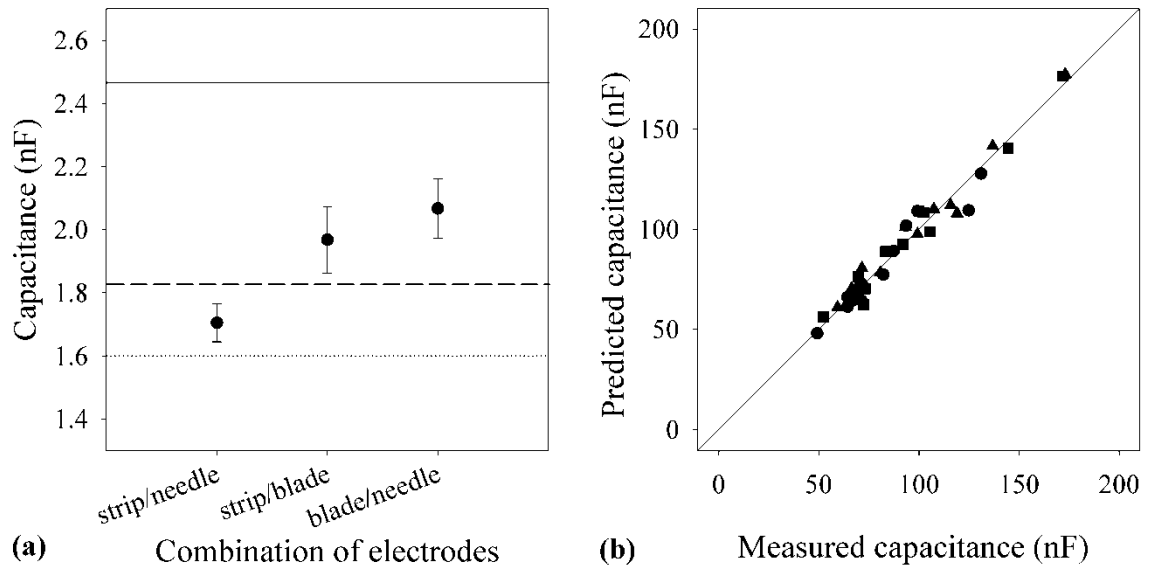


Figure 5-12. (a) Capacitance normalized by the cross-sectional area (C/A_s , nF mm^{-2}) and measured with pairs of blade-electrodes (—), needle-electrodes (---), and strip-electrodes (···) and combinations of two different electrodes of 12 potato tuber cores. Data represent the mean \pm SE. (b) Relationship between capacitance predicted for (C_p) and measured with (C_m) a combination of two different electrodes. The predicted values result from averaging the capacitances measured with two sets of electrodes of the same kind. Symbols represent the different electrode combinations strip/needle (\bullet), strip/blade (\blacksquare), and blade/needle (\blacktriangle). Linear regression was $C_p = 1.001 (\pm 0.010) C_m$ (mean \pm SE, $R^2 = 0.962$). The line indicates a 1:1 relationship.

The results are reasonably consistent with the general principle of plate capacitors, where capacitance is proportional to the average plate area. The blades have the greatest area of contact, whilst the needle- and strip-electrodes present very different electrical field geometry within the plant tissue (Fig. 5-9).

(iii) *Simulating barley experiments in hydroponics and field soil*

Expt iii-1. Fig. 5-5a: Simulating whole root systems in hydroponic solution (Figs 3-3a)

Potato tuber cores were submerged in water (Fig. 5-5a) to simulate individual roots submerged in nutrient solution (Fig. 3-3a). The first of two simulations included cores of same diameter being successively reduced in number (analogous to various numbers of identical roots in solution). The second simulation included cores of two different diameters (analogous to thick and thin roots). The number of cores was successively reduced.

In the first simulation capacitance was well correlated with both core mass in water (Fig. 5-14a) and core cross-sectional area at the water surface (Fig. 5-14b). In the second simulation, the regression lines of capacitance against core mass in water (Fig. 5-14c) and core cross-sectional area at the water surface (Fig. 5-14d) varied in their gradients for cores of non-uniform dimensions.

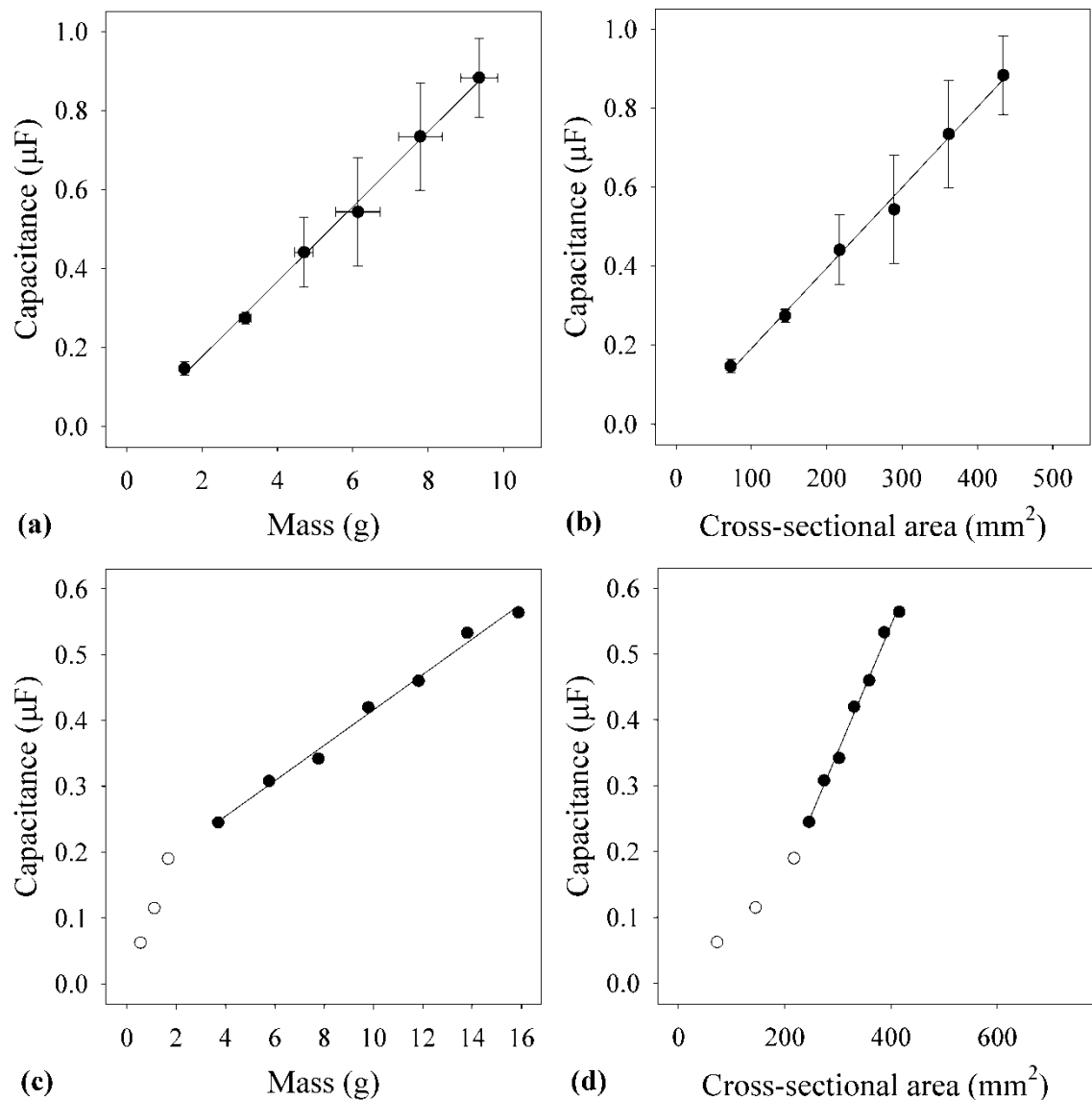


Figure 5-13. (a,c) Relationship of the capacitance (C , μF) of partly submerged potato tuber cores and the core mass in water (M , g) and (b,d) the core cross-sectional area (A_c , mm^2) at the water surface. (a,b) Data represent the mean \pm SD of three replicate measurements of cores of $72 \text{ mm}^2 A_c$. (c,d) Data represent the mean \pm SD of three replicate measurements of cores of (○) $72 \text{ mm}^2 A_c$ and (●) $41 \text{ mm}^2 A_c$. The linear regressions were for (a): $C = 0.095 (\pm 0.003) M$

(mean \pm SE, $n = 6$, $R^2 = 0.996$, $P < 0.0001$); for (b): $C = 0.020 (\pm 6.7 \times 10^{-5}) A_c$ (mean \pm SE, $n = 6$, $R^2 = 0.994$, $P < 0.0001$); for (c) (\bullet) $C = 0.027 (\pm 0.001) M + 0.147 (\pm 0.011)$ (mean \pm SE, $n = 7$, $R^2 = 0.990$, $P < 0.0001$); for (d) (\bullet) $C = 0.002 (\pm 7.5 \times 10^{-5}) A_c - 0.225 (\pm .025)$ (mean \pm SE, $n = 7$, $R^2 = 0.991$, $P < 0.0001$). Linear regressions for \circ -data were not significant.

The first simulation demonstrates that samples of same dimensions show proportionalities between capacitance, mass and cross-sectional area. The second simulation demonstrates that when samples of different dimensions are used linear relationships can be obtained with regression line intercepts far from the origin. By removing the thicker cores at last and excluding their values from regression analysis, the second simulation is consistent with the explanation for the offset linear regression line found between capacitance and root system mass in the simulated barley experiment (Fig. 3-4): The regression line was offset, because seminal roots provided more capacitance per cross-sectional area than nodal roots (Fig. 3-5b).

Expt iii-2. Fig. 5-5b, c: Simulating the partial submergence and trimming of roots in solution (Fig.3-3b, c)

Potato cores of various sizes were incrementally lowered into water, incrementally raised out of water, and trimmed below the water surface, respectively (Fig. 5-5b, c) (analogous to manipulations of barley roots; Fig. 3-3b, c). In the first test, cores of even cross-sectional area were lowered incrementally into water (Fig. 5-5b). Capacitance increased non-linearly with each increment (Fig. 5-15a) and increased nonlinearly with the mass in solution (Fig. 5-15b). Capacitances showed almost linear relationships with the reciprocal of the distance between plant-electrode and water surface (Fig. 5-15c). The distance between regression line intercept and the origin increased with increasing core cross-sectional area (Table 5-3). Trimming cores below the water surface had a negligible effect on the capacitance (Fig. 5-15d).

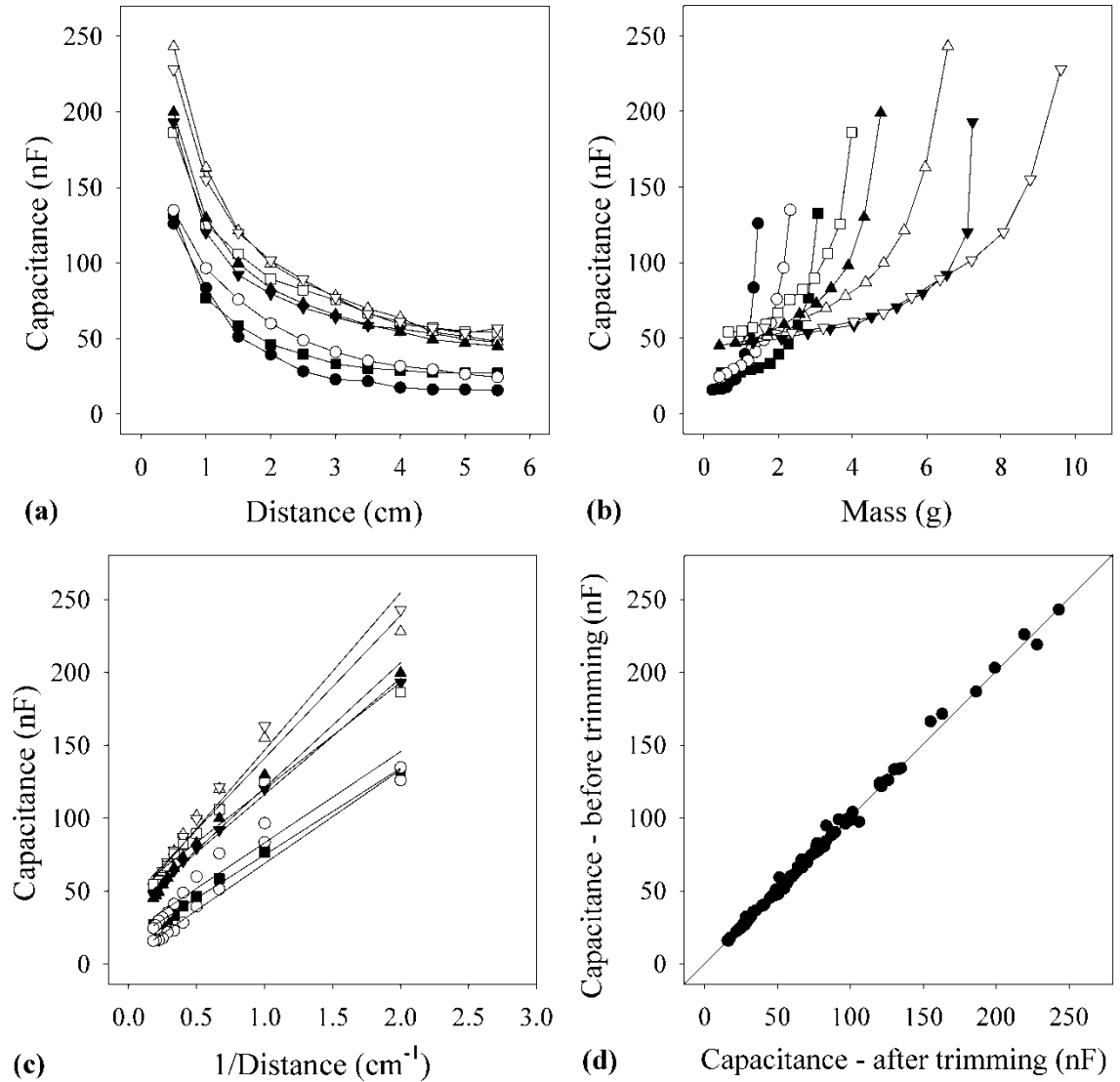


Figure 5-14. Relationship between the capacitance of potato tuber cores and (a) the distance between plant electrode and water surface (D , cm), (b) the tissue mass in water (g), and (c) the reciprocal of D . Symbols represent different bore-sizes (Table 5-1) ranging from 2,3 (circles) over 4,5 (squares) and 6,7 (triangles up) to 8,9 (triangles down). Full symbols represent cores of smaller, hollow symbols cores of greater diameter. (d) Capacitance before (C_b , nF) and after (C_a , nF) the excision of submerged core parts. Linear regressions for (c) see Table 5-2 and for (d) was $C_b = 1.01 (\pm 0.003) C_a$ (mean \pm SE, $n = 92$, $R^2 = 0.996$) when forced through the origin. The line indicates a 1:1-relationship.

Table 5-2. Linear regression equations for capacitance against distance between plant electrode and water surface for partly submerged potato cores (Fig. 5-15c).

Key: *D*: distance between plant electrode and water surface

Core cross-sectional area (mm ²)	$C = b \times \frac{1}{D} \pm y_0$						
	n	b	SE	y ₀	SE	R ²	P
28	9	64	3.5	4.6	2.6	0.971	< 0.0001
41	9	63	5.2	21	3.9	0.935	< 0.0001
55	9	59	1.1	15	0.8	0.997	< 0.0001
72	9	73	4.0	47	3.0	0.970	< 0.0001
92	9	86	3.5	35	2.6	0.984	< 0.0001
113	9	108	5.7	39	4.3	0.973	< 0.0001
137	9	80	1.6	37	1.2	0.996	< 0.0001
163	9	98	5.6	43	4.2	0.969	< 0.0001

The results of the simulations with potato cores are analogous to the findings of the respective barley experiments (Fig. 3-6): The capacitance of cores in water was (1) non-linearly related to the distance between water surface and plant electrode (*D*), (2) non-linearly related to the tissue mass in water, (3) linearly related to the reciprocal of *D*, and (4) proportional to the capacitance measured after trimming. However, increase pattern of capacitance with the reciprocal of *D* (Fig. 5-15c) appeared slightly curved which might be due by bypass-effects of solution at the cut core surface.

When cores of uneven diameter were raised out of water (Fig. 5-5c) capacitance showed a shallower decrease with *D* for greater core diameters and a steeper decrease for smaller diameters

(Fig. 5-16a). The complex relationship between capacitance, core cross-sectional area, and *D* became linear through weighting the *D* values according to the variations in cross-sectional area following Equation 8 (Fig. 5-16b).

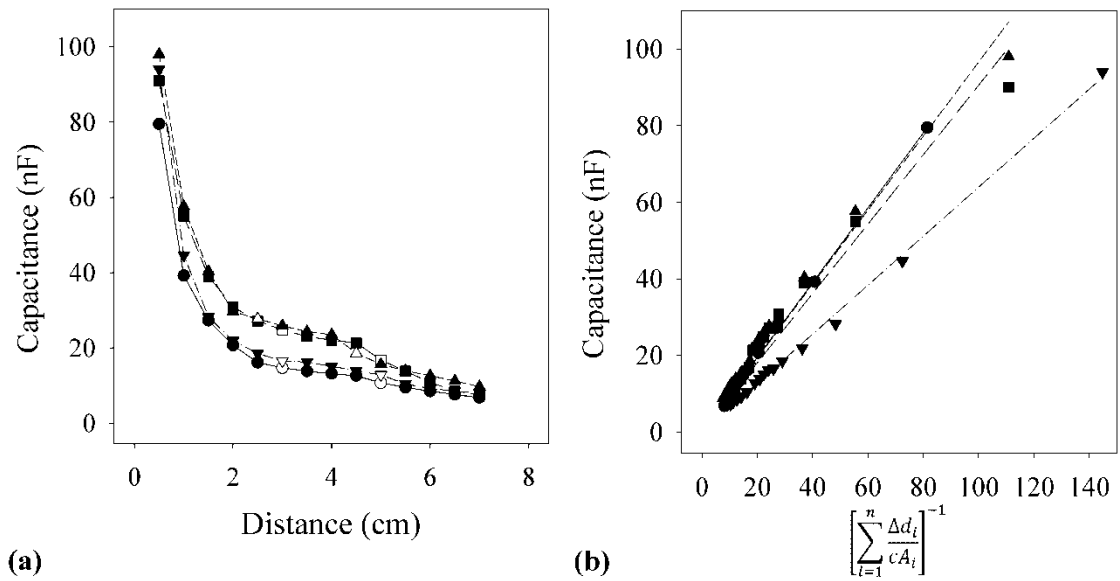
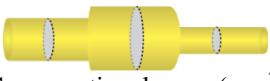


Figure 5-15. Relationship between (a) capacitance (C , nF) and the distance between water surface and plant electrode (d , cm) and (b) between C and reciprocal of cumulative d per cross-sectional area A (mm^2) of four incrementally submerged potato tuber cores. Linear regression equations see Table 5-3. The cross-sectional areas along the core length were 55,137, 41 mm^2 (circles); 41,137, 55 mm^2 (squares); 55, 163, 41 mm^2 (triangles up); and 72, 163, 55 mm^2 (triangles down). Hollow symbols mark changes of the cross-sectional area within an increment.

Table 5-3. Linear regression equations for the relationship between capacitance and the reciprocal of cumulative distance/area for potato tuber cores with three sections of different diameter.

Key: C : capacitance (nF); A_i : cross-sectional area of the i^{th} segment (mm^2); Δd : length of the i^{th} segment (cm)

 Cross-sectional areas (mm^2)	$C = b \times \left[\sum_{i=1}^n \frac{\Delta d_i}{A_i} \right]^{-1}$				
	n	b	SE	R ²	P
41,137,55	14	0.977	0.006	0.999	< 0.0001
55,137,41	13	0.966	0.028	0.970	< 0.0001
55,163,41	14	0.905	0.034	0.951	< 0.0001
72,163,55	15	0.639	0.006	0.997	< 0.0001

The results of this simulation were analogous to the findings of the original barley experiment (Figs 3-7a, 3-11). This confirms (a) the second statement of the new model that capacitances of tissues along an unbranched root or stem can be considered as connected in series and (b) the

fourth statement that capacitances of individual roots or stems are directly proportional to their cross-sectional area.

Expt iii-3. Fig. 5-5d: Simulation of partially submerged roots with the plant electrode at the solution surface (Fig.3-3d)

Capacitance was measured at different positions on potato tuber cores of stepped diameter (Fig. 5-1b). The plant electrode was reattached 5 mm above the water surface (Fig. 5-5d) for each measurement in order to simulate the respective barley experiment in hydroponics (Fig. 3-3d).

Complex relationships were observed between capacitance and the electrode position at the core (Fig. 5-17a). Maximal capacitance occurred where the cross-sectional area at the water surface was greatest (Fig. 5-17b). There was a close linear relationship found between capacitance (nF) and cross-sectional area (mm^2): $C = 1.23 (\pm 0.027) A_c$ (mean \pm SE, $n = 46$, $R^2 = 0.917$, $P < 0.0001$).

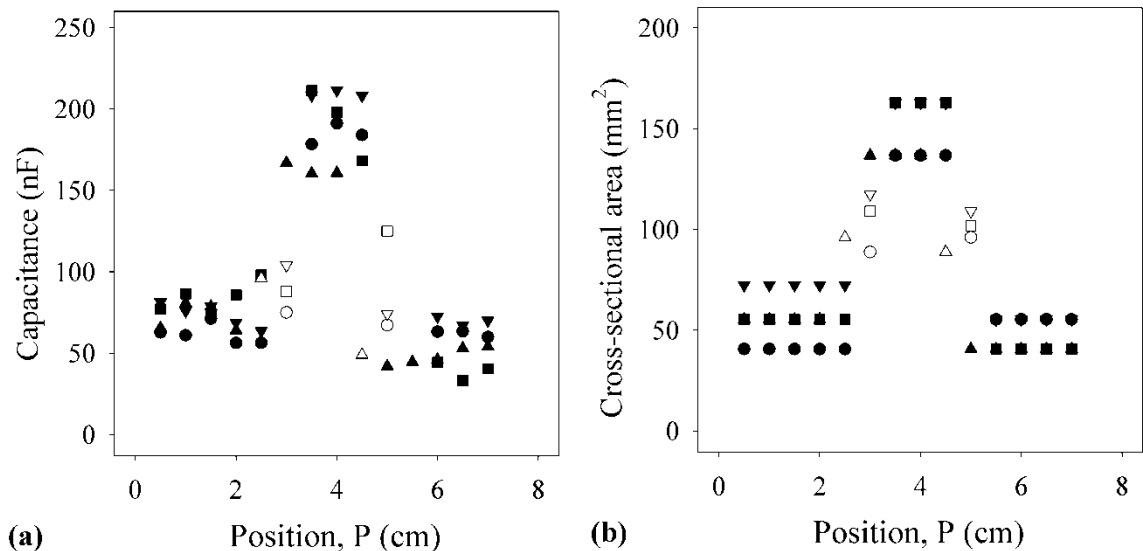


Figure 5-16. The relationship between (a) capacitance and (b) the cross-sectional area of four potato tuber cores that were incrementally raised out of water and position of the water surface on the cores (Fig. 5-5d). The cross-sectional areas along the core length were 41,137, and 55 mm^2 (circles); 55,162, and 41 mm^2 (squares); 55, 137, and 41 mm^2 (triangles up); and 72, 163, and 55 mm^2 (triangles down). Hollow symbols mark changes of the cross-sectional area within an increment.

Plotting the capacitance and cross-sectional area against the position of the water level on a core displayed equally well the differences in core thickness. This demonstrated that the water surface acts like an electrode. The finding of a direct proportionality between capacitance and cross-sectional area was possible, because the distance between water and plant electrode was kept constant. The results are consistent with findings of the respective barley experiments (Fig. 3-8a, c) and confirm (a) the first statement of the new model that the capacitances of the plant tissue and the rooting medium are in series and (b) the fourth statement that the capacitances of individual roots or stems are directly proportional to their cross-sectional area.

Expt iii-4. Fig. 5-5e: Simulation of capacitance measurements of roots in air (Fig.3-3e)

The capacitance of the same cores used in the previous two experiments was measured with two plant electrodes in air (Fig. 5-7e) to simulate the respective barley experiment in hydroponics (Fig. 3-3e).

Capacitance decreased non-linearly with increasing electrode separation (Fig. 5-18a) and showed a complex relationship with the electrode position when the electrode distance was kept constant (Fig. 5-18c). The values showed approximately a 1:1-relationship (Fig. 5-18b, d) with the respective values measured for cores submerged in water (Figs 5-16a and 5-17a).

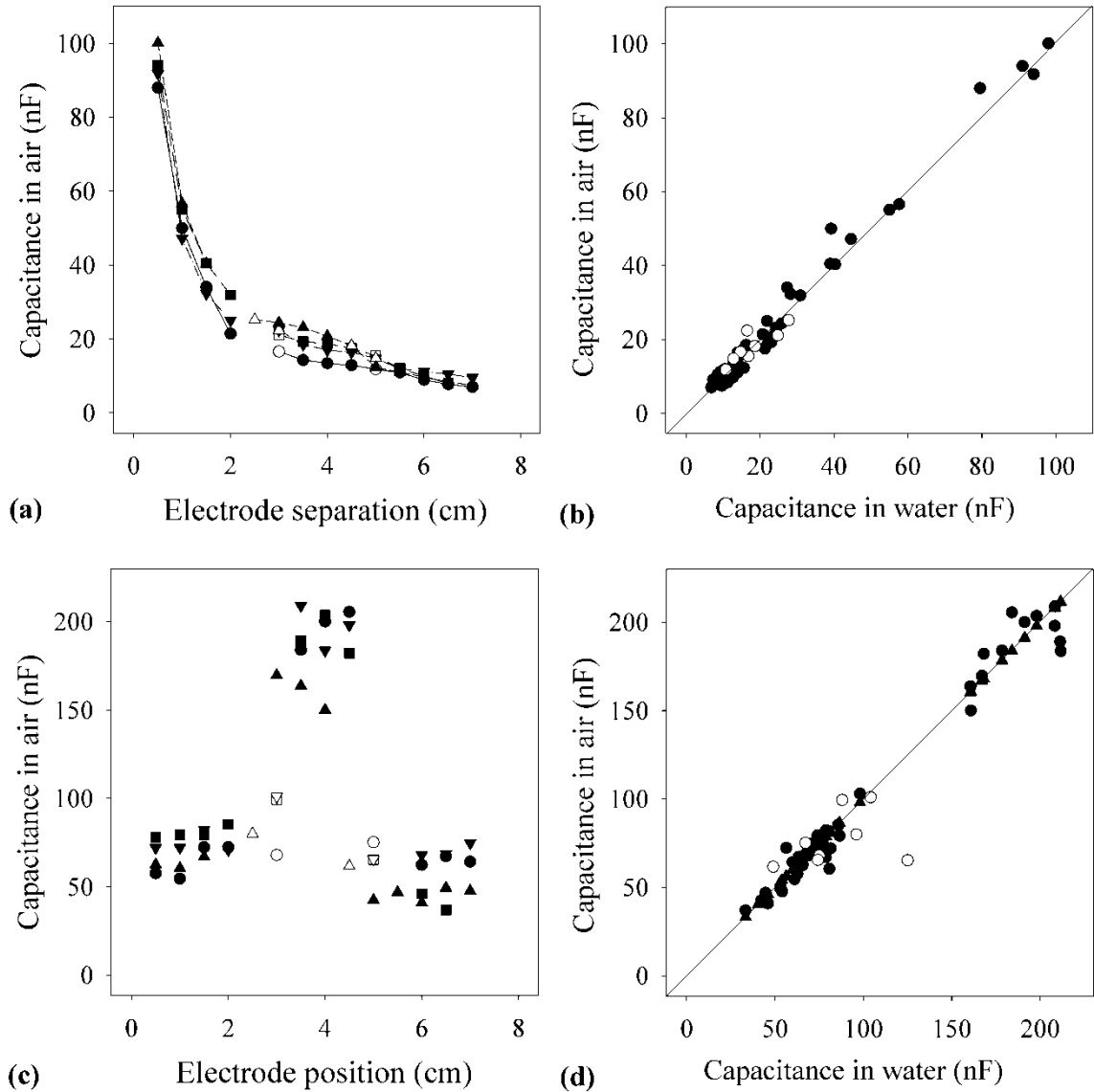


Figure 5-17. Relationship between the capacitance of four potato cores with stepped circumference (Fig. 5-1) measured in air (C_a , nF) and (a) electrode separation and (b) capacitance measured in water (C_w ; Fig. 5-16a). Relationship between the capacitance of four different cores with stepped circumference measured in air and (c) electrode position along the core and (d) capacitance measured in water (C_w ; Fig. 5-17a). The linear regression was for (c) $C_a = 1.026 (\pm 0.012) C_w$ (mean \pm SE, $n = 52$, $R^2 = 0.984$) and for (d) $C_a = 0.978 (\pm 0.016) C_w$ (mean \pm SE, $n = 50$, $R^2 = 0.946$). Open symbols mark data for increments with two circumferences. Lines indicate a 1:1 relationship.

The observation that plant capacitance measured in air differs negligibly from plant capacitance measured water is consistent with the results of the respective barley experiment (Fig. 3-9).

Expt iii-5. Fig. 5-6: Simulating field barley experiment (Fig. 4-6)

In the simulation of an field experiment where capacitance was measured for two neighbouring barley plants in the field (Fig. 4-6) potato cores represented the barley tillers and a wet paper towel the soil (Fig. 5-6d).

The capacitance measured from core to core was much lower than the capacitance of any of the cores (Fig. 5-19a) and fairly proportional to the capacitance of the paper towel (C_p , nF), though the values were slightly lower (Linear regression: $C_p = 1.093 (\pm 0.021) C_t$ (mean \pm SD, $n = 18$, $R^2 = 0.979$, $P < 0.0001$). Total capacitance could be fairly accurately predicted by applying the equation for capacitors in series (Fig. 5-19b), given by

$$C = \left[\sum \frac{1}{C_i} \right]^{-1}$$

(13)

where C_i is the capacitance of the i^{th} component. Applying this equation to capacitances of two cores (C_i , $i = 1, 2$; nF) of various diameters in direct connection (Fig. 5-6c) gave a fairly accurate prediction of the total capacitance (C_t , nF), too (Linear regression: $C_t = 0.988 (\pm 0.019)$

$$\left[\sum \frac{1}{C_i} \right]^{-1} \text{ (mean } \pm \text{ SE, } n = 18, R^2 = 0.977, P < 0.001).$$

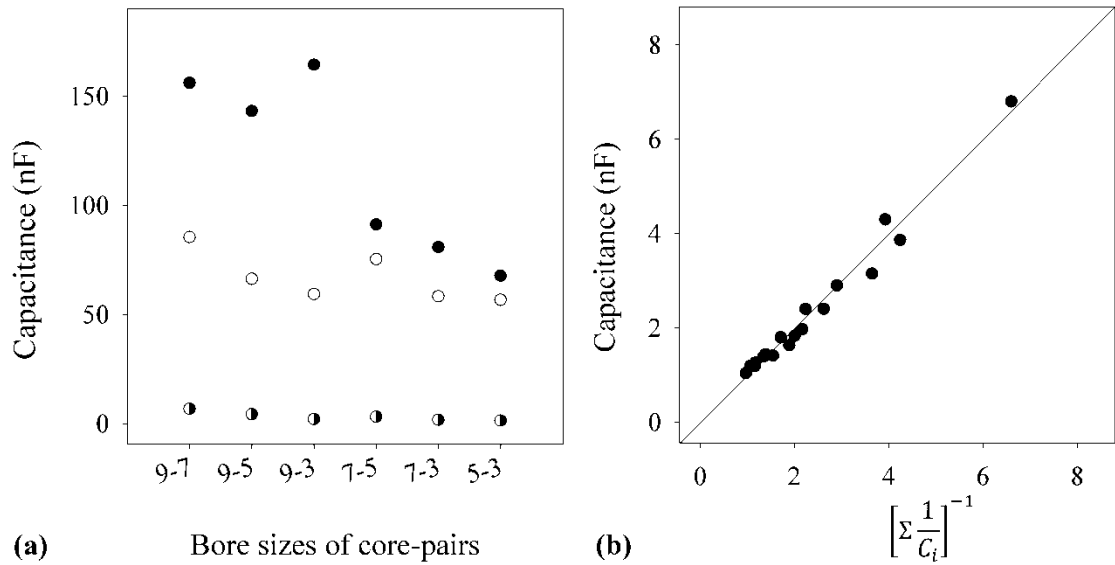


Figure 5-18. (a) Capacitances of the components in Figure 5-6d: two potato cores (●, ○) of different bore-size (Table 5-1) and of the paper towel connecting them (●). (b) Relationship between the total capacitance and the reciprocal of cumulative reciprocals of the component-capacitances, $\left[\sum \frac{1}{C_i}\right]^{-1}$ where C_i is the capacitance of the i^{th} -component.

The findings in the simulation and the field experiment are consistent and thus confirm the first statement of the new model that the capacitances of the plant tissue and the rooting medium are in series.

5.3.2 Electrical circuit analogies

Electrical components on an electrical breadboard were used to test circuit analogies of the cereal experiments in hydroponics (Ch. 3) and the field (Ch. 4) and for the potato core experiments (S. 5.3.1).

Whole root systems in hydroponic solution (Fig. 3-3a)

Capacitance was measured for an increasing number of capacitors connected in parallel (Fig. 5-20a, b). In the first of two tests all capacitors were of same size. In the second test, capacitors of two different sizes were measured. Large capacitors represented seminal roots, small capacitors nodal roots of barley root systems in hydroponic solution (Fig. 3-3a), because seminal roots provide more capacitance than nodal roots (Fig. 3-5b). Larger capacitors were omitted from the regression analysis, because all seminal roots had already emerged when the capacitance measurements started in the experiment with barley plants in hydroponics.

Analogous to the simulation of the barley experiment with potato cores (Fig. 5-14) capacitance increased proportionally to the number of components (Fig. 5-20c). The increase was steeper for the larger capacitors than for smaller capacitors. Thus the electrical analogy for root systems of various sizes in solution gave a regression line that had a positive intercept when capacitance was correlated with the number of “nodal root”.

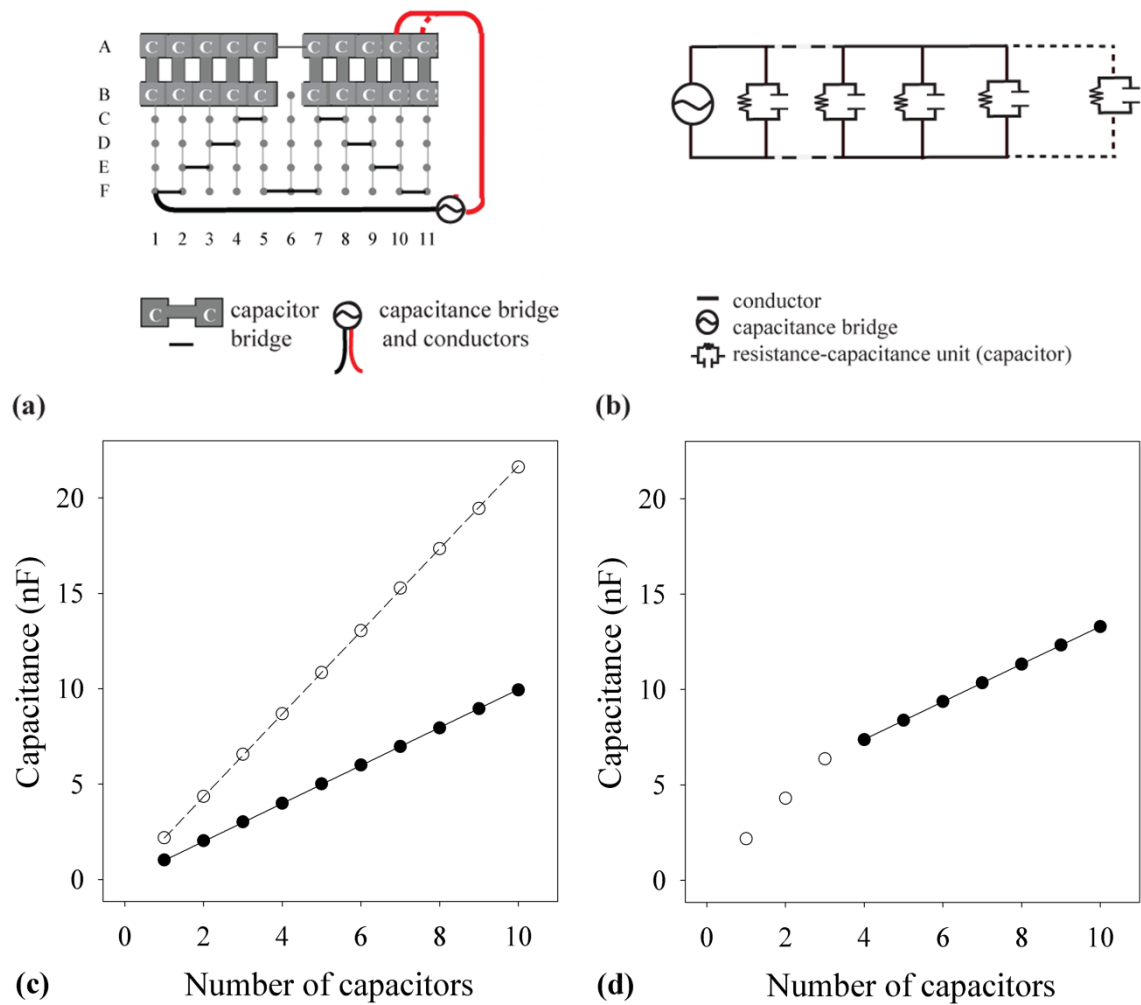


Figure 5-19. (a) Breadboard scheme and (b) RC circuit for the successive removal of capacitors from a set of capacitors connected in parallel. Solid lines show the recent, short dashes the previous connection. Long dashes indicate repetitions in the scheme pattern. Relationship between capacitance (C , nF) and the number of capacitors (N) for a set of (c) equally and (d) unequally large capacitors (●: 1.02 nF; ○: 2.22 nF) added incrementally. The linear regressions were for (c, ●): $C = 1.00 (\pm 0.001) N$ (mean \pm SE, $n = 10$, $R^2 = 1.000$) and for (c, ○) $C = 2.20 (\pm 0.003) N$ (mean \pm SE, $n = 10$, $R^2 = 1.000$) when forced through the origin and for (d; filled symbols only) $C = 0.99 (\pm 0.003) N + 3.44 (\pm 0.018)$ (mean \pm SE, $n = 10$, $R^2 = 1.000$, $P < 0.0001$).

The results are consistent with findings of the respective barley experiment (Fig. 3-4) and their simulation with potato cores (Fig. 5-14). This suggests that the offset regression line in the plant experiment (Fig. 3-4) based on different root capacitances. These results are in agreement with the third proposal of the new model that the capacitance of multiple unbranched root or stem axes in solution can be added in parallel.

The partial submergence of roots in solution (Fig. 3-3b, c)

Capacitance was measured for an increasing number of capacitors in series. In the first of two tests capacitors were of same size. In the second test capacitors of two different sizes were used. Large capacitors represented sections along a root axis of large cross-sectional areas, small capacitors sections of small cross-sectional areas to simulate the partial submergence of root systems in hydroponic solution (Fig. 3-3b, c).

Capacitance decreased non-linearly with the number of capacitors (Fig. 5-21a). The gradient of the curve decreased when large capacitors were added to the RC circuit and increased when small capacitors were added to the RC circuit (Fig. 5-21b). The measured capacitance showed an approximate 1:1 relationship to the capacitance following from the equation of capacitors in series (Eqn 1).

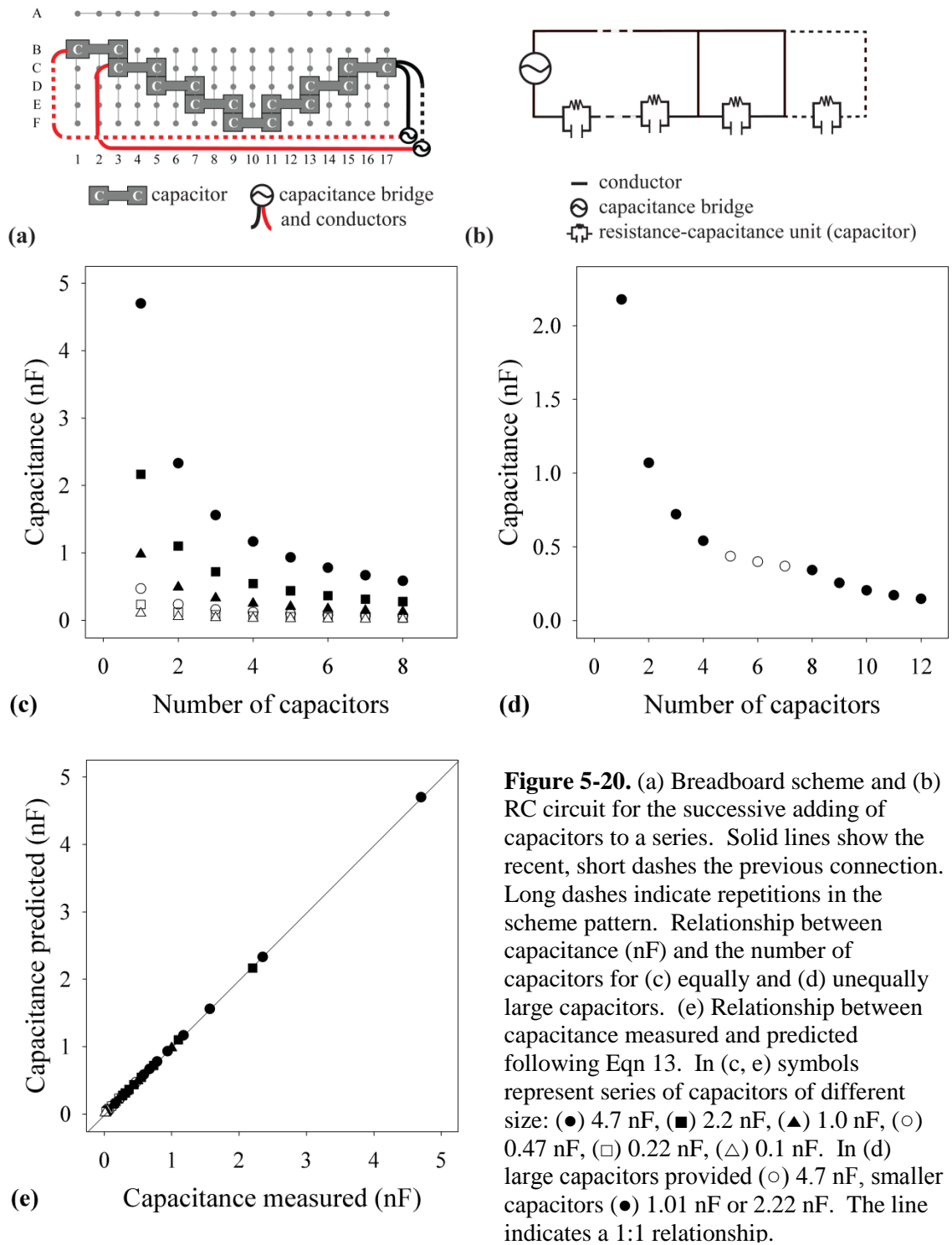


Figure 5-20. (a) Breadboard scheme and (b) RC circuit for the successive adding of capacitors to a series. Solid lines show the recent, short dashes the previous connection. Long dashes indicate repetitions in the scheme pattern. Relationship between capacitance (nF) and the number of capacitors for (c) equally and (d) unequally large capacitors. (e) Relationship between capacitance measured and predicted following Eqn 13. In (c, e) symbols represent series of capacitors of different size: (●) 4.7 nF, (■) 2.2 nF, (▲) 1.0 nF, (○) 0.47 nF, (□) 0.22 nF, (△) 0.1 nF. In (d) large capacitors provided (○) 4.7 nF, smaller capacitors (●) 1.01 nF or 2.22 nF. The line indicates a 1:1 relationship.

The results are consistent with findings of the respective barley experiment (Fig. 3-6a, 3-7a) and their simulation with potato cores (Figs 5-15a, 5-16a and 5-18a), respectively. This confirms

the second statement of the new model that capacitance of tissues along an unbranched root or stem can be connected in series.

Simulation of partially submerged roots with the plant electrode at the solution surface (Fig.3-3d)

Capacitance was measured along a series of capacitors of two different sizes on one capacitor at a time (Fig. 5-22a, b). Large capacitors represented sections of large cross-sectional areas along a root system axis, small capacitors sections of small root cross-sectional areas to simulate capacitance measurements on partially submerged root systems with the plant electrode at constant distance to the solution surface (Fig. 3-3d).

The capacitance readings displayed the capacitances of the capacitors (Fig. 5-22c) and formed pattern similar to the respective barley experiment (Fig. 3-8a, b) and the corresponding with potato core experiment (Fig. 5-17a, b).

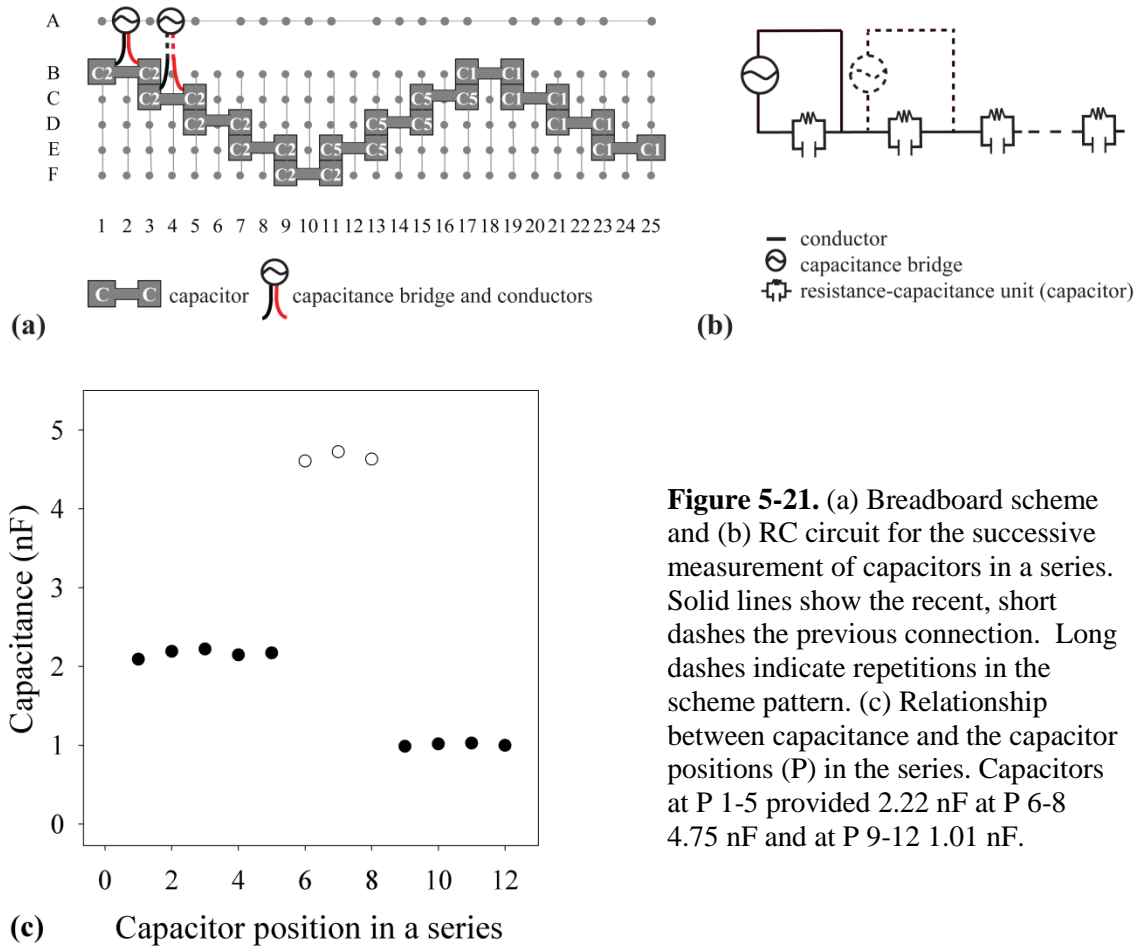


Figure 5-21. (a) Breadboard scheme and (b) RC circuit for the successive measurement of capacitors in a series. Solid lines show the recent, short dashes the previous connection. Long dashes indicate repetitions in the scheme pattern. (c) Relationship between capacitance and the capacitor positions (P) in the series. Capacitors at P 1-5 provided 2.22 nF at P 6-8 4.75 nF and at P 9-12 1.01 nF.

The results are consistent with findings of the respective barley experiment (Fig. 3-8a, b) and their simulation with potato cores (Fig. 5-18).

Capacitance and resistance

A capacitor was connected in series with resistors of different resistance to examine the effect of resistance on the capacitance. The capacitors used had the approximate size of a small barley plant in dry compost (4.6 nF), a large individual root in solution (46 nF), and a large barley root system in solution (1 μ F) (see Table 5-4).

A significant ($\geq 5\%$) under-estimation of the capacitance of the capacitors was found when resistance was greater than 100 k Ω (4.6 nF), 39 k Ω (46 nF), and 22 k Ω (1 μ F), respectively (Fig. 5-22).

Table 5-4. Average capacitances and impedances for barley grown in hydroponics and compost
Key: RS: Root System; SR: Seminal Root; NR: Nodal Root; C: Capacitance; Z: Impedance

	RS in solution		SR in solution		NR in solution		Plant in wet soil		Plant in dry soil	
n	12		12		12		70		70	
	<u>mean</u>	<u>SE</u>	<u>mean</u>	<u>SE</u>	<u>mean</u>	<u>SE</u>	<u>mean</u>	<u>SE</u>	<u>mean</u>	<u>SE</u>
C (nF)	444	47	27	4.3	17	1.8	76	3.4	5.6	0.3
Z (k Ω)	3.5	0.7	72	9.2	49	6.4	10	1.6	78	4.6

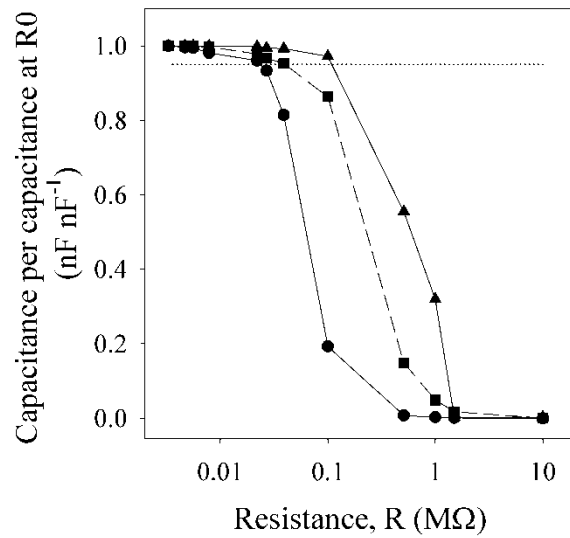


Figure 5-22. The capacitance of a capacitor and a resistor connected in series normalized by the capacitance of the capacitor plotted against the resistance of the resistor. Capacitor size was (●) 1 μ F, (■) 46 nF, and (▲) 4.6 nF. The dotted line shows the significance-level at and above that the variation from the capacitor-capacitance was $\leq 5\%$.

Impedances (Z) measured for barley in hydroponics and compost were at levels that exclude that the resistance (R ; Eqn 6) had a significant effect on the capacitance readings.

5.4 Conclusions

Potato tissues had different dielectric constants: The suberized periderm provides much less capacitance than parenchyma tissue. Tissue with a dense concentration of plant vessels showed much more capacitance than tissue with sparse concentrations of plant vessels, possibly due to differences in the water content.

Capacitance was affected by the nature of plant electrode: Destructive electrodes covering the total cross-section of a plant sample measure maximal capacitance, possibly because the area of contact is maximised and the electric field generated will be uniform (Fig. 5-9a). Non-invasive and minimally-invasive electrodes, e.g. strip- and needle-electrodes, measured lower values, possibly because only a fraction of the plant tissue was connected to the electrode.

Solution at the surface of tissue that had been cut interfered with the capacitance reading in potato cores. However, after removing the surface moisture, potato tissue capacitance was direct proportional to cross-sectional area and inversely proportional to the electrode separation.

The results of simulating cereal experiments with potato tuber cores were all consistent with the results obtained for cereal plants. This confirms the new model and its applicability to plant tissue in general. The finding of an offset regression line for capacitance versus root system mass (Fig. 3-4) can be explained with root-type related differences in the dielectric constant.

The results of testing the electrical analogies circuit components for the cereal experiments (and their equivalent with tuber cores) also agreed well with results for cereal experiments.



6 GENERAL DISCUSSION AND CONCLUSIONS

6.1 Objectives

The overall aim of this thesis was to investigate the applicability of capacitance measurement for the estimation of plant root mass. This required an evaluation of the physical basis underlying the measurement of electrical capacitance of plants. Dalton's widely accepted conceptual model for root capacitance measurement (1995) predicts a linear relationship between the capacitance of a plant in soil and its root mass. This model is based on the three assumptions: (1) all roots are connected as parallel capacitors; (2) capacitance is provided by all root surface cells in electrical connection to the rooting medium; and (3) plant vessels are electrical conductors so that the root cortex acts as the dielectric of a cylindrical capacitor. Dalton (1995) also hypothesized that the root tips contribute the majority of the capacitance.

There had been some suggestions in the literature that this model does not always work. So the experiments conducted in this study aimed to clarify the physical basis of electrical capacitance measurement, both in hydroponics and in solid rooting media.

6.2 Re-evaluation of the physical basis for the electrical capacitance of plants in hydroponics

Preliminary tests

Chapter 2 outlines the general methods used in the thesis and some preliminary experiments aimed to optimise the methods. These preliminary experiments explored variations in root capacitance measurement on barley plants in hydroponics. Hydroponic systems were used to promote easy access to the root system and avoid complications due to variations in the rooting medium. The experiments suggested that linear correlations of capacitance and root system mass may be circumstantial. The work suggests that these correlations result from a close correlation between root system mass and the root dimensions at the solution surface, i.e. the root cross-sectional area. Plant material between electrode and solution surface behaved like a dielectric between two capacitor plates. This analogy is supported by the finding that electrodes with a greater contact area to the plant measure higher capacitances. The tentative conclusion was that the plant material between plant electrode and solution surface determines the capacitance reading. This conclusion however conflicts with the key prediction of the Dalton (1995) model that capacitance would reflect the size of a root system in the ground. Therefore, experiments in Chapter 3 aimed to test Dalton's model (1995) more thoroughly.

Manipulations of the barley root system in hydroponics to test Dalton's model

The Dalton (1995) model was more thoroughly tested in Chapter 3 by using a range of treatments that included: raising roots out of solution, cutting roots at positions below the solution surface, and varying the distance between plant electrode and the solution surface. From the three key statements of Dalton's (1995) model it follows that capacitance should be proportional to the submerged root mass. Another indirect prediction from Dalton's model is that trimming of roots in solution would open the plant vessels effectively causing a short circuit. In this case total capacitance would equal solution capacitance.

Initial experiments showed that there was indeed a good linear correlation between capacitance and the whole root system mass (Fig. 3-4). This result agreed with Dalton's observations and those of a number of other authors (e.g. Ozier-Lafontaine and Bajazet, 2005; Kendall *et al.*, 1982; Chloupek, 1977; van Beem *et al.*, 1998; McBride *et al.*, 2008; Preston *et al.*, 2004; Pitre *et al.*, 2010; Tsukahara *et al.*, 2009). It was found, however, that the linear regression line intercepted the capacitance axis far from the origin. Similar offset regression lines had been found previously (e.g. Dalton, 1995; Chloupek, 1977; van Beem *et al.*, 1998; McBride *et al.*, 2008; Pitre *et al.*, 2010). Further manipulative experiments were designed to test the basis of the observed linear relationship (Fig. 3-3). These clearly showed that the relationship was fortuitous, possibly arising from a linear relationship between root system mass and the root cross-sectional area at the solution surface (Figs 3-5a,b; 3-8a,b). Excision of roots in the solution had negligible effect on the measured capacitance. In conclusion, these results for barley roots were inconsistent with the Dalton model (1995) in many respects. Instead, capacitance was proportional to the total root cross-sectional area at the solution surface (Figs 3-5b, 3-8c) and inversely related to the distance between plant electrode and solution surface (Fig. 3-6c).

These results necessitated the development of a new model to explain the capacitance measured in hydroponic systems. The basic features of the new model were: (1) the capacitances of root and rooting medium are in series; (2) the capacitances of tissues along any unbranched root can be considered as connected in series; (3) the capacitances of multiple unbranched roots at any level act in parallel so reduce to the equivalent of a single capacitor; and (4) the capacitances of individual roots are directly proportional to their cross-sectional area though different constants of proportionality may apply to different tissues. These four statements are consistent with all our observations obtained hitherto. From the first statement it follows that high capacitance of

the solution negligibly affects the total capacitance and therefore is generally irrelevant for the capacitance measurement of plants. The electrical impedance measurements of Cao *et al.* (2010; 2011) using willow plants can be interpreted in a similar way.

The capacitance of submerged root material added to the solution capacitance (as two capacitors connected in series) and thus has a negligible effect on the capacitance. This conclusion depends on the observations that root tissue showed lower capacitance than the solution (by at least an order of magnitude), and root trimming had a negligible effect on the capacitance. Further evidence was found when roots were incrementally raised out of or lowered into the solution and also when capacitance was measured at roots in solution and then in air. First, a 1:1 relationship was found between the capacitances measured in solution and air: this supported the first statement of the new model above. Then, proportionality was found between capacitance and the reciprocal of cumulative distance between electrode and solution surface per total root cross-sectional area: this supported the second to fourth statements of the new model.

6.3 Re-evaluation of the physical basis for the electrical capacitance of plants in solid media

It is of particular interest to determine the value of capacitance measurements for the study of root morphology in soils where access to the roots for observation is much less easy than in hydroponics. Therefore experiments in Chapter 4 aimed to extend the testing of the new model to solid media. The foci of the studies were the soil water distribution, the role of above-ground plant material, the estimation of total capacitance according to standard electrical laws, and the role of the plant electrode.

The effects of soil water distribution

Experiments were conducted in a range of media including a sand-mix, potting compost, and soil in the field. Different soil water properties were achieved by wetting the top surface of only or wetting the soil from below. One finding was that maximal capacitance required only dampening the soil surface right around the plant shoot. Raising the water level had almost negligible effect until the top soil was wet, again. Both findings were consistent with the new model. The new model explains the first finding with an increase of the top soil capacitance due to the wetting, and the second with the greater distance between plant electrode and the wet current-conducting soil.

Plant material between plant electrode and wet soil surface dominated the measurements

From the new model it follows that the aboveground plant tissue between soil surface and electrode is a key component of the capacitance reading. Analogous to capacitance readings on roots in solution and in air (Ch. 3-3) capacitance was measured on a whole plant in wet soil and on the shoot in air after its removal from root system and soil. Here too, a 1:1 relationship was found confirming the first statement of the new model (Fig. 4-5c). Further evidence was the finding of high proportionality between capacitance and the shoot cross-sectional area at the soil surface (Fig. 4-5b).

Calculations of total capacitance according to standard electrical laws confirmed the model

The first statement of the new model, of a serial connection between the capacitances of plant and soil implies that standard electrical laws can be used to calculate the capacitance of combinations of plant tissue and soil capacitance. Measurements of soil capacitance and plant capacitance were used to predict the overall capacitance of the plant in soil in a field experiment, where capacitance was measured between two neighbouring plants (Fig. 4-6).

6.4 Reevaluating the physical basis for the electrical capacitance of plant material in general

Because of the difficulties in experimentation with mature cereal plants, experiments of Chapter 5 used a more simplified system based on cores taken from potato tubers as a source of homogeneous plant material. Core cutting allowed accurate definition of the dimensions of a plant sample. Furthermore, potato tubers provide large areas of same tissue allowing comparisons between different types of potato tissue.

Experiments of Chapter 5 explored tissue- and electrode-related differences in the measurement of capacitance and attempted to simulate the preceding cereal experiments, on which the new model is based, with tuber cores. In a further set of experiments the RC circuits following from our model for these cereal experiments were tested with man-made capacitors on an electrical breadboard and using the same capacitance meter.

Tissue-related differences in the measurement are related to the water content.

The capacitance of different tuber tissues varied as a function of their vessel concentration. The orientation of the vessels however was irrelevant. These findings are in agreement with Urban *et al.*'s (2011) conclusion that electrical current propagates in all directions in plant tissues.

This implies that all capacitive material between two electrodes affect the capacitance reading, and predominately root material as suggested by Chloupek (1972, 1977), Dalton (1995), Aubrecht *et al.* (2006), and many other researchers.

The plant water content of potato tissue largely governed the dielectric constant of a plant tissue and thus its capacitance. Al Hagrey (2007) showed that there is a relationship between capacitance and plant water content by visualizing wet wood in tree trunks by capacitance tomography. Such relationship explains why potato skin with a relatively low water content

provided very little capacitance (Ch. 5, S. 4, *(i) Capacitance of different stem tissues*). The insulating effect of such tissue results obviously from its smaller capacitance being in series with the larger capacitance of inner plant tissue. As the smaller capacitance governs the reading, suberized outer tissue may need to be removed or penetrated by the plant electrode to determine the capacitance of the inner plant tissue.

Another observation was the fact that moisture at the outer surface of a sample increases the capacitance (Ch. 5, S. 4, *(ii) Plant electrode tests*). This capacitance-noise became stronger with increasing electrode separation (Fig. 5-8c) and supported a linear relationship between capacitance and circumference (Figs 5-10c). Both findings suggest that surface moisture serves as electrical bypass. Surface drying however lowered the capacitance and ensured its linear relationship with the cross-sectional area, as included in the new model (Fig. 5-11a).

Electrode-related differences between capacitance measurements are related to the plant/electrode-connection

The highest capacitance was measured when the electrode covered the full cross-section of a plant sample (Fig. 5-12a) necessitating the destruction of the plant. Only then was capacitance linearly related to the reciprocal of electrode separation as would be expected for the new model and as found for roots (Fig 3-6c) and shoots (Fig. 4-3) in the cereal experiments. To avoid destruction, non- or minimally-invasive electrodes can be used, though they can only measure a fraction of full capacitance. This could possibly be corrected by normalizing the capacitance by the ratio of electrode contact area per shoot cross-sectional area, although there may be geometrical effects of electrode shape on the capacitance measured.

Simulating preceding cereal experiments caused analogous results

The results of the simulation of experiments with tuber cores agreed well with results for cereal plants. This confirms the applicability of the new model for plant tissue in general. Testing the RC circuits with electrical components also gave consistent results.

6.5 Knowledge that was gained for practical application

The findings in this thesis suggest that a major reappraisal of the use of capacitance to estimate root mass is needed. Capacitance was determined by the plant tissue between the plant electrode and wet soil surface, and not by the presence of the bulk of the root system. Correlation between root mass and capacitance only occurs if root mass happens to correlate with the plant tissue cross-sectional area between the plant electrode and soil surface. The primary condition for estimating the root mass of a plant in the ground from capacitance, proportionality between root mass and plant dimensions at the ground surface (cf. Introduction of Ch. 6) may often occur (Table 1-2). However, great caution must be exercised in interpreting capacitance measurements, as root systems respond greatly to soil conditions.

In terms of making consistent measurements of plant capacitance, it is necessary to ensure a consistent height and a horizontal orientation of the lower edge of the plant electrode whatever the shape of the plant electrode is. A wet ground surface ensures measurement of the maximum plant capacitance, although this can be mathematically extracted from total capacitance and soil capacitance by applying the equation for capacitors in series, if all capacitance components are known. Dry soil conditions however may influence the relationship between capacitance and root mass, because (1) neither drying, nor necrosis of root tissue might be reflected by the capacitance causing an overestimation of root size and (2) changes in the water content in the

shoot may change the dielectric constant of this tissue and cause an underestimation of root size in relation to wet soil conditions.

We observed a noticeable, but small effect of the distance between plant and soil electrode within the range of several metres. A strong insulator is usually also a weak capacitor. When suberized plant tissue insulates the plant electrode from inner plant tissue the low capacitance it provides dominates the capacitance reading. To avoid this effect electrodes may be used that penetrate through the insulating tissue, e.g. needles, screws, or nails. Irrigation preceding the capacitance measurement should be carried out carefully, because splashes of water wetting the plant surface below the plant electrode can interfere with readings.

6.6 Future work

The results from this thesis show many dangers as well as some limited potential for estimating root mass from plant capacitance. For such estimations to be valid, root mass must be proportional to the plant dimensions at the ground surface. Considering the many findings of correlations between capacitance and root mass in the literature, this often seems to be the case for many crop species, under particular conditions. The proportionality constant varies among different plant species and will almost certainly depend on environmental conditions that influence root and shoot growth. Capacitance offers potential as a fast preliminary screen of plant size at the soil surface, when such proportionality is found. Sentence added: Though measuring the shoot dimensions with a calliper would provide the same information about a plant, this appears to be an inferior alternative, because it is much more labour-intensive, especially for crops producing more than just one tiller.

7 REFERENCES

- United Nations DoEaSA.** 2010. 2010 Revision of the world population prospects. *Population and Development Review*, Vol. 36. New York, NY, USA: United Nations, 854-855.
- Monfreda C, Ramankutty N, Hertel T.** 2007. Global agricultural land use data for climate change analysis. In: Hertel T, Rose S, Tol R, eds. *Economic analysis of land use in global climate change policy*. London, UK: Routledge.
- Gibbs HK, Ruesch AS, Achard F, Clayton MK, Holmgren P, Ramankutty N, Foley JA.** 2010. Tropical forests were the primary sources of new agricultural land in the 1980s and 1990s. *Proceedings of the National Academy of Sciences of the United States of America* **107**, 16732-16737.
- DeFries RS, Rudel T, Uriarte M, Hansen M.** 2010. Deforestation driven by urban population growth and agricultural trade in the twenty-first century. *Nature Geoscience* **3**, 178-181.
- Geist HJ, Lambin EF.** 2001. What drives tropical deforestation? - A meta-analysis of proximate and underlying causes of deforestation based on subnational case study evidence. In: Office LIP, ed. *LUCC report series*. Louvain-la-Neuve, Belgium: Land-Use and Land-Cover Change (LUCC).
- West PC, Gibbs HK, Monfreda C, Wagner J, Barford CC, Carpenter SR, Foley JA.** 2010. Trading carbon for food: Global comparison of carbon stocks vs. crop yields on agricultural land. *Proceedings of the National Academy of Sciences of the United States of America* **107**, 19645-19648.
- Dasgupta S, Laplante B, Meisner C, Wheeler D, Yan J.** 2009. The impact of sea level rise on developing countries: a comparative analysis. *Climatic Change* **93**, 379-388.
- Rahmstorf S, Ganopolski A.** 1999. Long-term global warming scenarios computed with an efficient coupled climate model. *Climatic Change* **43**, 353-367.
- Trachsel S, Kaeppler SM, Brown KM, Lynch JP.** 2011. Shovelomics: high throughput phenotyping of maize (*Zea mays* L.) root architecture in the field. *Plant Soil* **341**, 75-87.

Dalton FN. 1995. In-situ root extent measurements by electrical capacitance methods. *Plant and Soil* **173**, 157-165.

White JW, Andrade-Sanchez P, Gore MA, Bronson KF, Coffelt TA, Conley MM, Feldmann KA, French AN, Heun JT, Hunsaker DJ, Jenks MA, Kimball BA, Roth RL, Strand RJ, Thorp KR, Wall GW, Wang G. 2012. Field-based phenomics for plant genetics research. *Field Crops Research* **133**, 101-112.

Chloupek O. 1972. The relationship between electrical capacitance and some other parameters of plant roots. *Biologia Plantarum* **14**, 227-230.

Bengough AG, McKenzie BM, Hallet PD, Dietrich RC, White PJ, Jones HG. 2009. Physical limitations to root growth: screening, scaling and reality. *Proceedings of 7th ISRR Symposium on Roots: Research and Applications (RootRAP)* Vienna: Institut für Hydraulik und landeskulturelle Wasserwirtschaft, 174.

Waisel Y, Eshel A, Kafkafi U. 2002. *Plant roots - The hidden half*. Tel Aviv: CRC Press Taylor & Francis Group.

Woodward FI, Sheehy JE. 1993. Radiation. *Principles and measurements in environmental biology*, Vol. 1. Kent, UK: Butterworth & Co Ltd 1983, 23-55.

Vandenhirtz J, Vandenhirtz D, Eberius M, Jung A, van der Heijden R, Koch M, Specht K. 2010. Future developments for non-destructive 3D plant and root imaging. *Journal of Biotechnology* **150**, S567-S567.

al Hagrey SA. 2007. Geophysical imaging of root-zone, trunk, and moisture heterogeneity. *Journal of Experimental Botany* **58**, 839-854.

Merrill SD, Tanaka DL, Hanson JD. 2005. Comparison of fixed-wall and pressurized-wall minirhizotrons for fine root growth measurements in eight crop species. *Agronomy Journal* **97**, 1367-1373.

Garrigues E, Doussan C, Pierret A. 2006. Water uptake by plant roots: I - Formation and propagation of a water extraction front in mature root systems as evidenced by 2D light transmission imaging. *Plant and Soil* **283**, 83-98.

Bottomley PA, Rogers HH, Foster TH. 1986. NMR imaging shows water distribution and transport in plant root systems in situ. *Proceedings of the National Academy of Sciences of the United States of America* **83**, 87-89.

Schulze-Till T, Kaufmann I, Sattelmacher B, Jakob P, Haase A, Guo SW, Zimmermann U, Wegner LH. 2009. A ^1H NMR study of water flow in *Phaseolus vulgaris* L. roots treated with nitrate or ammonium. *Plant and Soil* **319**, 307-321.

Jahnke S, Menzel MI, van Dusschoten D, Roeb GW, Bühler J, Minwuyet S, Blümmler P, Temperton VM, Hombach T, Streun M, Beer S, Khodaverdi M, Ziemons K, Coenen HH, Schurr U. 2009. Combined MRI-PET dissects dynamic changes in plant structures and functions. *Plant Journal* **59**, 634-644.

Van As H. 2007. Intact plant MRI for the study of cell water relations, membrane permeability, cell-to-cell and long distance water transport. *Journal of Experimental Botany* **58**, 743-756.

Van As H, Scheenen T, Vergeldt FJ. 2009. MRI of intact plants. *Photosynthesis Research* **102**, 213-222.

Iwaya-Inoue M, Matsui R, Sultana N, Saitou K, Sakaguchi K, Fukuyama M. 2004. H-1-NMR method enables early identification of degeneration in the quality of sweet potato tubers. *Journal of Agronomy and Crop Science* **190**, 65-72.

Terskikh VV, Feurtado JA, Ren CW, Abrams SR, Kermode AR. 2005. Water uptake and oil distribution during imbibition of seeds of western white pine (*Pinus monticola* Dougl. ex D. Don) monitored in vivo using magnetic resonance imaging. *Planta* **221**, 17-27.

Homan NM, Windt CW, Vergeldt FJ, Gerkema E, Van As H. 2007. 0.7 and 3 T MRI and sap flow in intact trees: Xylem and phloem in action. *Applied Magnetic Resonance* **32**, 157-170.

Windt CW, Soltner H, van Dusschoten D, Blümmler P. 2011. A portable Halbach magnet that can be opened and closed without force: The NMR-CUFF. *Journal of Magnetic Resonance* **208**, 27-33.

Blümmler P. 2007. Application of a portable NMR cuff. In: Dietrich R, ed. Forschungszentrum Jülich, Germany.

Moradi AB, Conesa HM, Robinson B, Lehmann E, Kuehne G, Kaestner A, Oswald S, Schulin R. 2009. Neutron radiography as a tool for revealing root development in soil: capabilities and limitations. *Plant and Soil* **318**, 243-255.

Elliot TR, Heck RJ. 2007. A comparison of optical and X-ray CT technique for void analysis in soil thin section. *Geoderma* **141**, 60-70.

Ketcham RA, Carlson WD. 2001. Acquisition, optimization and interpretation of X-ray computed tomographic imagery: applications to the geosciences. *Computers & Geosciences* **27**, 381-400.

Perret JS, Al-Belushi ME, Deadman M. 2007. Non-destructive visualization and quantification of roots using computed tomography. *Soil Biology & Biochemistry* **39**, 391-399.

Ketcham RA. 2011. X-ray computed tomography (CT). In: College SERCaC, ed. *Geochemical Instrumentation and Analysis*. Northfield, MN, USA.

Haberthür D, Hintermüller C, Marone F, Schittny JC, Stampanoni M. 2010. Radiation dose optimized lateral expansion of the field of view in synchrotron radiation X-ray tomographic microscopy. *Journal of Synchrotron Radiation* **17**, 590-599.

Gregory PJ, Bengough AG, Grinev D, Schmidt S, Thomas WTB, Wojciechowski T, Young IM. 2009. Root phenomics of crops: opportunities and challenges. *Functional Plant Biology* **36**, 922-929.

Gregory PJ, Hutchison DJ, Read DB, Jenneson PM, Gilboy WB, Morton EJ. 2003. Non-invasive imaging of roots with high resolution X-ray micro-tomography. *Plant and Soil* **255**, 351-359.

Lontoc-Roy M, Dutilleul P, Prasher SO, Han LW, Brouillet T, Smith DL. 2006. Advances in the acquisition and analysis of CT scan data to isolate a crop root system from the soil medium and quantify root system complexity in 3-D space. *Geoderma* **137**, 231-241.

Tracy SR, Black CR, Roberts JA, Mooney SJ. 2011. Soil compaction: a review of past and present techniques for investigating effects on root growth. *Journal of the Science of Food and Agriculture* **91**, 1528-1537.

Hargreaves CE, Bengough AG, Gregory PJ. 2009. Measuring root traits in barley (*Hordeum vulgare* ssp. *vulgare* and ssp. *spontaneum*) seedlings using gel chambers, soil sacs and X-ray microtomography. *Plant and Soil* **316**, 285-297.

Oswald SE, Menon M, Carminati A, Vontobel P, Lehmann E, Schulin R. 2008. Quantitative imaging of infiltration, root growth, and root water uptake via neutron radiography. *Vadose Zone Journal* **7**, 1035-1047.

Vereecken H, Huisman JA, Bogaen H, Vanderborght J, Vrugt JA, Hopmans JW. 2008. On the value of soil moisture measurements in vadose zone hydrology: A review. *Water Resources Research* **44**, 21.

Vendl M. 2009. Ground Penetrating Radar. Chicago. IL, USA: U.S. Environmental Protection Agency.

Daniels JJ. 2000. Ground penetrating radar fundamentals. Lewis Center, OH, USA: Ohio State University, 1-21.

Hirano Y, Dannoura M, Aono K, Igarashi T, Ishii M, Yamase K, Makita N, Kanazawa Y. 2009. Limiting factors in the detection of tree roots using ground-penetrating radar. *Plant and Soil* **319**, 15-24.

al Hagrey SA. 2004. GPR application for mapping toluene infiltration in a heterogeneous sand model. *Journal of Environmental and Engineering Geophysics* **9**, 79-85.

Cui X, Chen J, Shen J, Cao X, Chen X, Zhu X. 2011. Modeling tree root diameter and biomass by ground-penetrating radar. *Science China earth sciences* **54**, 711-719.

Ley TW, Stevens SG, Topielec RR, Neibling WH. 1994. Soil water monitoring and measurement. *Soil water monitoring and measurement*.

Wu SY, Zhou QY, Wang G, Yang L, Ling CP. 2011. The relationship between electrical capacitance-based dielectric constant and soil water content. *Environmental Earth Sciences* **62**, 999-1011.

Butnor JR, Doolittle JA, Kress L, Cohen S, Johnsen KH. 2001. Use of ground-penetrating radar to study tree roots in the southeastern United States. *Tree Physiology* **21**, 1269-1278.

Zenone T, Morelli G, Teobaldelli M, Fischanger F, Matteucci M, Sordini M, Armani A, Ferre C, Chiti T, Seufert G. 2007. Preliminary use of ground-penetrating radar and electrical resistivity tomography to study tree roots in pine forests and poplar plantations. *5th International Workshop on Functional Structural Plant Models*. Napier, NEW ZEALAND: Csiro Publishing, 1047-1058.

Robinson DA, Kelleners TJ, Cooper JD, Gardner CMK, Wilson P, I L, Logsdon S. 2005. Evaluation of a capacitance probe frequency response model accounting for bulk electrical conductivity: Comparison with TDR and network analyzer measurements. *Vadose Zone Journal* **4**, 992-1003.

Robinson DA, Gardner CMK, Cooper JD. 1999. Measurement of relative permittivity in sandy soils using TDR, capacitance and theta probes: comparison, including the effects of bulk soil electrical conductivity. *Journal of Hydrology* **223**, 198-211.

Robinson DA, Gardner CMK, Evans J, Cooper JD, Hodnett MG, Bell JP. 1998. The dielectric calibration of capacitance probes for soil hydrology using an oscillation frequency response model. *Hydrology and Earth System Sciences* **2**, 111-120.

Kizito F, Campbell CS, Campbell GS, Cobos DR, Teare BL, Carter B, Hopmans JW. 2008. Frequency, electrical conductivity and temperature analysis of a low-cost capacitance soil moisture sensor. *Journal of Hydrology* **352**, 367-378.

Celinski VG, Zimback CRL. 2010. Evaluation of an electrical capacitance sensor an correlation with soil attributes. *Energia na Agricultura* **25**, 157-170.

Fuchs A, Moser MJ, Zangl H. 2008. Investigation on the dependency of the electrical capacitance on the moisture content of wood pellets. In: Mukhopadhyay S, ed. *2008 3rd International Conference on Sensing Technology (Icst 2008)*. Tainan: IEEE, 661-665.

Mizukami Y, Sawai Y, Yamaguchi Y. 2006. Moisture content measurement of tea leaves by electrical impedance and capacitance. *Biosystems Engineering* **93**, 293-299.

- Tattar TA, Blanchar RO, Saufley GC.** 1974. Relationship between electrical-resistance and capacitance of wood in progressive stages of discoloration and decay. *Journal of Experimental Botany* **25**, 658-662.
- Lekas TM, Macdougall RG, Maclean DA, Thompson RG.** 1990. Seasonal trends and effects of temperature and rainfall on stem electrical capacitance of spruce and fir trees. *Canadian Journal of Forest Research* **20**, 970-977.
- Qu Z, Wang X, Liang J.** 2005. Electrical capacitance and resistance assessing tree vigor. *Chinese Forestry Science and Technology* **4**, 37-42.
- Kato K.** 1997. Electrical density sorting and estimation of soluble solids content of watermelon. *Journal of Agricultural Engineering Research* **67**, 161-170.
- Maurício R, Dias CJ, Santana F.** 2006. Monitoring biofilm thickness using a non-destructive, on-line, electrical capacitance technique. *Environmental Monitoring and Assessment* **119**, 599-607.
- MacCuspie RI, Nuraje N, Lee SY, Runge A, Matsui H.** 2008. Comparison of electrical properties of viruses studied by AC capacitance scanning probe microscopy. *Journal of the American Chemical Society* **130**, 887-891.
- Boyce ST, Supp AP, Harriger MD, Pickens WL, Wickett RR, Hoath SB.** 1996. Surface electrical capacitance as a noninvasive index of epidermal barrier in cultured skin substitutes in athymic mice. *Journal of Investigative Dermatology* **107**, 82-87.
- Wickett RR, Mutschelknaus JL, Hoath SB.** 1993. Ontogeny of water sorption-desorption in the perinatal rat. *Journal of Investigative Dermatology* **100**, 407-411.
- Yamada EF, Villaverde AGJB, Munin E, Zangaro RA, Pacheco MTT.** 2004. Effect of low power laser therapy on edema dynamics: sensing by using the electrical capacitance method. *Laser Interaction with Tissue and Cells Xv* **5319**, 355-362.
- Inagaki T, Ong AM, Allaf ME, Rha KH, Bove P, Petresior D, Patriciu A, Varkarakis I, Bhayani SB, Stoianovici D, Jarrett TW, Kavoussi LR.** 2004a. Differentiating between renal

carcinoma and normal parenchyma utilizing electrical capacitance measurements. *Journal of Urology* **171**, 268-268.

Inagaki T, Bhayani SB, Allaf ME, Ong AM, Rha KH, Petresior D, Patriciu A, Varkarakis IM, Jarrett TW, Stoianovici D, Kavoussi LR. 2004b. Tumor capacitance: Electrical measurements of renal neoplasia. *Journal of Urology* **172**, 454-457.

Hope AB. 1955. The electric properties of plant cell membranes I. The electric capacitance of suspensions of mitochondria, chloroplasts, and *Chlorella sp.* *Australian Journal of Plant Biological Science* **9**, 53.

Tittor J, Hansen U-P, Gradmann D. 1983. Impedance of the electrogenic Cl⁻ pump in *Acetabularia*: Electrical frequency entrainments, voltage-sensitivity, and reaction kinetic interpretation *Journal of Membrane Biology* **75**, 129.

Beilby MJ, Beilby BN. 1983. Potential dependence of the admittance of *Chara coralline* *Journal of Membrane Biology* **75**, 371.

Hodgkin AL, Huxley AF. 1952. A quantitative description of membrane current and its application to conduction and excitation in nerve. *Journal of Physiology* **117**, 500-544.

Zimmermann U, Büchner K-H, Benz R. 1982. Transport properties of mobile charges in algal membranes: influence of pH and turgor pressure. *Journal of Membrane Biology* **67**, 183-197.

Zhang MIN, Stout DG, Willison HM. 1990. Electrical impedance analysis in plant tissues: Symplasmic resistance and membrane capacitance in the Hayden model. *Journal of Experimental Botany* **41**, 371-380.

Hayden RI, Moyses CA, Calder FW, Crawford DP, Fenson DS. 1969. Electrical impedance studies on potato and alfalfa tissue. *Journal of Experimental Botany* **20**, 177-200.

Degouys V, Cerckel I, Garcia A, Hearfield J, Dubois D, Fabry L, Miller AOA. 1993. Dielectric spectroscopy of mammalian cells. *Cytotechnology* **13**, 195-202.

Mishima K, Mimura A, Takahara Y, Asami K, Hanai T. 1991. On-line monitoring of cell concentrations by dielectric measurements. *Journal of Fermentation and Bioengineering* **72**, 291-295.

Markx GH, Davey CL, Kell DB, Morris P. 1991. The dielectric permittivity at radio frequencies and the Bruggman probe: novel techniques for the on-line determination of biomass concentrations in plant cell cultures. *Journal of Biotechnology* **20**, 279-290.

Asami K, Yamaguchi T. 1999. Electrical and morphological changes of human erythrocytes under high hydrostatic pressure followed by dielectric spectroscopy. *Annals of Biomedical Engineering* **27**, 427-435.

Matanguihan RM, Konstantinov KB, Yoshida T. 1994. Dielectric measurement to monitor the growth and the physiological states of biological cells. *Bioprocess Engineering* **11**, 213-222.

Morita S, Umakoshi H, Kuboi R. 1999. Characterization and on-line monitoring of cell disruption and lysis using dielectric measurement. *Journal of Bioscience and Bioengineering* **88**, 78-84.

Kiviharju K, Salonen K, Moilanen U, Eerikäinen T. 2008. Biomass measurement online: the performance of in situ measurements and software sensors. *Journal of Industrial Microbiology & Biotechnology* **35**, 657-665.

Asami K, Yamaguchi T. 1992. Dielectric spectroscopy of plant protoplasts. *Biophysical Journal* **63**, 1493-1499.

Asami K, Yonezawa T, Wakamatsu H, Koyanagi N. 1996. Dielectric spectroscopy of biological cells. *Bioelectrochemistry and Bioenergetics* **40**, 141-145.

Banasiak R, Soleimani M. 2010. Shape based reconstruction of experimental data in 3D electrical capacitance tomography. *Ndt & E International* **43**, 241-249.

Banasiak R, Wajman R, Betiuk J, Soleimani M. 2009. Feasibility study of dielectric permittivity inspection using a 3D capacitance CT method. *Ndt & E International* **42**, 316-322.

Banasiak R, Wajman R, Sankowski D, Soleimani M. 2010. Three-dimensional nonlinear inversion of electrical capacitance tomography data using a complete sensor model. *Progress in Electromagnetics Research-Pier* **100**, 219-234.

Warsito W, Marashdeh Q, Fan LS. 2007. Electrical capacitance volume tomography. *IEEE Sensors Journal* **7**, 525-535.

Soleimani M, Mitchell CN, Banasiak R, Wajman R, Adler A. 2009. Four-dimensional electrical capacitance tomography imaging using experimental data. *Progress in Electromagnetics Research-Pier* **90**, 171-186.

Niedostatkiewicz M, Tejchman J, Chaniecki Z, Grudziń K. 2009. Determination of bulk solid concentration changes during granular flow in a model silo with ECT sensors. *Chemical Engineering Science* **64**, 20-30.

Gamio JC, Castro J, Rivera L, Alamilla J, Garcia-Nocetti F, Aguilar L. 2005. Visualisation of gas-oil two-phase flows in pressurised pipes using electrical capacitance tomography. *Flow Measurement and Instrumentation* **16**, 129-134.

Waterfall RC, He R, Wolanski P, Gut Z. 2001. Flame visualizations using electrical capacitance tomography (ECT). *Process Imaging for Automatic Control* **4188**, 242-250.

Jiang F, Liu S, Liu J, Wang XY. 2009. Measurement of ice movement in water using electrical capacitance tomography. *Journal of Thermal Science* **18**, 8-12.

Rimpiläinen V, Poutiainen S, Heikkinen LM, Savolainen T, Vauhkonen M, Ketolainen J. 2011. Electrical capacitance tomography as a monitoring tool for high-shear mixing and granulation. *Chemical Engineering Science* **66**, 4090-4100.

Floyd TL. 2010. *Principles of electric circuits: electron flow version*. Upper Saddle River, NJ, USA: Pearson Education Inc., publishing as Prentice Hall.

Aaltonen J. 2001. Ground monitoring using resistivity measurements in glaciated terrains. Dissertation, Royal Institute of Technology, Stockholm, 61.

- Celano G, Palese AM, Ciucci A, Martorella E, Vignozzi N, Xiloyannis C.** 2011. Evaluation of soil water content in tilled and cover-cropped olive orchards by the geoelectrical technique. *Geoderma* **163**, 163-170.
- Michot D, Benderitter Y, Dorigny A, Nicoullaud B, King D, Tabbagh A.** 2003. Spatial and temporal monitoring of soil water content with an irrigated corn crop cover using surface electrical resistivity tomography. *Water Resources Research* **39**, 1-20.
- Paillet Y, Cassagne N, Brun JJ.** 2010. Monitoring forest soil properties with electrical resistivity. *Biology and Fertility of Soils* **46**, 451-460.
- Robain H, Descloitres M, Ritz M, Atangana QY.** 1996. A multiscale electrical survey of a lateritic soil system in the rain forest of Cameroon. *Journal of Applied Geophysics* **34**, 237-253.
- Samouëlian A, Cousin I, Tabbagh A, Bruand A, Richard G.** 2005. Electrical resistivity survey in soil science: a review. *Soil & Tillage Research* **83**, 173-193.
- Samouëlian A, Cousin I, Richard G, Tabbagh A, Bruand A.** 2003. Electrical resistivity imaging for detecting soil cracking at the centimetric scale. *Soil Science Society of America Journal* **67**, 1319-1326.
- Nowroozi AA, Horrocks SB, Henderson P.** 1999. Saltwater intrusion into the freshwater aquifer in the eastern shore of Virginia: a reconnaissance electrical resistivity survey. *Journal of Applied Geophysics* **42**, 1-22.
- Samsudin AR, Haryono A, Hamzah U, Rafek AG.** 2008. Salinity mapping of coastal groundwater aquifers using hydrogeochemical and geophysical methods: a case study from North Kelantan, Malaysia. *Environmental Geology* **55**, 1737-1743.
- al Hagrey SA.** 2006. Electrical resistivity imaging of tree trunks. *Near Surface Geophysics* **4**, 179-187.
- Amato M, Bitella G, Rossi R, Gómez JA, Lovelli S, Gomes JJF.** 2009. Multi-electrode 3D resistivity imaging of alfalfa root zone. *European Journal of Agronomy* **31**, 213-222.

Garré S, Javaux M, Vanderborght J, Pagès L, Vereecken H. 2011. Three-dimensional electrical resistivity tomography to monitor root zone water dynamics. *Vadose Zone Journal* **10**, 412-424.

Werban U, al Hagrey SA, Rabbel W. 2008. Monitoring of root-zone water content in the laboratory by 2D geoelectrical tomography. *Journal of Plant Nutrition and Soil Science - Zeitschrift für Pflanzenernährung und Bodenkunde* **171**, 927-935.

al Hagrey SA, Petersen T. 2011. Numerical and experimental mapping of small root zones using optimized surface and borehole resistivity tomography. *Geophysics* **76**, G25-G35.

Goulet E, Barbeau G. 2006. Contribution of soil electric resistivity measurements to the studies on soil/grapevine water relations. *Journal International Des Sciences De La Vigne Et Du Vin* **40**, 57-69.

Srayeddin I, Doussan C. 2009. Estimation of the spatial variability of root water uptake of maize and sorghum at the field scale by electrical resistivity tomography. *Plant and Soil* **319**, 185-207.

Rossi R, Amato M, Bitella G, Bochicchio R, Gomes JJF, Lovelli S, Martorella E, Favale P. 2011. Electrical resistivity tomography as a non-destructive method for mapping root biomass in an orchard. *European Journal of Soil Science* **62**, 206-215.

Fukue M, Minato T, Horibe H, Taya N. 1999. The micro-structures of clay given by resistivity measurements. *Engineering Geology* **54**, 43-53.

McCarter WJ. 1984. The electrical resistivity characteristics of compacted clays. *Geotechnique* **34**, 263-267.

Ozier-Lafontaine H, Bajazet T. 2005. Analysis of root growth by impedance spectroscopy (EIS). *Plant and Soil* **277**, 299-313.

Rajkai K, Végh KR, Nacsá T. 2002. Electrical capacitance as the indicator of root size and activity. *Agrokémia és Talajtan* **51**, 89-98.

Rajkai K, Végh KR, Nacsa T. 2005. Electrical capacitance of roots in relation to plant electrodes, measuring frequency and root media. *Acta Agronomica Hungarica* **53**, 197-210.

Repo T, Laukkanen J, Silvennoinen R. 2005. Measurement of the tree root growth using electrical impedance spectroscopy. *Silva Fennica* **39**, 159-166.

Repo T, Zhang G, Ryyppö A. 2002. The electrical impedance spectroscopy of Scots pine needles during cold acclimation. *Physiologia Plantarum* **115**, 385-392.

Repo T, Zhang G, Ryyppö A, Rikala R. 2000. The electrical impedance spectroscopy of Scots pine (*Pinus sylvestris* L.) shoots in relation to cold acclimation. *Journal of Experimental Botany* **51**, 2095-2107.

Räisänen M, Repo T, Lehto T. 2007. Cold acclimation was partially impaired in boron deficient Norway spruce seedlings. *Plant and Soil* **292**, 271-282.

Zhang G, Ryyppö A, Repo T. 2002. The electrical impedance spectroscopy of Scots pine needles during cold acclimation. *Physiologia Plantarum* **115**, 385-392.

Wu L, Ogawa Y, Tagawa A. 2008. Electrical impedance spectroscopy analysis of eggplant pulp and effects of drying and freezing-thawing treatments on its impedance characteristics. *Journal of Food Engineering* **87**, 274-280.

Cao Y, Repo T, Silvennoinen R, Lehto T, Pelkonen P. 2010. An appraisal of the electrical resistance method for assessing root surface area. *Journal of Experimental Botany* **61**, 2491-2497.

Aubrecht L, Stanek Z, Koller J. 2006. Electrical measurement of the absorption surfaces of tree roots by the earth impedance method: 1. Theory. *Tree Physiology* **26**, 1105-1112.

Čermák J, Ulrich R, Stanek Z, Koller J, Aubrecht L. 2006. Electrical measurement of tree root absorbing surfaces by the earth impedance method: 2. Verification based on allometric relationships and root severing experiments. *Tree Physiology* **26**, 1113-1121.

- Butler AJ, Barbier N, Čermák J, Koller J, Thornily C, McEvoy C, Nicoll B, Perks MP, Grace J, Meir P.** 2010. Estimates and relationships between aboveground and belowground resource exchange surface areas in a Sitka spruce managed forest. *Tree Physiology* **30**, 705-714.
- Dvořák M, Černohorská J, Janáček K.** 1981. Characteristics of current passage through plant tissue. *Biologia Plantarum* **23**, 306-310.
- Urban J, Bequet R, Mainiero R.** 2011. Assessing the applicability of the earth impedance method for *in situ* studies of tree root systems. *Journal of Experimental Botany* **62**, 1857-1869.
- Kendall WA, Pederson GA, Hill RR, Jr.** 1982. Root size estimates of red clover and alfalfa based on electrical capacitance and root diameter measurements. *Grass and Forage Science* **37**, 253-256.
- Matsumoto N, Homma T, Morita S, Abe J.** 2001. Capacitance as a possible indicator for size of maize root system. *Proceedings of 6th Symposium of the International Society of Root Research*. Nagoya: Japanese Society for Root Research, 578-579.
- Chloupek O.** 1977. Evaluation of the size of a plant's root system using its electrical capacitance. *Plant and Soil* **48**, 525-532.
- Chloupek O, Dostál V, Středa T, Psota V, Dvořáčková O.** 2010. Drought tolerance of barley varieties in relation to their root system size. *Plant Breeding* **129**, 630-636.
- van Beem J, Smith ME, Zobel RW.** 1998. Estimating root mass in maize using a portable capacitance meter. *Agronomy Journal* **90**, 566-570.
- Chloupek O, Skácel M, Ehrenbergerova J.** 1999. Effect of divergent selection for root size in field-grown alfalfa. *Canadian Journal of Plant Science* **79**, 93-95.
- McBride R, Candido M, Ferguson J.** 2008. Estimating root mass in maize genotypes using the electrical capacitance method. *Archives of Agronomy and Soil Science* **54**, 215-226.
- Chloupek O, Forster BP, Thomas WTB.** 2006. The effect of semi-dwarf genes on root system size in field-grown barley. *Theoretical and Applied Genetics* **112**, 779-786.

Preston GM, McBride RA, Bryan J, Candido M. 2004. Estimating root mass in young hybrid poplar trees using the electrical capacitance method. *Agroforestry Systems* **60**, 305-309.

Pitre FE, Brereton NJB, Audoire S, Richter GM, Shield I, Karp A. 2010. Estimating root biomass in *Salix viminalis* x *Salix schwerinii* cultivar "Olof" using the electrical capacitance method. *Plant Biosystems* **144**, 479-483.

Psarras G, Merwin IA. 2000. Water stress affects rhizosphere respiration rates and root morphology of young 'Mutsu' apple trees on M.9 and MM.111 rootstocks. *Journal of the american society for horticultural science* **125**, 588-595.

Tsukahara K, Yamane K, Yamaki Y, Honjo H. 2009. A nondestructive method for estimating the root mass of young peach trees after root pruning using electrical capacitance measurements. *Journal of Agricultural Meteorology* **65**, 209-213.

Blomme G, Blanckaert I, Tenkouano A, Swennen R. 2004. Relationship between electrical capacitance and root traits. *Infomusa* **13**, 14-18.

Schwan HP. 1992. Linear and nonlinear electrode polarization and biological materials. *Annals of Biomedical Engineering* **20**, 269-288.

Atkins PW. 1994. *Physical Chemistry*. Oxford, UK: Oxford University Press.

Patel P, Markx GH. 2008. Dielectric measurement of cell death. *Enzyme and Microbial Technology* **43**, 463-470.

Hall G. 2008. Maxwell's electromagnetic theory and special relativity. *Philosophical Transactions of the Royal Society a-Mathematical Physical and Engineering Sciences* **366**, 1849-1860.

Dietrich RC, Bengough AG, Jones HG, White PJ. 2012. A new physical interpretation of plant root capacitance. *Journal of Experimental Botany* **63**, 6149-6159.

Esau K. 1977. *Anatomy of seed plants*. New York: John Wiley & Sons.

Cao Y, Repo T, Silvennoinen R, Letho T, Pelkonen P. 2011. Analysis of the willow root system by electrical impedance spectroscopy. *Journal of Experimental Botany* **62**, 351-358.

Lulai E. 2005. Non-wound-induced suberization of tuber parenchyma cells: A physiological response to the wilt disease pathogen *Verticillium dahliae*. *American Journal of Potato Research* **82**, 433-440.

Rastovski A, Van Es A. 1981. *Storage of Potatoes*. Leiden, Netherlands: Backhuys Publishers.

APPENDIX

The figure shows the relationship between the change in capacitance following the removal of an individual root (Δ capacitance) and its fresh mass in the preliminary experiments (a) expt. II ($n = 266$) and (b) expt. III ($n = 216$) (Ch2, S. 2). There was no correlation found between the two measures. Whilst the average root mass was equal ($0.13 \text{ g} \pm 0.015 \text{ g SE}$, expt. II; $\pm 0.013 \text{ g SE}$, expt. III), the average capacitance was 2.4-times higher in expt. II than in expt. III possibly due to the different water regimes used (Fig. 2-1).

